Role of Secreted Protein Acidic Rich in Cysteine in Pulmonary Vascular Remodeling of Pulmonary Hypertension

Inaugural Dissertation

submitted to the

Faculty of Veterinary Medicine and Medicine

in partial fulfillment of the requirements

for the PhD-Degree of the Faculties of Veterinary Medicine and Medicine

of the Justus Liebig University Giessen

by Vartürk-Özcan, İpek

of

Üsküdar/ İstanbul

Giessen 2019

From the Department of Internal Medicine

Director: Prof. Dr. Werner Seeger of the Faculty of Medicine of the Justus Liebig University Giessen

First Supervisor and Committee Member: Prof. Dr. Norbert Weißmann

Second Supervisor and Committee Member: Prof. Dr. Reinhard Lakes-Harlan

Committee Members: Prof. Dr. Klaus-Dieter Schlüter

Date of Doctoral Defense: 17.10.2019

1. Introduction

1.1 Lung anatomy and respiratory system

The lungs are the main organs of the respiratory system in humans as well as many other animals and are crucial for gas exchange. In humans, the right lung consists of three, while the left lung consists of two major lobes because of the asymmetrical placement of the heart [1, 2]. The lung lies along the upper and lower respiratory tract. The upper respiratory tract consists of nose, nasal cavity, sinuses, and pharynx[3], while the lower respiratory tract consists of trachea, main bronchus, lobar bronchus, segmental bronchus, subsegmental bronchus, conducting bronchiole, terminal bronchiole, respiratory bronchiole, alveolar duct, alveolar sac and alveolus[4]. Human and other mammals are critically dependent on gas exchange, which takes place in the alveoli. They need oxygen (O_2) for energy production and have to dismiss the produced carbon dioxide (CO_2). O_2 is required for a metabolic process called cellular respiration, which takes place in the mitochondria. Cellular respiration converts biochemical energy from nutrients into adenosine triphosphate (ATP)[5]. Those steps involve an electron transfer to O_2[5]. There are two types of cellular respiration, aerobic and anaerobic respiration. Aerobic respiration requires O_2, however when O_2 is limited , anaerobic respiration is used for survival[6]. Aerobic respiration makes total 30-32 ATP while anaerobic respiration 2 ATP. ATP has a role in providing energy to cells, regulating biochemical processes, driving active transport of macromolecules (proteins and lipids) into and out of the cell, cell signaling and muscle contraction[7]. In this regard, the respiratory system has a critical function in keeping the organism alive[5].

When atmospheric air has been brought to the surface of the lungs, O_2 will start moving from the air space (alveoli) into the blood (alveolar capillaries). Oxygenated blood is then pumped via the left ventricle into the systemic circulation, delivering O_2 to the body´s cells. CO_2 moves the reverse direction[5]. CO_2 is produced during cellular respiration. It moves out from the cells, enters the bloodstream, moves back to the lungs, and is then expired out of the body during exhalation[8]. Both O_2 and CO_2 move passively via diffusion. Diffusion describes the movement of molecules from a higher to a lower concentration[9]. If there is an increase in the surface area of the lung for gas exchange, the O_2 diffusion rate increases[5]. In the lung, a partial pressure gradient for O_2 and CO_2 exists. Since the partial pressure of O_2 (PO_2) in the atmosphere is greater than the PO_2

of the blood, the net diffusion of O_2 is always from the atmosphere to the blood and for CO_2 vice versa[9]. Next to the surface area size, the thickness of the diffusion barrier affects the diffusion rate[5]. An increase in the alveolar-capillary membrane thickness, leads to an attenuated diffusion[5]. Thus, an optimal respiratory system should have the following main features:

1) A short distance for O_2 and CO_2 diffusion,
2) A large surface area for gas exchange
3) A system that maximizes the partial pressure gradient for O_2 and CO_2 and avoids edema formation[5].

Pulmonary edema is characterized by an abnormal accumulation of fluid in the lung impairing gas exchange[10], due to an increase in diffusion distance. Since humans have high metabolic rates and high requirements for O_2, the human respiratory system is associated with those main features for maximizing the rate of O_2 uptake from the atmosphere[5]. The human respiratory system has a large surface area for gas exchange (100m²-145 m^2) and an excessively thin but robust barrier (0.2 µm) for gas diffusion[5, 11].

The respiratory system, which is critically involved in gas exchange, closely works with the circulatory system. The blood circulatory system, also called cardiovascular system, contains the heart and a network of blood vessels, delivering nutrients and O_2 via the blood stream to all body´s cells[12]. Arteries carry the blood away from the heart, whereas veins carry the blood back to the heart[12]. The system of blood vessels has a tree-like structure. The main artery (aorta) branches into large arteries, smaller vessels, a capillary network and finally to a network of tiny vessels[12]. Pulmonary artery and bronchus lie next to each other, keeping diffusion distance as short as possible, ensuring optimal blood oxygenation under physiological conditions[12].

However, besides the structure of the air-blood barrier and the close proximity of bronchus and artery, there is a physiological phenomenon called hypoxic pulmonary vasoconstriction (HPV), increasing the efficiency of gas exchange.

1.2 Hypoxic pulmonary vasoconstriction

Hypoxic pulmonary vasoconstriction (HPV) is a vascular feedback control mechanism in the lung, which was first described by von Euler and Liljestrand in 1946[13]. In this mechanism, a drop in alveolar O_2 concentration (hypoxia) causes a constriction of small pulmonary vessels, shifting blood away from poorly ventilated (hypoxic) areas into better ventilated (normoxic) areas of the lung, ensuring optimal blood oxygenation (**Figure 1)**[14]. The effect of hypoxia differs in the pulmonary and systemic circulation, which typically vasodilates in response to hypoxia[15]. In the lung, acute, regional hypoxia and HPV occurring within seconds to minutes is beneficial, matching perfusion of the lung to ventilation. However, global hypoxia and thus generalized HPV due to chronic hypoxia, which occurs at high altitude or during respiratory diseases, is detrimental[16]. Generalized HPV leads to a global increase in pulmonary vascular resistance (PVR) and mean pulmonary arterial pressure (mPAP)[17]. Moreover, under generalized hypoxia, vasoconstriction is fixed by pulmonary vascular remodeling leading to PH. In addition to vessel constriction, pulmonary vascular remodeling causes vessel lumen obliteration and vessel wall thickening, leading to insufficient oxygenation of arterial blood and poor oxygen supply of the body[17]. The condition of chronic elevated mPAP within the pulmonary arteries is known as pulmonary hypertension (PH)[17].

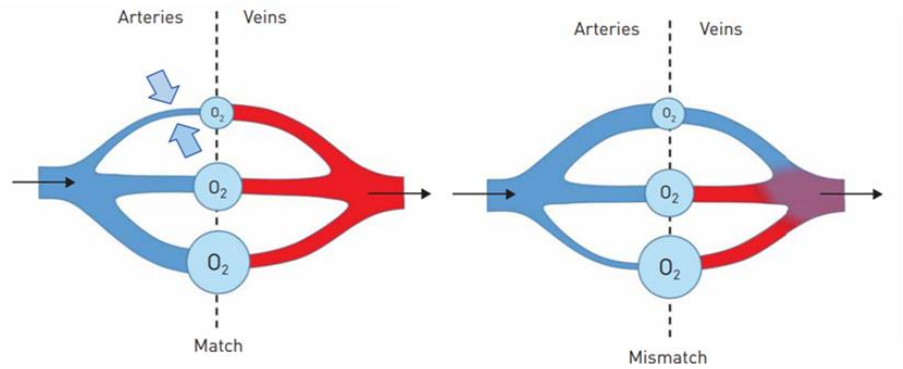

Figure 1: Hypoxic pulmonary vasoconstriction

Optimization of gas exchange by matching perfusion to ventilation. In a healthy individual, blood flow is directed to the areas of the lung that are well ventilated and oxygenated (O_2) (depicted by large blue circles). Here, an optimal gas exchange and oxygenation of the blood (shown in red) is ensured. A very small proportion of the blood reaches areas that are badly ventilated and oxygenated (smaller and medium blue circles). In individuals with lung diseases, the mechanism of hypoxic pulmonary *v*asoconstriction is disturbed, causing perfusion of not or poorly ventilated areas of the lung and thus leads to a reduced/decreased oxygenation of the blood (shown in blue/purple). Blue arrows show the constriction of pulmonary arteries, black arrows show the direction of blood flow. The big circles symbolize a high, small a low pO_2[18]. (Figure is reproduced with permission of the © ERS 2019).

1.3 Pulmonary hypertension

Pulmonary hypertension (PH) is a severe disease, causing high mortality[19]. The estimated prevalence of PH is about 15 cases per million patients[20]. PH is a pathophysiological condition defined by an increase in the mPAP of ≥ 25 mmHg at rest, accompanied by right heart hypertrophy and eventually right heart failure[21, 22].

Early symptoms of PH include shortness of breath during routine activity, chest pain, fatigue, racing heartbeat, decreased appetite and pain in the upper right side of the abdomen. Later symptoms include feeling light-headed especially during physical activity, fainting, bluish lips or skin and swelling in the ankles or legs[23]. Factors causing PH are: drugs and chemicals, diseases (chronic obstructive lung disease (COPD), scleroderma, human immunodeficiency virus (HIV), liver cirrhosis, etcetera), phenotype (age, gender), mutations (bone morphogenic protein receptor 2, BMPR2), single nucleotide polymorphisms, possible epigenetic inheritance, environmental triggers, chronic hypoxia, vasoconstrictor/vasodilator and/or growth factor imbalance[22, 24].

The diagnosis of PH needs a wide evaluation such as, history of the patient, physical examination, laboratory tests which include biomarker testing such as brain natriuretic peptide and N-terminal pro-brain natriuretic peptide, pulmonary function testing, echocardiography, cardiac catheterization, connective tissue disease serology and some tests to exclude chronic thromboembolic disease[21, 25]. By pulmonary function testing, normal lung volumes or a mild restriction can be seen[26]. Echocardiography, which is a sonogram of heart, is mostly used as a first diagnostic test to check the possibility of PH[27]. However, if diagnostic evaluation suggests PH, right heart catheterization will be used for confirmation and determination of the severity of PH[25]. This helps to exclude left-sided heart disease[25]. Lung scintigraphy, computed tomography, cardiac magnetic resonance imaging, positron emission tomography scanning and exercise testing are used as well[28]. To see the enlarged central pulmonary arteries and right heart dilation, chest radiographs are performed. Electrocardiogram, which records the electrical activity of heart, can show right axis deviation and RV hypertrophy[26].

PH is associated with a broad spectrum of histological patterns and abnormalities and occurs in a variety of clinical situations[22, 29]. Since it has such a diversity, a classification

system for PH has been developed and recently modified to organize the diseases into categories based on common clinical parameters, potential etiologic mechanisms and responses to treatment[30].

The clinical classification of PH was first proposed in 1998, during the 2nd World Symposium on Pulmonary Hypertension held in Evian, France[31] and modified in 2003 during the 3rd Symposium on Pulmonary Hypertension in Venice[29]. In the 4rd Symposium on Pulmonary Hypertension in Dana Point, 2008, PH was divided in five groups[32]. Group 1 is pulmonary arterial hypertension (PAH), group 2 is PH associated with left heart disease, group 3 is PH associated with lung diseases and/or hypoxemia, group 4 is PH due to chronic thrombotic and/or embolic disease and category 5 is PH with unclear multifactorial mechanisms. Modifications and updates were proposed in the 6th World Symposium on Pulmonary Hypertension held in Nice, 2018 ([19, 33]; **Table 1**). Two subgroups "pulmonary arterial hypertension (PAH) long-term responders to calcium channel blockers", due to the specific prognostic and management of these patients, and "PAH with overt features of venous/capillaries (pulmonary veno-occlusive disease/pulmonary capillary haemangiomatosis) involvement", due to evidence suggesting a continuum between arterial, capillary and vein involvement in PAH were added in group 1[33].

Table 1: Clinical classification of PH according to the 6th World Symposium in Nice, France (Modified from Simonneau 2018[33])

1. Pulmonary Arterial Hypertension (PAH)
1.1 Idiopathic PAH
1.2 Heritable PAH
1.2.1 BMPR2
1.2.2 ALK-1, ENG, SMAD9, CAV-1, KCNK3
1.2.3 Unknown
1.3 Drug or toxin induced
1.4 Associated with:
1.4.1 Connective tissue diseases
1.4.2 HIV infection
1.4.3 Portal hypertension
1.4.4 Congenital heart disease
1.4.5 Schistosomiasis

1.5 Long-term responders to calcium channel blockers
1.6 With overt features of venous/capillaries
1.7 Persistent pulmonary hypertension of the newborn (PPHN)
2. Pulmonary hypertension due to left heart disease
2.1 Due to heart failure with preserved LVEF
2.2 Due to heart failure with reduced LVEF
2.3 Valvular heart disease
2.4 Congenital/acquired cardiovascular conditions leading to post-capillary PH
3. Pulmonary hypertension due to lung disease and/or hypoxia
3.1 Obstructive pulmonary disease
3.2 Restrictive lung disease
3.3 Other pulmonary diseases with mixed restrictive and obstructive pattern
3.4 Hypoxia without lung disease
3.5 Developmental lung disorders
4. Pulmonary hypertension due to pulmonary artery obstructions
4.1 Chronic thromboembolic pulmonary hypertension (CTEPH)
4.2 Other pulmonary artery obstructions
5. Pulmonary hypertension with unclear multifactorial mechanisms
5.1 Hematologic disorders
5.2 Systemic disorders
5.3 Others
5.4 Complex congenital heart disease

BMPR2: bone morphogenetic protein receptor, type 2, ALK1: activin receptor-like kinase-1, HIV: human immunodeficiency virus. CAV-1: caveolin-1, ENG: endoglin, KCNK3: potassium channel subfamily K member 3; LVEF: left ventricular ejection fraction; SMAD9: mothers against decapentaplegic 9.

1.3.1 Group 1

After the 2nd World Symposium in 1998, different subcategories of **Group 1** (PAH) have markedly developed in 2013 and additional modifications were made in the Nice classification. All subcategories have similar pathological abnormalities, primarily in the small pulmonary arterioles[19]. The subgroups include:

Idiopathic PAH

Idiopathic PAH is a heterogeneous group, which includes idiopathic forms of the disease, known as idiopathic PAH (IPAH)[22]. In IPAH neither a family history of PAH, nor an identified risk factor, is known[22].

Heritable PAH

In heritable PAH, mutations of the bone morphogenetic protein receptor type 2 (BMPR2), a member of the tumor growth factor (TGF)-β super family, can be identified in 80% of the families. More rarely, mutations in other genes belonging to the TGF-β super family, which are activin-like receptor kinase-1 (ALK1)[34], endoglin (ENG)[35], and mothers against decapentaplegic 9 (Smad 9) can be identified in 5% of the patients [36]. Recently, two new gene mutations have been identified, occurring in caveolin-1 (CAV1)[37] and KCNK3, a gene encoding the outwardly rectifying potassium channel super family K member 3[38].

Drug- and Toxin-Induced Pulmonary Hypertension

Classic drugs causing PAH include anorexigens, aminorex and fenfluramine derivatives, and toxic rapeseed oil[39].

PAH Associated With Connective Tissue Diseases

The rate of prevalence of PAH in systemic sclerosis patients is between 7% and 12% [40,41]. Most of the long-term studies showed that the outcome of patients with PAH associated with systemic sclerosis is markedly worse than that of patients with IPAH, despite the use of modern therapies[42].

PAH Associated With HIV Infection

The prevalence of PH associated with human immunodeficiency virus (HIV) infection has been estimated to be 0.5%[43]. In the early 1990s, the development of specific PAH drugs and highly active antiretroviral therapies were extremely poor as well as, the prognosis for HIV-PAH. The mortality rate in a year was 50%[44].

PAH Associated With Portal Hypertension

Portopulmonary hypertension (POPH) means the development of PAH in association with elevated pressure in the portal circulation[45, 46]. Some of the hemodynamic studies revealed that, 2% to 6% of patients with portal hypertension have PH[47, 48].

PAH Associated With Congenital Heart Disease in Adults

Untreated patients with congenital heart disease (CHD), in particular those with relevant systemic-to-pulmonary shunts, will develop PAH[49].

PAH Associated With Schistosomiasis

In 2008, schistosomiasis-associated PAH (Sch-PAH) was included in Group 1. Today, Sch-PAH is potentially the most prevalent cause of PAH worldwide[19].

PAH long-term responders to calcium channel blockers

In 1992, patients with an acute vasodilator response to calcium channel blockers had effectively improved survival when treated with long-term calcium channel blockers[33]. In 2005, 6.8% of patients had a long-term clinical and hemodynamic improvement in using calcium channel blockers[33]. Long-term response to calcium channel blockers is characterized by clinical improvement (New York Heart Association Functional Class I or II) and sustained hemodynamic improvement after at least 1 year, only using calcium channel blockers[33].

PAH with overt features of venous/capillaries

Pulmonary veno-occlusive disease (PVOD) and pulmonary capillary hemangiomatosis (PCH) do not share common conditions with PH, but they have been categorized as reasons of PH[32]. As PVOD and PCH have similar clinical presentations and pathologic features, e.g. pulmonary parenchyma changes, these disorders are combined in one subgroup in the PH classification system[22].

Persistent pulmonary hypertension of the newborn

Persistent pulmonary hypertension of the newborn (PPHN) is a syndrome defined by sustained elevation of pulmonary vascular resistance (PVR) and is often related with normal or low systemic vascular resistance (SVR)[50].

1.3.2 Group 2

PH due to left heart disease belongs to group II and it is the most common cause of PH[51]. Left-sided ventricular or valvular diseases may elevate left atrial pressure, with passive backward transmission of the pressure that leads to elevation of PAP[30].

1.3.3 Group 3

In Group III (PH due to lung diseases and/or hypoxia), the main cause of PH is alveolar hypoxia[22]. Hypoxia in the lung can occur due to impaired control of breathing, residence at high altitude or lung diseases[22]. Triggers are chronic obstructive pulmonary disease (COPD), obstructive sleep apnea (OSA), interstitial lung disease (ILD), alveolar hypoventilation disorders, developmental lung abnormalities and chronic exposure to high altitude[52]. Elevation of pulmonary vascular resistance, inflammation of lung tissue and airways, fibrotic lung changes, hypoxic vasoconstriction are the main pathological features found in this group[53].

1.3.4 Group 4

Group 4 (chronic thromboembolic pulmonary hypertension) is characterized by occlusion of pulmonary arteries which increase PVR and mPAP[54]. Severe CTEPH can lead to right heart failure due to progressive right ventricular dysfunction[54].

1.3.5 Group 5

Group 5 contains several forms of PH with unclear multifactorial mechanisms[22]. The first subgroup contains several hematologic disorders [22], the second subgroup comprises systemic disorders, which are associated with an increased risk of developing PH[55]. The third subgroup includes metabolic disorders[22] and the fourth subgroup contains a number of miscellaneous conditions such as tumor growth in the central pulmonary arteries[56]. The present thesis mainly deals with PH group one and three, thus in the following paragraphs focuses on pulmonary vascular remodeling in these two groups.

1.4 Pulmonary vascular remodeling

PH is characterized by pulmonary vascular remodeling, affecting all three layers of the blood vessel wall[57]. Each layer consists of a special cell type. The adventitia consists of fibroblasts, the media of pulmonary arterial smooth muscle cells (PASMC) and the intima of endothelial cells, which face the blood. Hypertrophy (cell growth) and/or hyperplasia (proliferation) of those cell types finally leads to lumen occlusion[58].

Stimuli inducing pulmonary vascular remodeling can be mechanical stretch and shear stress (physical stimuli) and/or hypoxia, vasoconstrictor/vasodilator and growth factor imbalance (chemical stimuli)[58].

In the adventitia, fibroblasts are activated by a variety of potentially injurious stimuli[59], leading to increased cell proliferation, expression of contractile and extracellular matrix (ECM) proteins and increased secretion of chemokines, cytokines, and growth/angiogenic factors[59], stimulating PASMC proliferation[59]. Moreover, hyper-proliferative fibroblasts can differentiate in SMC, migrating in the media layer[59].

However, media hypertrophy is suggested as the main pathological hallmark of PH[60]. It takes place consistently in arteries, at all levels of the pulmonary arterial tree, and less constantly in veins[61]. Especially in distal pulmonary arteries the abnormal muscularization and thus the vessel lumen occlusion is of major importance, since those arteries are normally non-muscularized and mainly determine the pulmonary vascular resistance (PVR)[62]. The *de-novo* muscularization is caused by migration of PASMC from proximal to distal and/or by differentiation of pericytes into PASMC that subsequently proliferate (**Figure 2)**[62].

In addition to adventitial and medial changes, endothelial dysfunction contributes to pulmonary vascular remodeling. Under physiological conditions endothelium regulates vascular tone, production of growth factors, homeostasis (coagulation) and barrier function[63]. However, under pathophysiological conditions, impaired vasoconstriction, aberrant endothelial-mesenchymal transition and altered production of endothelial vasoactive mediators (nitric oxide (NO), prostacyclin, endothelin-1) and growth factors vascular endotheial growth factor (VEGF), platelet-derived growth factor (PDGF) occurs[64]. In addition, hyper-proliferation of endothelial cells leads to plexiform lesion formation[63]. Plexiform lesions are most abundant in small pulmonary artery branches, immediately after their origin from a parent artery[65]. They consist of proliferating

myofibroblasts, endothelial and/or fibrillary cells, embedded in an ECM[66-68]. Moreover, encroachment of myofibroblasts and deposition of ECM proteins leads to neo-intima formation[69] (**Figure 2**) which is a characteristic response of arteries to several forms of injury[70]. The neo-intima is located between the endothelium and the internal elastic lamina[70]. Besides media hypertrophy, a rise in neo-intima increases PVR[64]. The initial stimulus or injury causing endothelial hyper-proliferation is unknown, but may include hypoxia, shear stress, reactive oxygen species, inflammation, or response to drugs or toxins on a background of genetic susceptibility[63, 71]. Moreover, apoptosis of endothelial cells (EC) and/or pericytes could lead to the loss of small precapillary arteries[72].

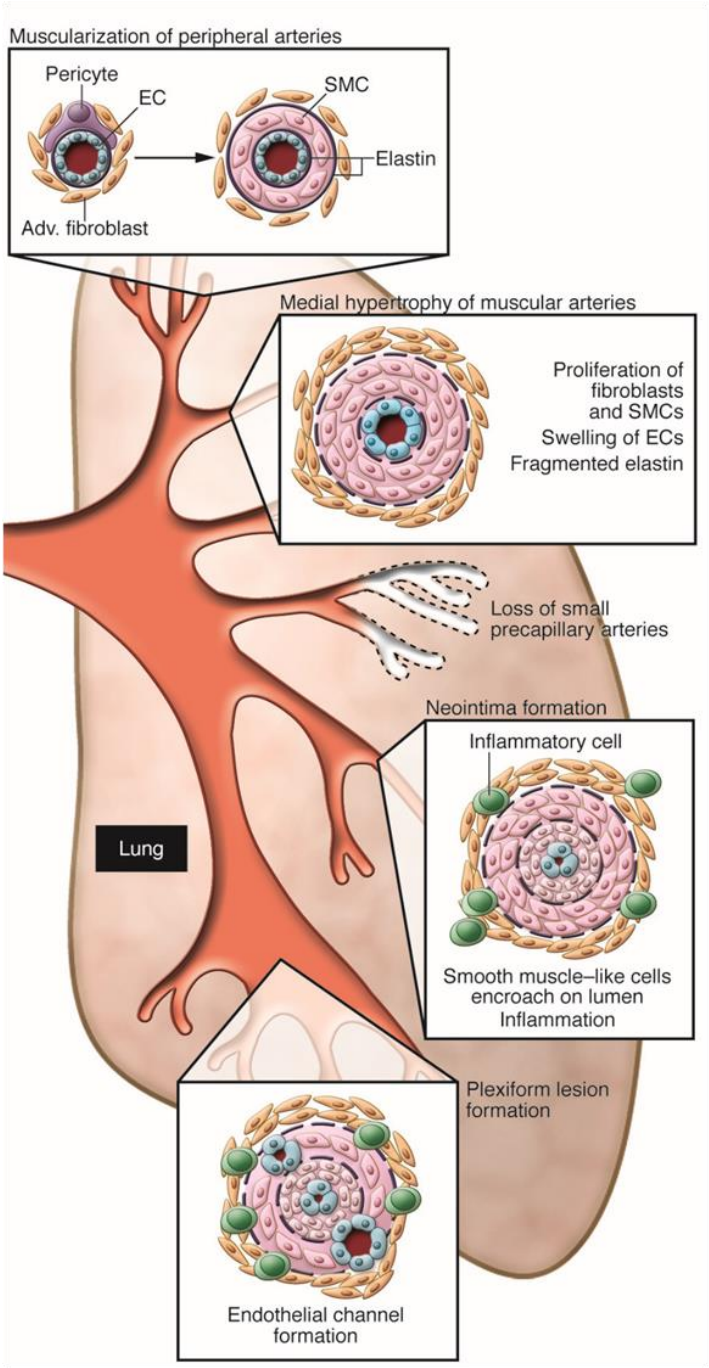

Figure 2: Pulmonary vascular remodeling.

Pulmonary vascular remodeling involves structural changes in the normal architecture of pulmonary arteries, including dysregulated proliferation, migration and apoptosis of pulmonary arterial smooth muscle cells (PASMC), fibroblasts and endothelial cells and deposition of extracellular matrix proteins. Due to PASMC dysregulation media hypertrophy (ii) and abnormal muscularization of previous non-muscularized distal pulmonary arteries occurs (i), leading to narrowing and lumen occlusion. In addition, in severe PH forms, vessel loss (iii), neo-intima (iv), and plexiform lesion (v) formation takes place[69, 72]. (Confirmation number of figure:11779725[69]).

Next to vascular cells, ECM structure proteins (collagen, elastin, fibronectin, laminin, etc.), providing structural support of surrounding cells, contribute to vessel wall thickening and lumen occlusion[61]. The ECM has a role in determining the physical properties of tissues such as mechanical stability, stiffness, porosity, insolubility[73] and characteristics of the cells within them[74]. Several studies showed that modifications in the composition of ECM lead to the onset and progression of vascular lesions[75]. Besides structure proteins, matricellular proteins are located in the ECM. They do not participate directly in the organization or physical properties of structures[75]. However, they possess regulatory cell functions such as angiogenesis, adhesion, migration and proliferation[76-78]. They are able to modulate cell-matrix interactions and they possess binding sites for many cell surface receptors, growth factor receptors and ECM structure proteins[79]. In this regard, matricellular proteins are expressed at high levels during development and responses to injury. The original group of matricellular proteins are thrombospondin-1 (TSP1), SPARC (secreted protein, acidic and rich in cysteine), tenascin-C, osteopontin (OPN) and tenascin X[76-78].

The mitogen transforming growth factor β (TGF-β), among other functions, is a potent modulator of ECM synthesis. It stimulates matrix synthesis in wounds and remodeling processes[80]. Other growth factors involved in dysregulation of cellular functions in PH are PDGF, VEGF, epidermal growth factor (EGF) and basic fibroblast growth factor (bFGF). They are involved in the abnormal proliferation and migration of vascular cells[81-85]. In this regard, it was shown that VEGF is highly expressed in EC of plexiform lesions in severe PAH[86]. PDGF acts as a potent mitogen and chemoattractant for SMC[82]. Both, PDGF and bFGF induce SMC and fibroblast proliferation and migration and thus work as key mediators in the progression of PH[87]. EGF is involved in a tenascin dependent SMC proliferation[75]. Studies revealed the colocalization of EGF with tenascin in PH lesions, suggesting a direct role in disease progression[87].

Beside of growth factors there are also transcription factors (TFs) which are implicated in the pathogenesis of PH[88]. TFs are sequence-specific DNA-binding proteins that control the process of transcription[88]. Some of the TFs in PH are forkhead box O1 (FOXO1), krüppel-like factor 4 (KLF4), peroxisome proliferator–activated receptor γ (PPARG1), snail family zinc finger 2 (SLUG), signal transducers and activators of transcription 3 (STAT3), nuclear factor of activated T-cells, cytoplasmic, calcineurin-dependent 2 (NFATc2), hypoxia-inducible factor 1α (HIF1α) and hypoxia-inducible factor 2α (HIF2α)[88]. HIFs are main regulators of the molecular response to hypoxia and strongly implicated in the pathogenesis of PH by targeting genes controlling vascularization, cellular proliferation, migration and metabolism[89, 90].

1.5 Treatment options

Over the past 20 years, more and more treatment options for PH came up[91], however PH is still not curable.

Conventional medical therapies with oral, inhaled and intravenous options are used for the treatment for PH. Heart or lung transplant may also be an option depending on the severity of PH[92]. Conventional medical therapies used in PH include: Calcium channel blockers, Digoxin, diuretics, oxygen and Warfarin (Coumadin®)[92]. Calcium channel blockers inhibit the calcium influx in cells and thus impair calcium-dependent vasoconstriction. They are the first vasodilator agents used in the treatment of PH[93]. However, calcium channel blockers are only appropriate for a small minority of patients, demonstrating a favorable response to vasodilator-testing during heart catheterization[92]. Digoxin supports the heart contractility[92]. Diuretics are used to increase diuresis and thereby decreasing blood pressure[92]. Oxygen therapy helps to improve blood oxygenation. Patients generally inhale oxygen by a nasal cannula or a face mask[92]. Warfarin prevents blood clotting and thus thrombus formation[92].

Next to conventional treatment options, oral, inhaled or intravenous medications are available. For several years prostacyclin analogues, phosphodiesterase 5 (PDE-5) inhibitors and endothelin receptor antagonists were used for treatment of PH[94]. These medications target prostacyclin, endothelin (ET)-1, and nitric oxide (NO) pathways that are dysregulated in PH[95].

Prostacyclin initiates vasodilation by cyclic adenosine monophosphate and has both anti-proliferative and anti-coagulative effects[96]. Available prostacyclins are: Treprostinil (Orenitram®), Iloprost (Ventavis®), Treprostinil (Tyvaso™ and Remodulin®) and Epoprostenol (Flolan® and Veletri®)[92].

ET-1 is an efficient vasoconstrictor, which is produced and secreted by the vascular endothelium[97]. Blockage of ET -1 receptors by Macitentan on PASMC reverses pulmonary vasoconstriction[98, 99]. Next to Macitentan (Opsumit®), Ambrisentan (Letairis®) and Bosentan (Tracleer®) are available endothelin receptor antagonists[92].

NO vasodilates the pulmonary arterial circulation by diffusing across the alveolar-capillary membrane into the pulmonary artery smooth muscle. It activates soluble guanylate cyclase and increases the levels of cyclic guanosine 3′5′-monophosphate (cGMP)[100].

PDE 5 inhibitors increase endogenous cGMP levels. Available PDE 5 inhibitors for treatment of PH are Sildenafil (Revatio™) and Tadalafil (Adcirca®)[92].

Newer approved drugs are: Riociguat (Adempas®), Treprostinil and Selexipag (Uptravi®)[91, 101]. Riociguat is a soluble guanylate cyclase stimulator, producing cGMP, which causes blood vessel relaxation. The pulmonary blood pressure decreases and the heart function is improved[102-104]. The advantages of the new approved drugs are delaying the time of clinical worsening[94], improving the 6-minute walk distance (6MWD), cardiopulmonary hemodynamics[105] and exercise capacity[94].

Targeting those pathways improves symptoms, survival and quality of life[106]. However, many of the medications have complex administration regimens and considerations, along with significant side effects and monitoring requirements[94].

However, until now there is no drug available which can fully reverse PH, thus research is still needed, identifying new pathways and targets[91].

1.6 Animal models of pulmonary hypertension

Using animal models of PH is a valuable tool to study the various underlying pathobiological mechanisms and to test new treatment strategies[107].

The most commonly used animal models of PH are the chronic hypoxia model in different species and the monocrotaline injury model in rats[107]. Both models are widely available, have well-described histopathological characteristics and possess good reproducibility[107].

However, nowadays, various additional experimental PH models are available. Those models include, physically, chemically and genetically-induced models as well as single and multiple stimuli models (**Figure 3**). Every model has its specific characteristics and thus is used to investigate a particular category of human PH.

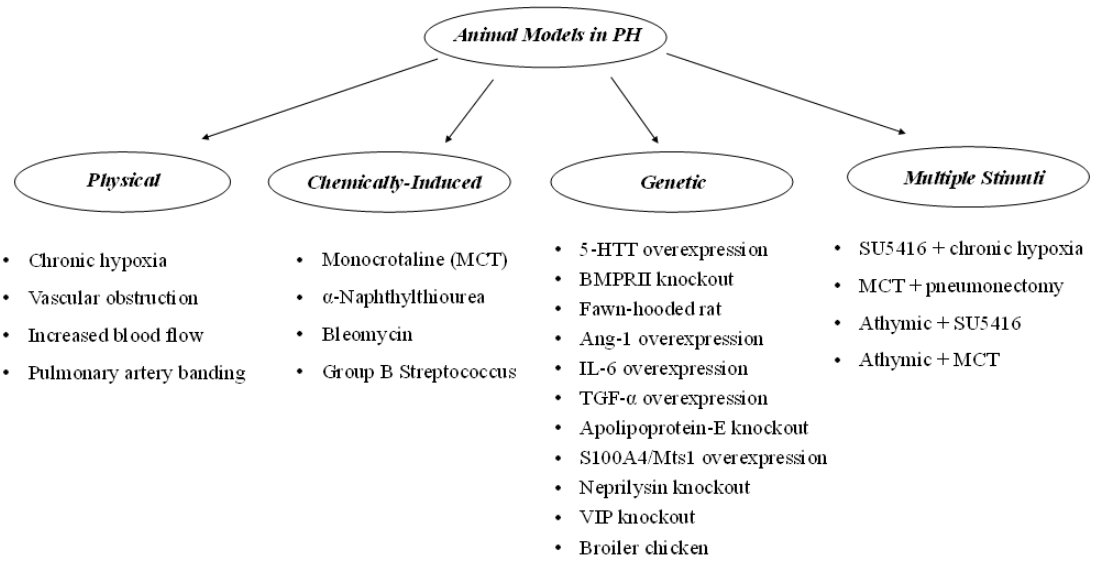

Figure 3: List of animal models used in PH research

Physical, chemically-induced, genetic and multiple stimuli models used in PH research[108].

An ideal PH model reflects the key clinical, hemodynamic and histopathological features of human PH[109]. However, until now each models has its limitations. So far, there is no perfect and ideal animal model that fully reflects the complex pathophysiological changes of human PH[30]. There are species-specific differences and the three critical points of the human disease: obliteration of pulmonary arterioles, non-reversibility and development of the right ventricle failure (RVF) are not reflected in each model[108]. In this regard, multiple stimuli approaches reflect the human disease better than single stimuli approaches[110]. However, single stimuli approaches are suggested to reflect the characteristics of early PH[110].

In the present thesis mice were exposed to chronic hypoxia, thus the following paragraphs provides more details about this specific model.

1.7 Chronic hypoxia-induced Pulmonary Hypertension

In a wide variety of animal species, such as mouse, pig, rat, and cattle, normobaric (normal pressure but reduced O_2 concentration (10% O_2, balanced by N_2) and hypobaric (O_2 concentration is constant and pressure is reduced (380mmHg ≈ 5500m)) hypoxia are frequently used to induce PH[108, 109]. As variety of genetically modified mice are available, they are a desirable tool for studying chronic hypoxia-induced PH[30].

Pathological findings from animals exposed to chronic hypoxia are muscularization of small previous non-muscularized arterioles, increased mPAP and right heart hypertrophy[30, 109].

Besides rats, mice are the most commonly used animals in this model[30]. Both develop similar pathological changes following exposure to chronic hypoxia. However, the degree of remodeling and hemodynamic changes are more severe in rats[108, 109]. In normoxic mice, RVSP is between 10-20 mmHg, whereas in hypoxic mice it is between 14-26 mmHg[108]. Moreover, factor of right ventricular hypertrophy (RVH) (RV/LV+S) in normoxic mice is 0.24, while it is 0.32 in hypoxic mice[108]. In normoxic rats, RVSP is 21 mmHg and in hypoxic rats is 47 mmHg[111]. RVH in normoxic rats is 0.18 and in hypoxic rats 0.44[112].

Limitations of the chronic hypoxia-induced animal models are;

1) The response to hypoxia is variable among animal species and age of animals,
2) There is a lack of right ventricular failure[109]
3) There is no intimal cell proliferation and
4) There are no complex pulmonary vascular lesions.

Moreover, when the hypoxic stimulus stops and mice/rats re-oxygenate to room air oxygen concentration, chronic hypoxia-induced PH is reversible, a process called reverse-remodeling[113]. The following paragraph deals with this phenomenon.

1.8 Reverse remodeling in mice

In 1960s it was observed that high altitude hypoxia leads to PH in humans[114], which can be partially reversed after returning to sea level[115]. In 1971, experimental studies showed that exposure of rats to hypobaric pressure (5500m) leads to PH, including right heart hypertrophy and muscularization of small pulmonary arteries[116]. The increase in right ventricular weight and muscularization was reversible after 37 days recovery[116].

In 1973, an experiment in rats was conducted, increasing the recovery time after chronic hypoxic exposure to 5 weeks. It was found that right ventricular hypertrophy was partially reversible. The thickness of the main pulmonary artery and the volume of the hypertrophied carotid body decreased[117].

The reversal of right heart hypertrophy and pulmonary artery muscularization after re-exposure of rats to normoxia was confirmed in 1977[118].

In 2014, reverse remodeling findings in rats were transferred to mice, revealing that chronic hypoxia-induced PH is fully reversible upon re-exposure to normoxia. Right heart hypertrophy as well as pulmonary vascular remodeling was completely reversible[113] (**Figure 4**).

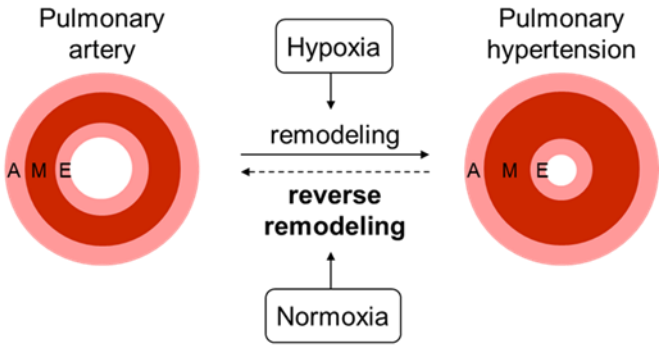

Figure 4: Reverse remodeling

Chronic hypoxic exposure leads to pulmonary vascular remodeling, which is reversible upon re-exposure to normoxia A: Adventitia, M: Media, E: Endothelium.

1.9 Aim of the study

Until now, research in the field of PH concentrates mostly on the onset and development of PH. In this study, we focus on mechanisms underlying the reversal of PH. It was previously shown that chronic hypoxia-induced vascular remodeling in mice can be reversed by re-exposure to normoxia[113]. In this regard, a microarray analysis from murine lung homogenate was performed, screening for potential candidate genes contributing to reverse remodeling. S-adenosylmethionine decarboxylase 1 (AMD-1) was identified as a novel potential candidate gene. AMD-1 is elevated expressed in chronic hypoxic mice and down-regulated following re-oxygenation of mice. Furthermore, it is critically involved in dysregulated PASMC proliferation and apoptosis. In addition, AMD-1 knockout mice possess less chronic hypoxia-induced PH than respective controls[113].

Going beyond this approach, we now wanted to specifically focus on the gene expression alterations in the lung vasculature, possibly enhancing the chance to detect additional relevant new pathways and targets for pulmonary vascular remodeling. In this regard, pulmonary vessels from mice, exposed under normoxia, chronic hypoxia and chronic hypoxia with subsequent normoxic exposure for different time points, will be laser-microdissected followed by microarray analysis. Expression of identified targets will be validated in chronic hypoxic mice, in IPAH patients and on cellular level. Moreover, the functional role will be assessed *in vitro* as well as *in vivo* by using respective knockout mice.

It is hypothesized that, the microarray technique leads to identification of new candidate genes and their relevant signaling pathways underlying pulmonary vascular remodeling which will help to identify novel treatment strategies for PH.

2. Materials and Methods

2.1 Materials

2.1.1 Equipment

Catheter - MiniVent type 848 Hugo Sachs	*Elektronik-Harvard Apparatus, March, Germany*
Cell incubator HERAcell 150	*Thermo Scientific, Dreieich, Germany*
Centrifuge Hematocrit 210	*Hettich, Tuttlingen, Germany*
Centrifuge Rotanta 460R	*Hettich, Tuttlingen, Germany*
CFX Connect™ Real-Time PCR Detection System	*Biorad, Munich, Germany*
ChemiDoc™ Touch Imaging System	*Biorad, Munich, Germany*
ChemiDoc™ XRS+	*Biorad, Munich, Germany*
Cooling Plate EG 1150C	*Leica Microsystems, Wetzlar, Germany*
Computer Q 550 IW	*Leica Microsystems, Wetzlar, Germany*
Digitale Camera DC 300F	*Leica Microsystems, Wetzlar, Germany*
GenePix 4100A Scanner	*Axon Instruments, Union City, NJ, USA*
Glass plates (1.5 mm)	*Biorad, Munich, Germany*
Hematocrit 210 Centrifuge	*Hettich, Tuttlingen, Germany*
Heating Block	*VWR, Bruchsal, Germany*
Heating Plate Hi 1220	*Leica Microsystems, Wetzlar, Germany*
HLC Heating-ThermoMixer	*DITABIS Digital Biomedical Imaging Systems, Pforzheim, Germany*
Homeothermic plate	*AD Instruments, Spechbach, Germany*
Homogenizer PRECELLYSR24	*PeqLab, Erlangen, Germany*
Hotplate/Stirrer (371)	*VWR, Bruchsal, Germany*

Infinite M200	*Tecan, Männedorf, Switzerland*
Laser Microdissection system LMD 600	*Leica Microsystems, Wetzlar, Germany*
Low Voltage Power Supplies Power pack P25T	*Biometra, Analytic Jena, Jena, Germany*
Magnet for Tubes (DynaMagTM-Spin Magnet)	*Thermo Fisher Scientifc Inc. Waltham, USA*
Micro-tip catheter SPR-671NR	*Millar Instruments, Houston, USA*
MiniVent type 845 Hugo Sachs	*Elektronik, March-Hugstetten, Germany*
Multimode microplate reader Infinite 200 PRO	*Tecan, Männedorf, Switzerland*
Multimode microplate reader Spark®	*Tecan, Männedorf, Switzerland*
NanoDrop (ND-1000)	*Kisker-Biotech, Steinfurt, Germany*
Ultrapure Milli-Q®	*Millipore, Schwalbach, Germany*
Paraffin cooling station Leica EG 1150C	*Leica, Wetzlar, Germany*
Paraffin embedding station Leica EG 1140H	*Leica, Wetzlar, Germany*
PCR Plate sealer PX1	*Biorad, Munich, Germany*
PEN membrane slides	*Leica Microsystems, Wetzlar, Germany*
pH meter-766 Calimatic	*Knick, Berlin, Germany*
Rectal thermometer	*Indus Instruments, Houston, TX, USA*
Table Centrifuge Mikro 200R	*Hettich, Tuttlingen, Germany*
Thermocycler, Tpersonal	*Biometra, Analytic Jena, Jena, Germany*
Thermocycler, T3000	*Biometra, Analytic Jena, Jena, Germany*
Tissue Tek	*Sakura Finetek, Staufen, Germany*
Ultrapure water-Milli Q®	*Millipore, Schwalbach, Germany*
Vortexer MS1 Minishaker	*IKA GmbH, Staufen, Germany*

Waterbath	*Memmert, Schwabach, Germany*

2.1.2 Chemicals and consumables

0,9 % NaCl-Solution	*B.Braun, Melsungen, Germany*
Aceton	*Sigma-Aldrich, Munich, Germany*
Agarose	*Fermentas, St. Leon-Rot, Germany*
Amersham ECL Plus Western Blotting Detections System	*GE Healthcare, Munich, Germany*
Ammonium persulfate (APS)	*Promega, Mannheim, Germany*
Ampuwa®	*Fresenius Kabi, Bad Homburg, Germany*
Antibody Diluent	*Zytomed Systems, Berlin, Germany*
β-Mercaptoethanol	*Sigma-Aldrich, Munich, Germany*
Bovines Serum Albumin (BSA)	*Sigma-Aldrich, Munich, Germany*
BSA-Solution	*Biorad, Munich, Germany*
Cell lysis buffer	*Cell Signaling Technology, Cambridge, UK*
Cpd 22, Calbiochem®	*Merck, Darmstadt, Germany*
Deionised Water (dH_2O)	*Milliporanlage in Laboratory*
Deoxynucleotide (dNTP)	*Promega, Mannheim, Germany*
Distilled Water (dH_2O, DNAse-/ RNAse-free)	*GibcoTM Invitrogen, Karlsruhe, Germany*
Disodiumhydrogenphosphate (Na_2HPO_4)	*Merck, Darmstadt, Germany*
Double distilled Water (ddH_2O)	*Carl Roth, Karlsruhe, Germany*
Dimethylsulfoxid (DMSO)	*Sigma-Aldrich, Munich, Germany*
Ethanol 70 %, 96 % und 100 %	*Otto Fischer GmbH, Saarbrücken, Germany*
Ethanol (pure) for molecular biology	*Merck, Darmstadt, Germany*
Ethylenediaminetetraacetic acid (EDTA)	*Sigma-Aldrich, Munich, Germany*

Flexi Buffer	*Promega, Mannheim, Germany*
Glycerol	*Sigma-Aldrich, Munich, Germany*
Glycin	*Carl Roth, Karlsruhe, Germany*
GoTaq polymerase	*Promega, Mannheim, Germany*
Hematoxylin	*Biocare Medical, Pacheco, CA*
Hydrochloride (HCl)	*Carl-Roth, Karlsruhe, Germany*
Hydrogen peroxide (H_2O_2)	*Merck, Darmstadt, Germany*
Isopropylalcohol (2-Propanol)	*Merck, Darmstadt, Germany*
Lysis Buffer (9803S)	*Cell Signaling Danvers, MA, USA*
Magnesium Chloride ($MgCl_2$)	*Promega, Mannheim, Germany*
Monopotassiumdihydrogenphosphate (KH_2PO_4)	*Merck, Darmstadt, Germany*
Methanol	*Sigma-Aldrich, Munich, Germany*
Methyl green	*Vector Laboratories, Burlingame, CA, USA*
Microarray Slides Mouse whole Genome 4x44K	*Agilent Technologies, Palo Alto, CA, USA*
Paraformaldehyde	*Carl Roth, Karlsruhe, Germany*
Phenylmethansulfonylfluorid (PMSF)	*Sigma-Aldrich, Munich, Germany*
Phenylmethylsulfonyl Fluoride (PVDF)-membrane	*Pall Corporation, Dreieich, Germany*
Potassiumchloride (KCl)	*Merck, Darmstadt, Germany*
Proteinase K Novocastra™	*Leica, Wetzlar, Germany*
Skimmed milk powder	*Sigma-Aldrich, Munich, Germany*
Sodiumchloride (NaCl)	*Carl Roth, Karlsruhe, Germany*
Sodium dodecyl sulfate (SDS)	*Promega, Mannheim, Germany*
Sodium hydroxide (NaOH)	*Carl Roth, Karlsruhe, Germany*

Sodium ortho vanadate (Na_3VO_4)	*Sigma-Aldrich, Munich, Germany*
SYBR® Safe	*Invitrogen, Karlsruhe, Germany*
SYBR® Safe DNA gel stain	*Invitrogen, Karlsruhe, Germany*
T-EDTA Buffer pH 9.0	*Zytomed Systems, Berlin, Germany*
Tetramethylethylenediamine (TEMED)	*Carl Roth, Karlsruhe, Germany*
Tergitol® (NP-40)	*Sigma-Aldrich, Munich, Germany*
TRIS Base	*Sigma-Aldrich, Munich, Germany*
TRIS-HCl	*Sigma-Aldrich, Munich, Germany*
Triton-X	*Sigma-Aldrich, Munich, Germany*
Tween® 20	*AppliChem, Darmstadt, Germany*
Xylol	*Carl Roth, Karlsruhe, Germany*

2.1.3 Cell culture

Canule 16G, 18 G	*BD Microlane, Franklin Lakes, USA*
Cell culture dishes, (35er, 60er)	*Sarstedt, Nümbrecht, Germany*
Cell culture flasks, (T-25, T-75)	*Greiner bio-one, Frickenhausen, Germany*
Cell culture plate (6, 12, 24, 96 well)	*Greiner bio-one, Frickenhausen, Germany*
Cell scrapers	*Greiner bio-one, Frickenhausen, Germany*
Cryo Tubes	*Sarstedt, Nümbrecht, Germany*
Falcon-Tubes	*Greiner bio-one, Frickenhausen, Germany*
Fetal calf serum (FCS)	*PAA Laboratories, Cölbe, Germany*
Filtered tips, 10, 100, 1000 µl	*Nerbe plus, Winsen, Germany*
Heparin, Heparin-Natrium	*Ratiopharm GmbH, Ulm, Germany*

-5000-ratiopharm®	
Ketaminhydrochlorid 100 mg/mL, Ketamin®, 10%ig	*Bela-Pharm, Vechta, Germany*
Lipofectamine 2000	*Invitrogen, Karlsruhe, Germany*
Medium 199 (M199)	*GIBCO Invitrogen, Karlsruhe, Germany*
Micro tube 0.5, 1.5, 2.0 ml	*Sarstedt, Nümbrecht, Germany*
Micro tube 0.5, 1.5, 2.0 ml DNA-/DNase-/RNase-/PCR-inhibitor free	*Sarstedt, Nümbrecht, Germany*
Neubauer counting chamber LO	*Laboroptik GmbH, Bad Homburg, Germany*
Opti-MEM Medium	*Gibco, Darmstadt, Germany*
PCR Plate 96-Well, Multiplate^{TM} PCR Plates, clear	*Biorad, Munich, Germany*
Penicilin/Streptomycin (Pen Strep, P/S)	*Gibco, Life Technologies, Carlsbad, USA*
Phosphate puffered saline (PBS)	*PAN Biotech, Aidenbach, Germany*
Pulmonary arterial smooth muscle cells (PASMC)	*Lonza, Köln, Germany*
Serological pipette 5, 10, 25, 50 ml	*BD Falcon, Heidelberg, Germany*
Smooth Muscle Cell Basal Medium	*PromoCell, Heidelberg, Germany*
Smooth Muscle Cell Growth Medium 2	*PromoCell, Heidelberg, Germany*
Smooth Muscle Supplement 2 mix	*Promo cell, Heidelberg, Germany*
Sterile filter 0,22 µm	*Millipore, Schwalbach, Germany*
Trypsin/EDTA (10x)	*PAN-Biotech, Aidenbach, Germany*
Xylazinhydrochlorid, Xylazin® 2%ig	*Ceva Tiergesundheit, Düsseldorf, Germany*

2.1.4 Ligands and inhibitors

Epidermal growth factor (EGF, human)	*Peprotech, Hamburg, Germany*

Platelet -derived growth factor (PDGF-BB, human)	*Peprotech, Hamburg, Germany*
Rapamycin	*Sigma Aldrich, Munich, Germany*
Transforming growth factor beta 1 (TGF-β1, human)	*Peprotech, Hamburg, Germany*
Vascular endothelial growth factor (VEGF, human)	*Peprotech, Hamburg, Germany*
Wortmannin	*Sigma Aldrich, Munich, Germany*

2.1.5 siRNA

HIF-1α ON-TARGETplus SMARTpool L-004018-00	*DharmaconThermo Scientific, Schwerte, Germany*
HIF-2α ON-TARGETplus SMARTpool L-004814-00	*DharmaconThermo Scientific, Schwerte, Germany*
ILK ON-TARGETplus SMARTpool L-004499-00	*DharmaconThermo Scientific, Schwerte, Germany*
siRNA Negative Control SR-CL000-005	*Eurogentec Cologne, Germany*
SPARC ON-TARGETplus SMARTpool L-003710-00	*DharmaconThermo Scientific, Schwerte, Germany*

2.1.6 Markers and enzymes

GeneRuler™ 100 bp DNA Ladder	*Fermentas, St. Leon-Rot, Germany*
GoTaq Polymerase	*Promega, Madison, USA*
Precision plus Protein™ Dual Color Standards	*Biorad, Munich, Germany*

2.1.7 Kits and assays

AP Polymer System	*Zytomed Systems, Berlin, Germany*
BCA assay	*Pierce, Rockford, IL, USA*
Cell proliferation ELISA, BrdU	*Roche, Mannheim, Germany*

(colorimetric)	
DAB Peroxidase Substrate Kit	*Vector Laboratories, Burlingame, CA, USA*
Dual-color QuickAmp Kit	*Agilent, Palo Alto, CA, USA*
iScript cDNA Synthesis Kit	*Biorad, Munich, Germany*
ImmPRESS Anti-Rabbit Ig Polymer Detection-Kit	*Vector Laboratories, Burlingame, CA, USA*
Mouse-on-mouse HRP-Polymer Kit	*Zytomed Systems, Berlin, Germany*
RNeasy®Mini Kit	*Qiagen, Hilden, Germany*
RNeasy®Micro Kit	*Qiagen, Hilden, Germany*
TGX FastCast Kit (12% gels)	*Biorad, Munich, Germany*
VECTOR VIP Peroxidase Substrate Kit	*Vector Laboratories, Burlingame, CA, USA*
VECTOR NovaRED Peroxidase Substrate Kit	*Vector Laboratories, Burlingame, CA, USA*
Warp Red Chromogen Kit	*Biocare Medical, Pacheco, CA, USA*

2.1.8 Antibodies

2.1.8.1 Primary antibodies

AKT (#9272S)	*Cell Signaling, Danvers, MA, USA*
β-Actin (A228)	*Sigma-Aldrich, Munich, Germany*
Cyclin D1 (#ab134175)	*Abcam, Cambridge, UK*
ERK1/2 (137F5, #4695S)	*Cell Signaling, Danvers, MA, USA*
HIF-1α (#10006421)	*Cayman Chemical, Ann Arbor, MI USA*
HIF-2α (#NB100-132)	*Novus Biologicals, Wiesbaden, Germany*
ILK (#3862)	*Cell Signaling, Danvers, MA, USA*
IgG	*Millipore, Schwalbach, Germany*

phospho-AKT (S473, #9271S)	*Cell Signaling, Danvers, MA, USA*
phospho-ERK1/2 (T202/Y204, #9101S)	*Cell Signaling, Danvers, MA, USA*
SPARC (D10F10, #8725s)	*Cell Signaling, Danvers, MA, USA*
Von-Willebrand-Factor (A0082)	*Dako, Hamburg, Germany*
α-smooth muscle actin (A2547)	*Sigma-Aldrich, Munich, Germany*

2.1.8.2 Secondary antibodies

Horseradish-peroxidase–labeled secondary antibodies Anti-mouse W4011 Anti-rabbit W4021	*Promega, Mannheim, Germany*

2.1.9 Computer programes

GraphPad Prism Version 7	*GraphPad Software, Inc., La Jolla, CA, USA*
Image Lab Version 4.1	*Biorad, Munich, Germany*
LabChart 7	*AD Instruments, Spechbach, Germany*
PowerLab data acquisition system (MPVS-Ultra Single Segment Foundation System)	*AD Instruments, Spechbach, Germany*
Qwin software	*Leica, Wetzlar, Germany*

2.1.10 Animals

C57Bl/6J	*Charles River Laboratories, Sulzfeld, Germany*
Secreted protein acidic and rich in cysteine knockout mice ($SPARC^{-/-}$)	*Jackson Laboratory, Bar Harbor, Maine, USA*

(JAX stock #003728)	
B6129SF2/J	*Jackson Laboratory, Bar Harbor, Maine, USA*

2.2 Methods

2.2.1 Experimental design

For microarray analysis, adult C57BL/6J mice were exposed to chronic hypoxia (10% O_2) in a ventilated chamber to induce pulmonary vascular remodeling as previously described[113]. Briefly, animals were age-matched and randomly distributed to groups that are either exposed to 21 days to normobaric normoxia [inspiratory O_2 fraction (FiO_2) 0.21] or normobaric hypoxia [FiO_2 of 0.10] with subsequent re-exposure to normoxia for 1, 3, 7 and 14 days.

For deciphering the role of SPARC in chronic hypoxia-induced PH, B6129SF2/J and $SPARC^{-/-}$ mice were obtained from Jackson Laboratory for breeding. Briefly, animals were age-matched and randomly distributed to groups that are either exposed to 28 days normoxia (21% O_2) or 28 days hypoxia (10% O_2).

All animal experiments were approved by the local authorities GI 20/10 22/2000, GI 20/10 77/2015 (Regierungspraesidium, Giessen, Germany).

2.2.2 Patient characteristics and measurements

Tissue samples from human explanted lungs were obtained from 11 donors (mean age 42 ± 31, 6 female, 5 male) and 14 IPAH patients (mean age 33 ± 28, 9 female, 5 male). Lung tissue was either snap-frozen in liquid nitrogen directly after explantation or placed in 4% m/v paraformaldehyde within 30 min. after lung explantation. The study protocol was approved by the Ethik-Komission des Fachbereichts Medizin (AZ 10/06) of the Justus-Liebig-University Giessen, Germany.

2.2.3 Genotyping

DNA isolation was performed from mouse tail cuts or ear marks. Per sample, 300 µl of 50 mM NaOH was added, following incubation in an HLC heating thermomixer (95°C, 800l/min, 15 min.). Afterwards, samples were vortexed for 10 sec. at 595g. After that, 50 µl 1 M Tris was added and samples were centrifuged for 5 min. at 16089g.

After the DNA isolation, PCR was performed using GoTaq polymerase. The following reaction conditions were used for PCR in the thermocycler T3000: 3 min. at 94°C, (30 sec. at 94°C, 1 min. at 65°C, 1 min. at 72°C) 35 times 30 sec. at 94°C, 5 min. at 72°C and stop at 10°C. The following master mix per sample was prepared and **Table 2** shows primer sequences used for genotyping.

Ampuwa®	3.80 µl
FlexiBuffer	3.00 µl
$MgCl_2$	1.20 µl
dNTPs	0.30 µl
Primer 1	1.50 µl
Primer 2	1.50 µl
Primer 3	1.50 µl
GoTaq-Polymerase	0.20 µl
DNA	2.00 µl
	15 µl

Table 2: Primer sequences for genotyping

Gene	Sequence
Primer 1	TTCTTCCTTGCAACCCTCTC
Primer 2	GGGGTTTGCTCGACATTG
Primer 3	TGTGGAGCTTCCTCTGTCCT

Following PCR, gel electrophoresis was performed to identify the genotype. An agarose gel (1.5%) was prepared as described below (**Table 3**), (**Table 4)**. The gel electrophoresis was performed at 400 Volt, 250 mA for 15 min. The gel was visualized using a ChemiDoc^{TM} XRS+ device. As shown in **Figure 5**, a double band referred heterozygous SPARC, lower single band referred homozygous SPARC$^{-/-}$ and the upper single band at the gel referred homozygous SPARC WT.

Table 3: Preparation of Agarose gel for Genotyping

Reagents	Amount
Agarose	0.75 g
1x SB Buffer	50 ml
SYBR® Safe Gel Stain	2 µl

Table 4: Preparation of SB Buffer for Genotyping

Reagents	Amount
1x SB Buffer	50 ml 20x SB Buffer 950 ml dH_2O
20x SB Buffer	8 g NaOH 42 g boric acid 1000 ml dH_2O

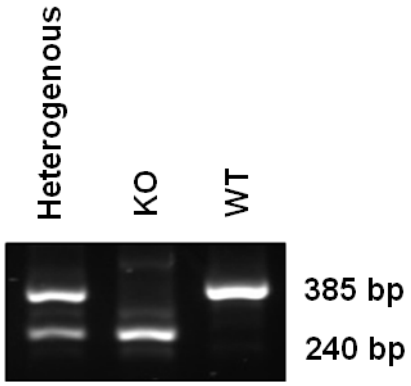

Figure 5: Gel electrophoresis for genotyping

Bands referring to heterozygous, KO and WT between the size of 240 to 385 bp.

2.2.4 Hemodynamic measurements

Hemodynamic measurements done by Karin Quanz. For hemodynamic measurements, normoxic/hypoxic wild-type/SPARC$^{-/-}$ mice were anesthetized with inhaled isoflurane in room air supplemented with 100% O_2. The mouse was placed supine on a homeothermic plate and after tracheotomy connected to a small animal ventilator MiniVent type. The body temperature was controlled by a rectal probe connected to the control unit and was kept at 37°C during the catheterization. The right external jugular vein was catheterized with a SPR-671NR micro-tip catheter and advanced into the right ventricle to assess the right ventricular systolic pressure (RVSP). Data were collected and analyzed using the PowerLab data acquisition system and LabChart 7 for Windows software. After exsanguination, the left lung was fixed for histological investigations in 3.5% neutral buffered formalin. The right lung was snap-frozen in liquid nitrogen for molecular biological investigations. For measuring the right heart hypertrophy, the right ventricle (RV) was separated from the left ventricle plus septum (LV+S) and the RV/(LV+S) ratio (fulton index) was determined.

2.2.5 Echocardiography

Echocardiography was done by Dr. Simone Kraut and performed as previously described[113]. In short, mice were anesthetized with isoflurane gas (3%) and maintained with 1.5% isoflurane in room air supplemented with 100% O_2. For monitoring heart rate (HR), mice were set in a flat position on a heating platform with all legs taped to ECG electrodes. A rectal thermometer was used to monitor the body temperature. After

shaving, a pre-warmed ultrasound gel was spread over the chest wall for providing a coupling medium for the transducer. A Vevo 2100 high-resolution imaging system equipped by a 55-MHz transducer (VisualSonics, Toronto, Canada) was used for transthoracic echocardiography. Cardiac output (CO) is the volume of blood being pumped by the heart, in particular by the left or right ventricle, per unit time[119]. CO was calculated as the product of the velocity-time integral of the pulsed-Doppler tracing in the LV outflow tract, the cross-sectional area of the LV outflow tract, and the heart rate[113]. Cardiac index (CI) relates heart performance to the size of the individual. CI was calculated by dividing CO by body weight. Following, B-mode derived right ventricular internal diameter (RVID) was measured. Right ventricular wall thickness (RVWT) was measured in AM-mode. AM-mode represents images in higher magnification than in the commonly used M-mode, allowing a more precise analysis.

2.2.6 Paraffin embedding, immunohistochemical staining and microscopy

Lungs were flushed with saline, using a vascular pressure of 22 cm H_2O and a tracheal pressure of 12 cm H_2O. A catheter from MiniVent type 848 into trachea and one saline catheter into pulmonary artery was inserted. Stroke volume of MiniVent was adjusted to 150-200 µl. Next, a catheter was put into pulmonary artery and afterwards, organs were harvested for molecular biological experiments. Finally, MiniVent pressure was decreased to <100 µl stroke volume and left lung was harvested and fixed by immersion in a 3.5% paraformaldehyde solution[113].

The left lungs were dissected in tissue blocks for paraffin embedding. Three µm sections of paraffin embedded lungs were used for the investigations. For assessing the degree of pulmonary vessel muscularization, lung sections were stained with antibodies against α-smooth muscle actin (α-sma) and von Willebrand factor (vWF) as described in the **Table 5**. As negative control, an isotype (IgG) control staining was performed.

Table 5: Protocol for double immunostaining against α-sma and vWF

Incubation time	Reagents	Comments
60 min.	by 58ºC	
10 min.	Xylol	
10 min.	Xylol	
10 min.	Xylol	

5 min.	Ethanol absolute 99.6%	
5 min.	Ethanol absolute 99.6%	
5 min.	Ethanol 96%	
5 min.	Ethanol 70%	
20 min.	H_2O_2- methanol mixture 3%	180 ml methanol + 20 ml H_2O_2 30%
2x5 min.	Aqua dest. (Millipore)	Shake
2x5 min.	1x-PBS	Shake
30 min.	Proteinase K	1,6 ml diluent + 1 drop of Proteinase K (40 x)
3x5 min.	1x-PBS	Shake
20 min.	10 % BSA	
3x5 min.	1x-PBS	Shake
30 min.	Rodent Block M (Mouse on Mouse HRP Polymer)	Zytomed Systems Blue
3x5 min.	1x-PBS	Shake
30 min.	Primary antibody (α-actin)	1:700 with antibody diluent 200 µl/slide
4x5 min.	1x-PBS	Shake
20 min.	Mouse on Mouse HRP Polymer	Zytomed systems yellow
3x5 min.	1x-PBS	Shake
1 to 4 min.	Vector Vip. Substrat Kit	5 ml PBS + 3 drops from Reagent 1 + 3 drops from Reagent 2 + 3 drops from Reagent 3 + 3 drops from H_2O_2
5 min.	H_2O	Shake
2x5 min.	1x-PBS	Shake
20 min.	10 % BSA	
3x5 min.	1x-PBS	Shake
20 min.	Serum Block 1	2.5 % Normal Horse Serum ImmPRESS kit Anti-Rabbit Ig Kit

30 min.	Primary antibody (37°C) (vWF)	1:1400 with antibody diluent 200 µl/slide
4x5 min.	1x-PBS	Shake
30 min.	Secondary antibody	ImmPRESS REAGENT Anti-Rabbit Ig Peroxidase Kit
4x5 min.	1x-PBS	Shake
1-40 sec.	DAB Substrate kit	5 ml aqua dest +2 drops from buffer pH 7.5 +4 drops from DAB Substrate +2 drops from H_2O_2
5 min.	H_2O	
1-3 min.	Methylgreen	on heating block (60°C)
1 min.	Aqua dest	
5 sec.	Ethanol 96 %	
5 sec.	Ethanol 96 %	
5 sec.	2-Propanol	
5 sec.	2-Propanol	
2 min.	Xylol	
2 min.	Xylol	
2 min.	Xylol	
	Cover the slide with Pertex	

After staining, the sections were analyzed with the help of a computer-aided analysis system. The macros used were developed by the company Leica. All sections were -counted blinded. Morphometric quantification was done with a microscope using the Qwin software. Firstly, vessels were marked, then the vessel volume was detected. After that, the vessel lumen was confirmed, the vessel wall area was marked and in the end, the muscularization of vessel was determined. Staining of α-sma, depicting the muscularized parts of the vessel wall, is in purple, whereas staining of vWF, depicting the endothelium of the vessels and thus the non-muscularized areas of the vessel wall, is in brown. The degree of muscularization was assessed from small (external diameter of 20 – 70 µm), medium (external diameter of >70 – 150 µm) and large (external diameter of >150 µm) pulmonary vessels from WT and $SPARC^{-/-}$ mice which are kept 28 days under normoxia (21% O_2) or hypoxia (10% O_2). Vessels were categorized as

fully- (>70% vessel circumference α-sma positive), partially- (5%-70% vessel circumference α-sma positive) or non-muscularized (<5% vessel circumference α-sma positive). The vessels were marked manually at a magnification of 400 times and their interior automatically detected by the computer to determine the degree of muscularization. 85 vessels of an outer diameter of 20-70 µm were analyzed from each lung lobe. The values measured automatically were transferred to Excel (Microsoft Corporation).

For assessing the localization of SPARC lung tissue of normoxic (N, 21% O_2, 28 days) or chronic hypoxic (H, 10% O_2, 28 days) mice was used. The protocol for detection of SPARC is given in **Table 6**. As negative control, an isotype (IgG) control staining was performed.

Table 6: Protocol for immunostaining against SPARC for mice

DAY 1		
Incubation time	Reagents	Comments
60 min.	by 58°C	
10 min.	Xylol	
10 min.	Xylol	
10 min.	Xylol	
5 min.	Ethanol absolute 99.6%	
5 min.	Ethanol absolute 99.6%	
5 min.	Ethanol 96%	
5 min.	Ethanol 70%	
2x5 min.	Aqua dest. (Millipore)	Shake
15 min. 20-25 min. 10 min. 30 min.	Waiting for boiling Cooking with T-EDTA Buffer, pH 9.0 Switch off the cooker Cooling in room room temperature	10x T-EDTA Buffer Per 1 cuvette: 90 ml Aqua dest.+10 ml T-EDTA Buffer
60 min.	10 % BSA	
4x5 min.	1x-PBS	Shake

30 min.	Rodent Block M (blocking solution) at room temperature	Zytomed System
4x5 min.	1x-PBS	Shake
overnight	Primary antibody (SPARC), +4°C	1:200 with antibody diluent 200µl/slide
DAY 2		
Incubation time	Reagents	Comments
6x20 min.	1x-PBS	Shake
30 min.	AP Polymer	AP Polymer kit
4x5 min.	PBS	Shake
1 to 4 min.	Warp Red Chromogen Kit	Add 1 drop of Warp Red Chromogen to 2.5 ml of Warp Red Buffer
5 min.	1x-PBS	Shake
1 min.	Aqua dest	Shake
2-3 sec.	Hematoxylin	Dilute hematoxylin with Aqua dest (1:10)
1 min.	Aqua dest	
1 min.	PBS	
5-10 min.	Tap water	
1 min.	Ethanol 96%	
1 min.	Ethanol 96%	
2 min.	2-Propanol	
2 min.	2-Propanol	
2 min.	Xylol	
2 min.	Xylol	
2 min.	Xylol	
	Cover the slide with Pertex	

2.2.7 Laser-microdissection

Cryo-sections (10 μm) of Tissue Tek-embedded lung tissue from C57BL/6J mice were mounted on PEN membrane slides. For visualization of cell nuclei, sections were stained with hemalaun for 45 sec., following immersion in water, 70% ethanol, 96% ethanol, and then stored in 100% ethanol until use. Intrapulmonary arteries with a diameter of 50–100 μm were selected and microdissected under optical control using the Laser Microdissection 6000. Microdissected material was collected in Eppendorf tubes filled with RNA lysis buffer with 1% β-mercaptoethanol and finally snap-frozen in liquid nitrogen until use.

2.2.8 Microarrays

Pulmonary vessels were laser-microdissected followed by RNA isolation and microarray analysis. Microarray was done by Dr. Friederike Weisel and Dr. Oleg Pak. In total vessels from 76 animals (23 controls – hypoxia, and 8-12 per time point) were analyzed by dual-color hybridizations in a balanced dye-swap design. RNA was isolated using the RNeasy Mini Kit following the kit's instructions. RNA quality was measured by capillary electrophoresis using the Bioanalyzer 2100. Purified total RNA was amplified and Cy-labeled using the dual-color QuickAmp Kit following the manufacturer's instructions. 1μg of total RNA was used per reaction. Cy3- and Cy5-labeled RNA were hybridized to 4x44K 60mer oligonucleotide spotted microarray slides (Mouse Whole Genome 4x44K, design ID 014868). Hybridization and subsequent washing and drying of the slides was performed following the Agilent hybridization protocol. The slides were scanned using a GenePix 4100A scanner. Images of Cy3 and Cy5 signals were analyzed using GenePix Pro 5.1 software, and calculated values for all spots were saved as GenePix results files. Stored data were evaluated using the R software[120] and the limma package[121] from BioConductor[122]. Log mean spot signals were taken for further analysis. Signals of replicate spots (same probes) within arrays were averaged. M/A data were LOESS normalized[123] before averaging over arrays. Genes were ranked for differential expression using a moderated t-statistic[124]. Pathway analyses were done using gene set tests on the ranks of the t-values[121].

2.2.9 cDNA synthesis and quantitative real-time PCR

Total RNA was isolated from human PASMC and from human and mouse lung homogenate by using the RNeasy Mini Kit according to the manufacturer's instructions. 200 ng / µl RNA was reverse-transcribed using the iScript cDNA Synthesis Kit according to manufacturer's instructions. The following reaction conditions were used for cDNA synthesis in the TPersonal thermocycler: 5 min. at 25°C, 20 min. at 46°C and 1 min. at 95°C and stop at 4°C.

Quantitative real-time polymerase chain reaction (q(RT)-PCR) was performed using the iQ SYBR Green Supermix according to the manufacturer's instructions.

iQ SYBR Green Supermix	5.0 µl
Ampuwa®	3.5 µl
Forward primer (10 pmol/µl)	
+	0.5 µl
Reverse primer (10 pmol/µl)	
cDNA (template)	1.0 µl
	10 µl

q-PCR was carried out in a CFX Connect™ Real-Time PCR Detection System under the following conditions: 1 cycle at 95°C for 10 min., then 40 cycles at 95°C for 10 sec., 59°C for 10 sec., 72°C for 10 sec., followed by a dissociation curve. Primers were designed by using Primer BLAST from NCBI and purchased from Metabion (Martinsried, Germany) **Table 7** shows the primer sequences for human and **Table 8** shows the primer sequences for mice. The Ct values were normalized to the endogenous control, porphobilinogen deaminase (PBGD) or beta-2-microglobulin (B2M), using the equation:

$$\Delta Ct = Ct_{reference} - Ct_{gene\ of\ interest}$$

Table 7: Primer sequences for human

Gene	Forward primer (5`→3`)	Reverse primer (5→ 3`)
PBGD	CCCACGCGAATCACTCT CAT	TGTCTGGTAACGGCAATGCG
SPARC	CCCTGTACACTGGCAGTT CG	ACATTGGGGGAAACACGAAG
Ki67	GCAAGCACTTTGGAGAG C	TCTTGACACACACATTGT
PCNA	CCTGTGCAAAAGACGGA GTG	TGAACTGGTTCATTCATCTCTAT GG
HIF-1α	TTACAGCAGCCAGACGA TCATG	TGGTCAGCTGTGGTAATCCACT
HIF-2α	CTGATGGCCATGAACAG CATCT	TCCTCGAAGTTCTGATTCCCGA
mTOR	TTAGAGGACAGCGGGGA AGG	AGGTCCGGTTCCAAGCATCT
Tenascin C	TCTGGTGCTGAACGAAC TGC	GTTTTCCAGAAGGGGCAGGG
ILK1	GGCTGGACAACACGGAG AAC	ATCTCAACCACAGCAGAGCG

Table 8: Primer sequences for mouse

Gene	Forward primer (5`→3`)	Reverse primer (5→ 3`)
B2M	AGCCCAAGACCGTCTAC TGG	TTCTTTCTGCGTGCATAAATTG
PBGD	GGTACAAGGCTTTCAGC ATCGC	ATGTCCGGTAACGGCGGC
SPARC	GGCCCGAGACTTTGAGA AGA	AATGTTCCATGGGGATGAGG
FSTL1	CGAGCACGATGTGGAAA CGA	CTCTGTGACGGCACATTCCC
SMOC1	CCGCATCCAACCTGCTGT C	CGGTCATGAACGGCGGAG

SMOC2	TGACAAGTCCATCACCG TGC	TCAGCATTTCCTCTGGGGGT
SPOCK1	CGTGGTGCTTCCTCCAAG TG	GGTTCCAGTACTTGTCACGGTC

PBGD: porphobilinogen deaminase, SPARC: secreted protein acidic and rich in cysteine, PCNA: proliferating-cell-nuclear-antigen, HIF-1α: hypoxia inducible factor 1 alpha HIF-2α: hypoxia inducible factor 2 alpha mTOR: the mammalian target of rapamycin, ILK: integrin linked kinase, B2M: beta-2-microglobulin FSTL1: follistatin like protein 1, SMOC1: secreted modular calcium binding protein 1, SMOC2: secreted modular calcium binding protein 2, SPOCK1: SPARC/osteonectin, CWCV, and kazal-like domains proteoglycans 1.

2.2.10 Cell culture

Primary human PASMC (hPASMC) were purchased from Lonza and maintained in Smooth Muscle Growth Medium 2, containing Smooth Muscle Supplement 2 mix. Cells were incubated at 37°C in a humidified atmosphere of 5% CO_2. Experiments were performed in between passage 3 to 8 using 10.000 cells/1cm^2.

Mouse PASMC (mPASMC) were isolated from pre-capillary pulmonary artery vessels from WT and SPARC$^{-/-}$ mice.

For cell isolation, mice were anesthetized and anticoagulated with a mixture of ketamine (100 mg/kg body weight), xylazine (20 mg/kg body weight) and heparin (1000 I.U/kg body weight). The lung preparation for cell isolation was performed with the help of the technical assistant Carmen Homberger and Dr. Monika Brosien. Tail and foot of the mice was pinched with forceps before starting to insure that the animal was fully anaesthetized. The skin was removed starting at the abdomen and the incision was vertically extended along the midline to the level of the mandible, exposing the trachea and a ligature was put around it. An incision was placed into the trachea which was subsequently cannulated with a tracheal tube or catheter. Following, the ligature was pulled tight. The abdomen was opened up and the diaphragm was removed from the thorax. Pericardium was removed carefully and the thorax was opened. Thymus was removed and an open ligature was placed around the aorta and the pulmonary artery. One incision was placed into the right ventricle and a catheter was inserted into the pulmonary artery. A second incision was placed in the left ventricle for drainage. Lungs were perfused with 3 ml Dulbecco's phosphate-buffered saline (DPBS). Afterwards, 15

mg agarose + 15 mg iron mixture was instilled. Following, 30 mg agarose was instilled into the trachea until the lung was completely filled. The catheter in the pulmonary artery was pulled out and the ligature was closed. Finally, the lung was transferred to ice cold (4°C) DPBS solution. The heart, trachea and coarse tissue residues were removed under the laminar flow hood and the five lung lobes were mechanically minced using the three-shaving technique. The iron-filled tissue pieces were washed several times in DPBS using a magnetic concentrator. Following, the tissue pieces were enzymatically digested in 37°C warm collagenase solution for 1 h. The tissue fragments were then mechanically sheared by 15 G and 18 G cannulas and separated from the iron-filled vessel pieces with the magnetic concentrator. M199 medium with 10% FBS and 1% Penicilin/Streptomycin was used to stop collagenase activity. The isolated vessel pieces were taken up in SMC medium with 10% FBS and 1% Penicilin/Streptomycin and seeded on cell culture dishes (seed 1, passage 0). Following 5 to 10 days, the vessel pieces were removed from the culture dish, washed in DPBS and transferred to a fresh culture dish in fresh SMC medium with 10% FBS and 1% Penicilin/Streptomycin (seed 2, passage 0). Those steps were also done for seed 3, passage 0. After 18 days of isolation, seeds 1 to 3 were detached by 1-fold trypsin, centrifuged at 338 g (1200 rpm) for 5 min. After cell counting in a Neubauer counting chamber, 5000 cells/1cm^2 cells were seeded on culture dishes for experiments (passage 1).

Hypoxia experiments were performed in a chamber equilibrated with a water-saturated gas mixture of 1% O_2, 5% CO_2 and 94% N_2 at 37°C. hPASMC and mPASMC were incubated in normoxic or hypoxia conditions for the indicated time points.

For growth factor stimulation experiments hPASMC were serum-starved overnight and stimulated with human TGF-β1 (2ng/ml), PDGF-BB (5ng/ml), VEGF (2ng/ml), or EGF (50ng/ml), for the indicated time-points.

The mTOR pathway was blocked using 0.5 μM rapamycin 20 h prior to TGF-β1 stimulation for 4 h. For AKT inhibition, cells were treated with 50 nM wortmannin 20 h prior to TGF-β1 stimulation for 4h. For ILK inhibition cells were treated with 1mM Cpd22 for 24 h. A solvent control was carried out for each experiment.

After experiment, cells were washed twice with ice cold PBS. Either, cells were harvested for protein or RNA isolation, using NP-40 respectively RLT buffer, or cells were used for proliferation assays.

2.2.11 siRNA transfection

Gene silencing was performed in hPASMC using siRNAs targeting SPARC, HIF-1α, HIF-2α, ILK and non-targeting control. hPASMC (90,000 cells/10cm^2) were transfected in serum-free medium with 100 nM small-interfering RNA (siRNA) diluted in Opti-MEM I medium, using Lipofectamine® 2000 reagent (0.5 µl/cm^2). The medium was replaced 8 h after transfection. Following siRNA transfection for the indicated time points, either RNA or proteins were isolated, or transfected cells were used for functional investigations.

2.2.12 Proliferation assay

Primary hPASMC were seeded on 6-well plates and transfected with control siRNA (siR) or siSPARC. 24, 48 or 72 h post siRNA transfection, proliferation was assessed by cell counting in a Neubauer counting chamber. Values were normalized to siR as depicted in the paragraph statistical analysis **2.2.15.**

mPASMC from WT and SPARC$^{-/-}$ mice were seeded on 24-well plates. 1 µL BrdU-labeling solution per 1 mL was added to the each well and incubated for 24 h. Proliferation was performed by using the Roche cell proliferation ELISA Kit, according to the manufacturer's instructions. Measurment was performed in a Tecan SPARK® multimode microplate reader at an absorbance of 370 nm for 20 min.

2.2.13 Western blot analysis

hPASMCs were scraped in 200 µl NP-40 buffer, containing 1 mM phenylmethylsulfonyl fluoride (PMSF). Human and mouse lung samples were grinded in 200 µl tissue lysis buffer containing 1mM PMSF using a homogenizer. After incubation on ice for 15 min., samples were centrifuged (10 min., 14000g, 4°C) and supernatant was transferred to a new tube. Protein concentrations were determined by a spectrophotometric assay (BCA assay). 20 µg/µl of protein extract was used for Western blotting. Samples were run on a 12% sodium dodecyl sulphate-polyacrylamide gel, following transfer to a polyvinylidene fluoride (PVDF) membrane. Membranes were blocked in blocking buffer. The following antibodies were applied over night at 4°C: SPARC, phospho-ERK1/2 (T202/Y204), ERK1/2, phospho-AKT (S473), AKT, ILK (all raised in rabbit and 1:1.000 diluted), rabbit cyclin D1 (1:10.000 diluted) and mouse β-actin (1:50.000 diluted). After washing 3 times for 10 minutes with PBS-T buffer, the

membrane was incubated for 1 h with horseradish-peroxidase–labeled secondary antibodies (1:5.000 diluted). Afterwards, the membranes were washed 3 x 15 min. with PBS-T buffer. Proteins were detected by Clarity™ Western ECL blotting substrate. Antigen-antibody complex was removed by incubating the membrane for 30 min. with stripping buffer prior to incubation with a new primary antibody. **Table 9** and **Table 10** shows the protocols for preparation of buffers used for Western blotting and immunohistochemistry.

Table 9: Preparation of buffers used for Western blotting

Buffer	Substance	Amount
NP-40 buffer (Protein-Isolation)	TRIS Base	20 mM;
		pH 7.6
	NaCl	150 mM
	EDTA	1 mM,
		pH 8.0
	EGTA	1 mM,
		pH 8.0
	NP-40	0.5% (v/v)
1x Elektrophoresis-Buffer	TRIS-Base	3.02 g
(Western blotting)	Glycin	18.8 g
	SDS	(10%); 10 ml
	H_2O	900 ml
1x Blotting-Buffer	Methanol	200 ml
(Western blotting)	TRIS-Base	2.42 g
	Glycin	11.2 g
	H_2O	700 ml
Stripping-Buffer	Glycin	1 M; 5 ml
(Western blotting)	H_2O	10 ml
	25 % HCl	0.750 ml

Table 10: Preparation of buffers used for Western blot and immunohistochemistry

Buffer	Substance	Amount
1x PBS; pH 7.4	NaCl	8 g
(Western blotting,	KCl	0.2 g
Immunohistochemistry)	Na_2HPO_4	1.44 g
	KH_2PO_4	0.24 g
	H_2O	1000 ml
PBS-T	1x-PBS	999 ml
(Western blotting)	Tween 20	1 ml
Blocking Buffer	Skimmed Milk powder	6 g
(Western blotting)	PBS-T	100 ml

12% Gel for Western blotting

TGX FastCast 12% gels were prepared in 1.5 mm Biorad glass plates for Western blotting as described in the **Table 11**.

Table 11: TGX FastCast protocol

Resolver solution for 1 gel				Resolver solution in total
Resolver A + Resolver B + 10% APS + TEMED				6 ml
3 ml	3 ml	30 µl	3 µl	
Stacker solution for 1 gel				Stacker solution in total
Stacker A + Stacker B + 10% APS + TEMED				2 ml
1 ml	1 ml	10 µl	2 µl	
Polymerization for 30 min.				

2.2.14 Promoter Analysis

Sense and antisense strands of the human SPARC promoter were screened upstream of the coding sequence of the SPARC gene (NM_002859) for potential hypoxia response elements (HRE:gcgtg). The SPARC promoter sequence was obtained online (http://www.ncbi.nlm.nih.gov/mapview).

2.2.15 Statistical analysis

The statistical evaluation of the cDNA microarrays was carried out by Dr. Jochen Wilhelm. Data were presented as mean ± SEM. Student's t-test was performed for comparing two groups. Differences between more than two groups were analyzed by one or two way ANOVA followed by Dunnett's, Bonferroni or Tukey`s multiple comparison post hoc tests. The evaluations were done by using GraphPad Prism 7 and Excel. The normalization was carried out according to the following formula: $(x_{i,\,treatment} - x_{i,\,control}) / (x_{i,\,control})$; where x_i is the measured value of the experiment i. A p value less than 0.05 was considered significant for all analyzes.

3. Results

Pulmonary hypertension (PH) is a severe and until now not curable disease[22]. In a previous study in mice, AMD-1 was identified as a novel key protein for the development and the reversal of PH. In this regard, it was shown that AMD-1 knockout mice possess less chronic hypoxia-induced PH than wild-type mice. Thus, targeting AMD-1 may represent a promising strategy for PH treatment.

Along these lines, the present work/thesis aims to identify further key candidates for pulmonary vascular remodeling and its reversal by using a microarray approach, possibly identifying additional treatment strategies for PH.

3.1 SPARC expression is attenuated in laser-microdissected pulmonary vessels following re-oxygenation of chronic hypoxic mice

To screen for candidate genes involved in reverse remodeling, C57BL/6J mice were either exposed to normoxia (21% O_2, 21 days, control group), hypoxia (10% O_2, 21 days, control group) or hypoxia (21 days) with a subsequent re-exposure to normoxia for 1, 3, 7, or 14 days (treatment group) **(Figure 6A)**. Pulmonary vessels of those mice were laser-microdissected. To decipher gene expression alterations, whole-genome DNA microarray analysis was performed, revealing secreted protein acidic and rich in cysteine (SPARC), a matricellular glycoprotein, as one gene consistently down-regulated in all re-oxygenation time-points investigated, compared to hypoxic controls **(Figure 6B and C)**. SPARC is also known as osteonectin or basement membrane protein-40 (BM-40)[125]. SPARC is suggested to be involved in in cell-matrix interactions during tissue remodeling and embryonic development[126]. Moreover, elevated SPARC levels correlate with cell proliferation, cancer metastasis[127] and the progression of bleomycin-induced pulmonary fibrosis[128].

As SPARC is suggested to be involved in hyper-proliferative diseases such as cancer and fibrosis, it is well conceivable that SPARC may play a major role in hypoxia-driven pulmonary vascular remodeling and its reversal. To confirm the down-regulation of SPARC following re-oxygenation, laser-microdissection of pulmonary vessels and q(RT)-PCR was performed from C57BL/6J mice, showing attenuated SPARC expression following 14 days of re-oxygenation **(Figure 6D)**. Moreover, there was no

difference in SPARC expression between the normoxic and hypoxic control group in the microarray as well as in the q(RT)-PCR analysis **(Figure 6B-D)**.

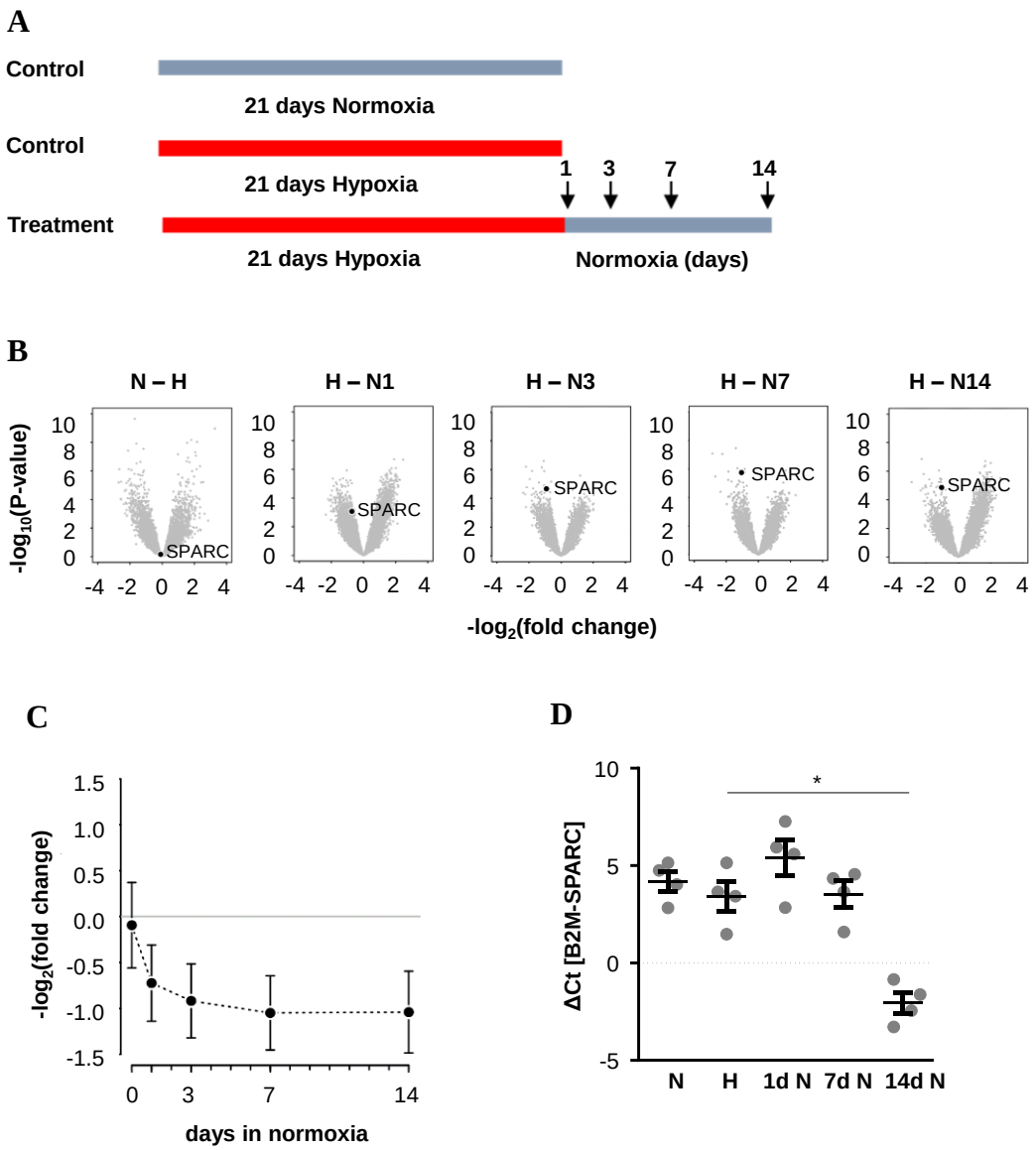

Figure 6: Down-regulation of secreted protein acidic and rich in cysteine (SPARC) in the pulmonary vasculature during the reversal of hypoxia-induced pulmonary hypertension (PH).

A. Schematic of the study design. Chronic hypoxic mice (H, 21 days, 10% O_2) were re-exposed to normoxia (N, 21 days, 21% O_2) for 1, 3, 7 and 14 days. B. Volcano plot: regulation versus statistical significance. Genes with log odds values ≥5 were considered to be regulated; black spot shows SPARC regulation in laser-microdissected pulmonary vessels isolated from mice after induction of PH (N-H) and reversal of PH (H-N1; H-N3, H-N7, H-N14). C. SPARC regulation in the pulmonary vasculature for the indicated time points of re-oxygenation. D. q(RT)-PCR depicting SPARC mRNA expression in the pulmonary vasculature during the reversal of PH. n=4 animals per time point. SPARC expression was normalized to B2M.

3.2 SPARC expression is elevated in the pulmonary vasculature of chronic hypoxic mice and idiopathic pulmonary arterial hypertension patients

Next, possibly altered SPARC expression in chronic hypoxic mice and in human idiopathic pulmonary arterial hypertension (IPAH) patients was assessed. Analysis of lung tissue samples from normoxic (21% O_2, 21 days) and chronic hypoxic (10% O_2, 21 days) mice showed no changes in SPARC mRNA expression. However, SPARC protein level was increased in chronic hypoxic mice (**Figure 7A and B**). Immunohistochemical staining showed predominant localization of SPARC in the pulmonary vessel wall (**Figure 7C**). Furthermore, hypoxia-induced SPARC expression seems to be specific for the pulmonary vasculature. In the systemic vasculature (Aorta) SPARC was not regulated (**Figure 7D**).

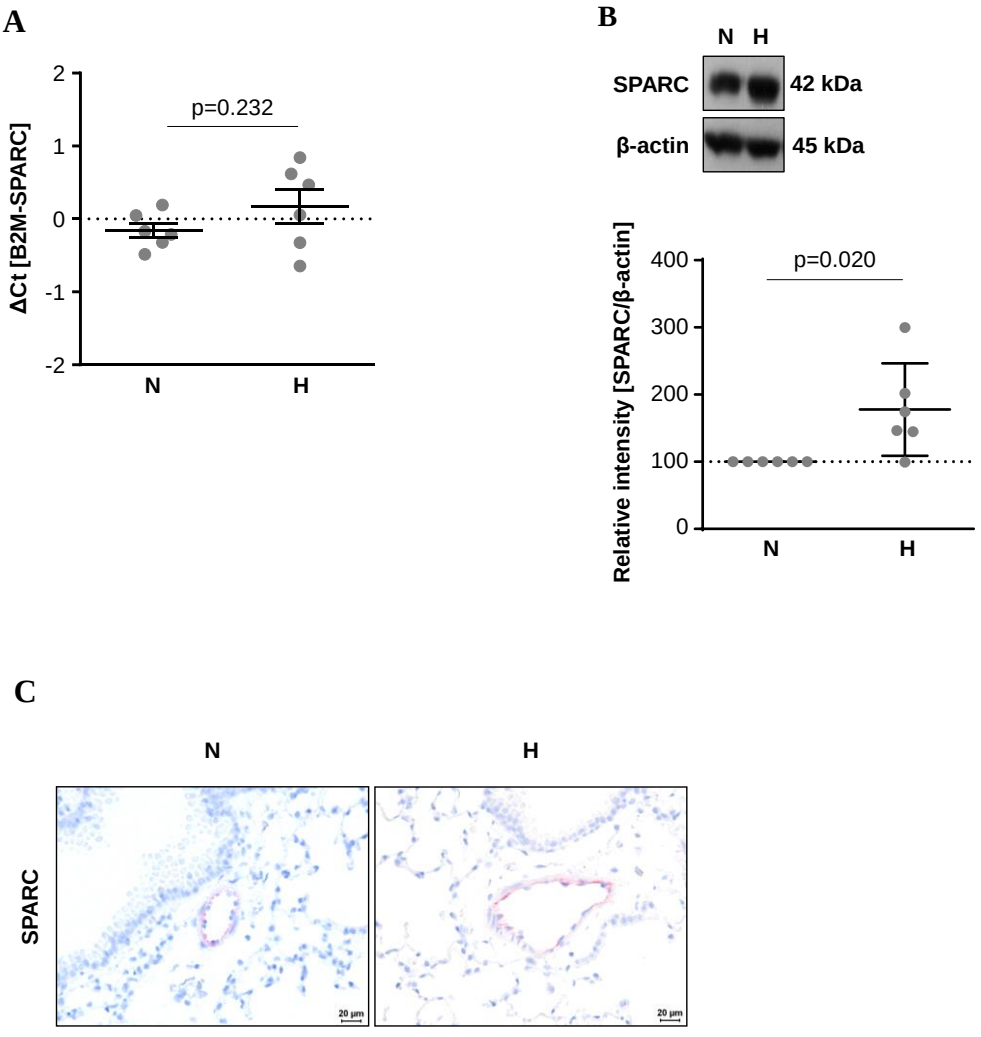

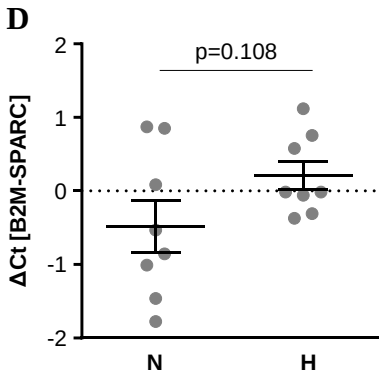

Figure 7: Elevated SPARC expression in the pulmonary vasculature of chronic hypoxic mice.

A. q(RT)-PCR depicting SPARC mRNA expression in lung homogenate from normoxic (N, 21% O_2, 28 days) or chronic hypoxic (H, 10% O_2, 28 days) mice. n=6 animals per time point. SPARC expression was normalized to B2M. B. Representative Western blot analysis and densitometry of SPARC expression in lung homogenate from normoxic or chronic hypoxic mice. n=6. C. Immunohistochemical staining of SPARC (in red) in normoxic and chronic hypoxic mouse lungs. D. q(RT)-PCR showing SPARC mRNA expression in isolated Aorta from normoxic and chronic hypoxic mice. n=8.

SPARC expression was elevated in an animal model of PH. Thus, next, its expression in human IPAH patients was assessed, demonstrating up-regulation of SPARC in lung homogenate from IPAH patients on both mRNA and protein level, compared to healthy donors (**Figure 8A** and **B**).

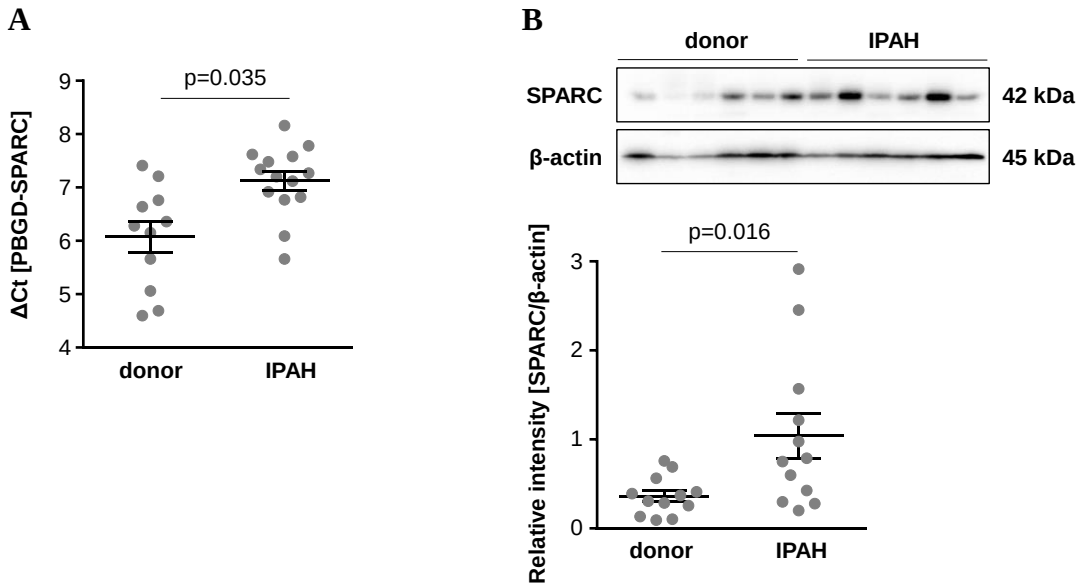

Figure 8: Elevated SPARC expression in the pulmonary vasculature of IPAH patients.

A. q(RT)-PCR depicting SPARC mRNA expression in lung homogenate from donor and idiopathic pulmonary arterial hypertension (IPAH) patients. n=11-14. SPARC expression was normalized to PBGD. B. Representative Western blot analysis and densitometry of SPARC expression in lung homogenate from donor and IPAH patients. n=12.

3.3 Hypoxia regulates SPARC expression via HIF-2α

Since abnormal proliferation of PASMC has a major role in pathogenesis of PH [72] and SPARC was localized in the medial layer, PASMC were used for *in vitro* studies. To unravel the molecular mechanisms regulating SPARC expression *in vitro*, primary hPASMC were exposed to normoxia (21% O_2), hypoxia (1% O_2) or hypoxia with a subsequent re-exposure to normoxia. SPARC mRNA expression was elevated following hypoxia and reversed following re-oxygenation (**Figure 9A**). SPARC protein level trended higher in hypoxic cells and was significantly down-regulated in re-oxygenated PASMC (**Figure 9B**).

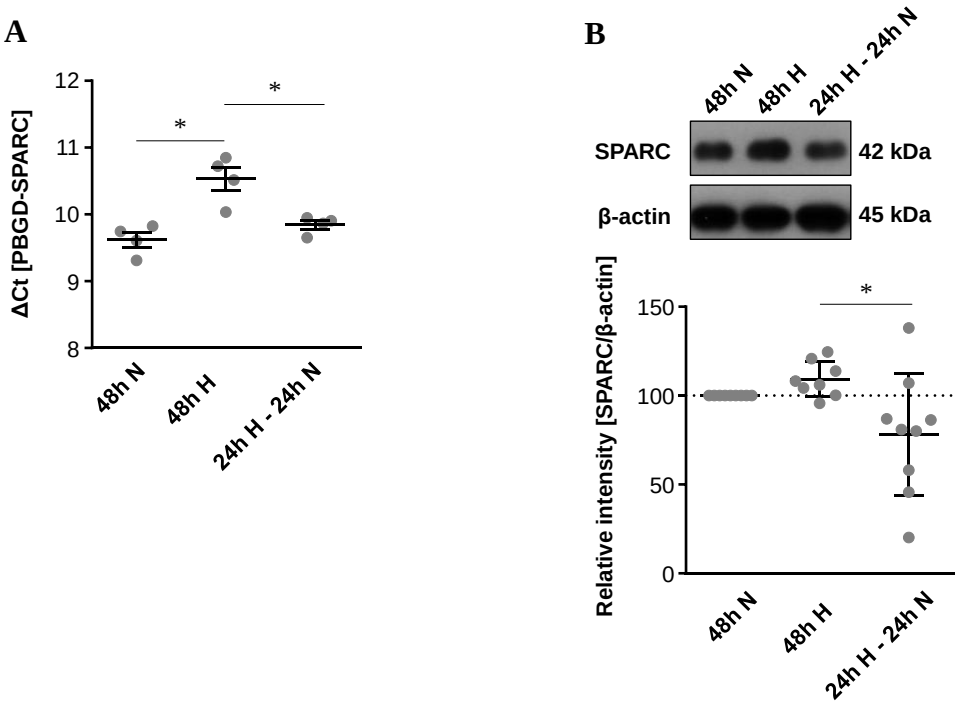

Figure 9: Hypoxia-dependent SPARC expression in primary hPASMC is reversed by re-oygenation.

A. q(RT)-PCR analyzing SPARC expression in primary hPASMC exposed to normoxia (48h H, 21% O_2), hypoxia (48h H, 1% O_2) or hypxia with subsequent re-exposure to normoxia (24h H - 24h N). n=4. SPARC expression was normalized to PBGD. B. Representative Western blot analysis and densitometry of SPARC expression in normoxic, hypoxic or hypoxic with subsequent re-oxygenated PASMC. n=8. Control (24h N) was set to 100%. *$p<0.05$ vs respective control.

Hypoxia triggers SPARC expression *in vivo* as well as *in vitro*, indicating that hypoxia-inducible factor (HIF), which is one of the main transcription factors regulating hypoxic effects[129], might be involved in regulating SPARC expression. For this purpose, HIF-1α and HIF-2α, respectively were silenced in hPASMC by specific siRNA transfection. Both, HIF-1α and HIF-2α knockdown led to significantly reduced HIF-1α and HIF-2α mRNA levels, respectively (**Figure 10A** and **C**). Moreover, following HIF-1α silencing SPARC mRNA expression was not altered. However, HIF-2α knockdown significantly impaired SPARC mRNA expression in hypoxic PASMC (**Figure 10B** and **D**). Promoter analysis revealed two potential hypoxia response elements (HRE) in the SPARC promoter region **(Figure 10E**), confirming our results.

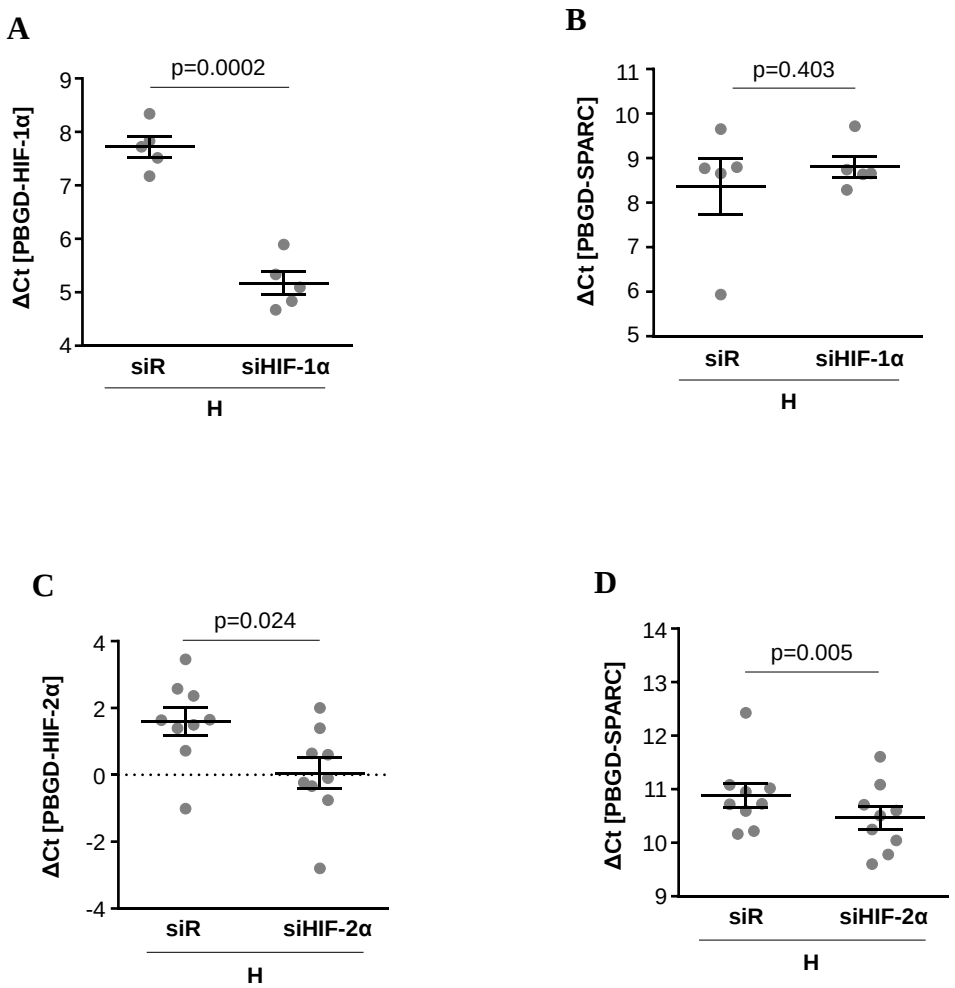

E

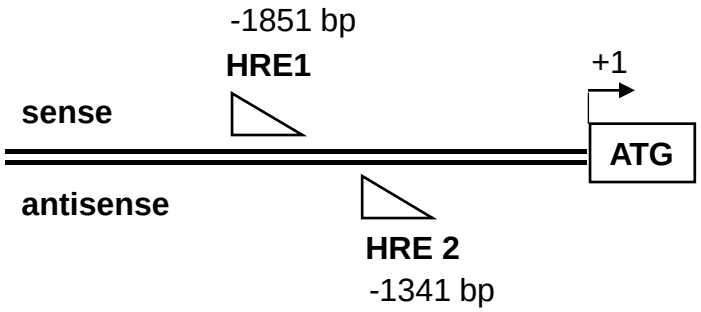

Figure 10: HIF-2α regulates SPARC expression in hypoxic primary hPASMC

A. q(RT)-PCR analyzing HIF-1α mRNA expression in hypoxic (H; 24h; 1% O_2) PASMC after siRNA transfection against HIF-1α (siHIF-1α) in comparison to control (siR). n=5. B. q(RT)-PCR depicting SPARC mRNA expression in hypoxic PASMC after siRNA transfection against HIF-1α in comparison to control. n=5. C. q(RT)-PCR showing HIF-2α mRNA expression in hypoxic PASMC after siRNA transfection against HIF-2α (siHIF-2α) in comparison to control. n=9. D. q(RT)-PCR analyzing SPARC mRNA expression in hypoxic (24h) PASMC after siRNA transfection against HIF-2α in comparison to control. n=9. E. SPARC promoter analysis. Potential hypoxia response elements (HRE) in the 2000bp promoter region are shown. The coding sequence of the SPARC gene is marked with +1.

3.4 TGF-β1-induced SPARC expression

To further identify factors regulating SPARC expression, primary hPASMC were stimulated with growth factors implicated in PH pathogenesis. Transforming growth factor-β1 (TGF-β1) induced a time-dependent increase in SPARC mRNA expression. A plateau was reached after 4 h of stimulation (**Figure 11A**). SPARC protein expression was elevated following 24 h of TGF-β1 stimulation (**Figure 11B**). Moreover, treatment of primary hPASMC with both, hypoxia and TGF-β1 induced no additive effect on SPARC mRNA expression (**Figure 11C**).

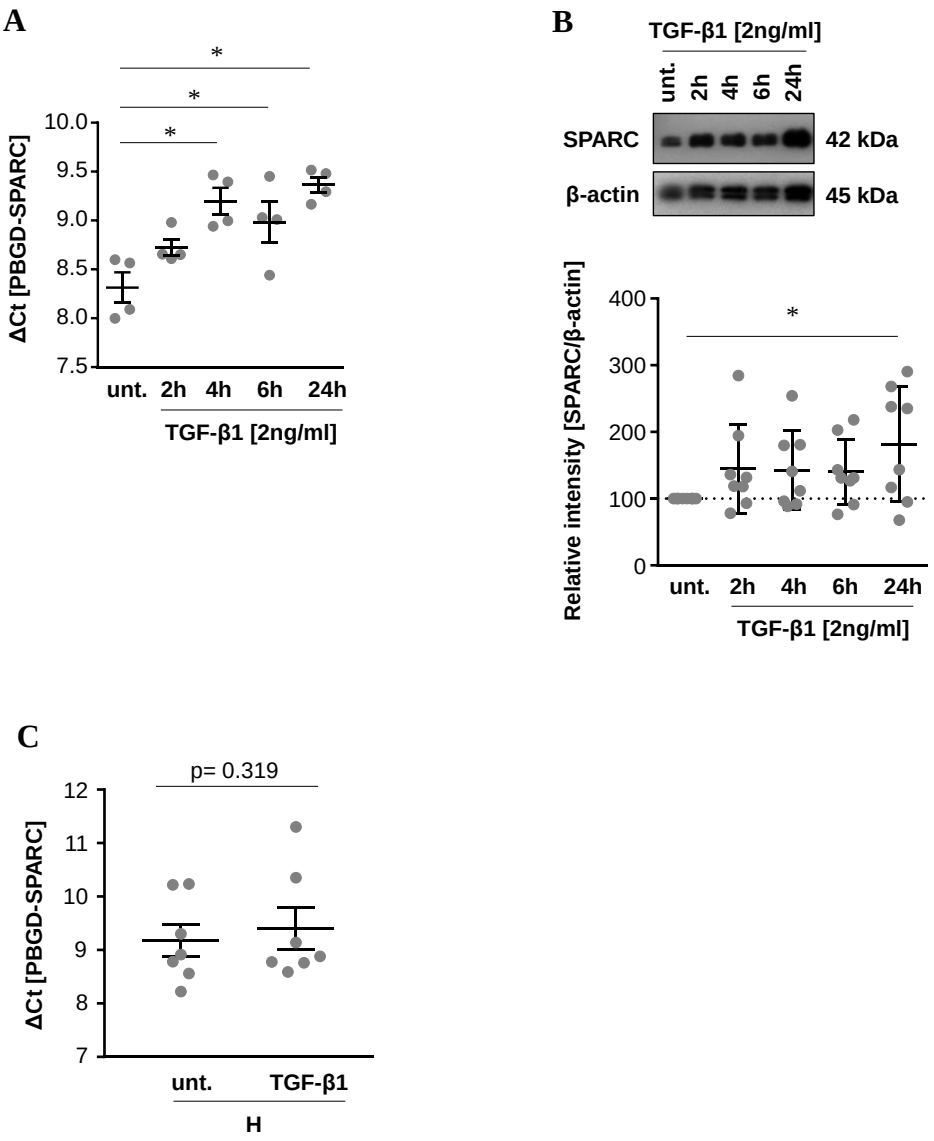

Figure 11: TGF- β1-induced SPARC expression in primary hPASMC

A. q(RT)-PCR analyzing SPARC mRNA expression in primary hPASMC stimulated with 2 ng/ml TGF-β1 for 2, 4, 6 and 24h in comparison to control (unt., solvent control). n=4. SPARC expression was normalized to PBGD. B. Representative Western blot analysis and densitometry of SPARC expression in TGF-β1 stimulated PASMC. n=8. Control (untreated) was set to 100%. C. q(RT)-PCR demonstrating SPARC mRNA expression in TGF-β1 (4h) stimulated normoxic or hypoxic (24h) PASMC. n=7. SPARC expression was normalized to PBGD. *p<0.05 vs respective control (untreated).

In addition, effect of PDGF-BB, EGF and VEGF stimulation was assessed on SPARC expression. However, none of those growth factors affected SPARC mRNA and protein expression (**Figure 12A-F).**

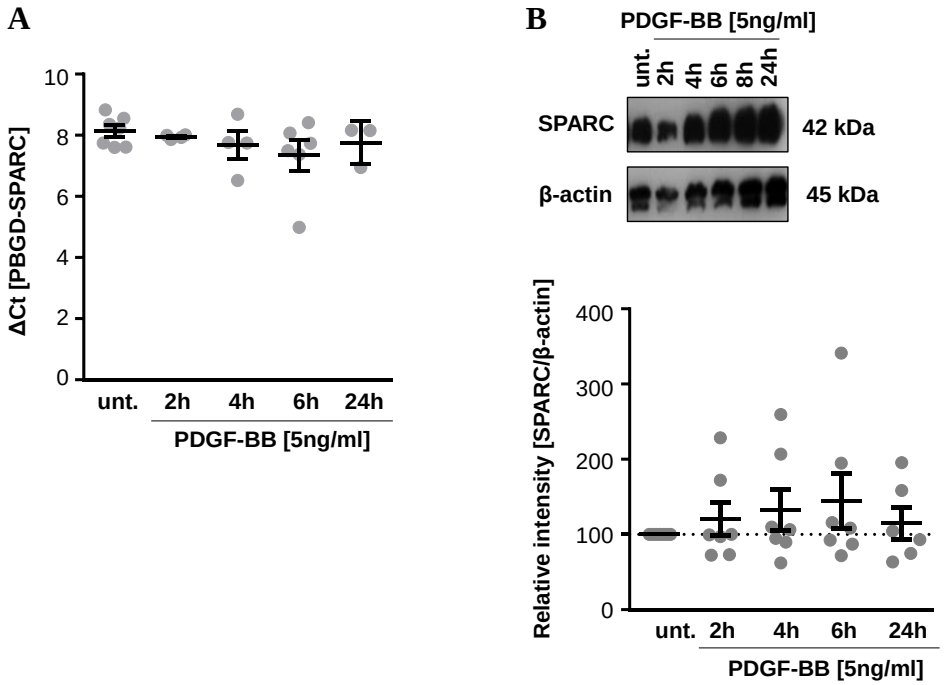

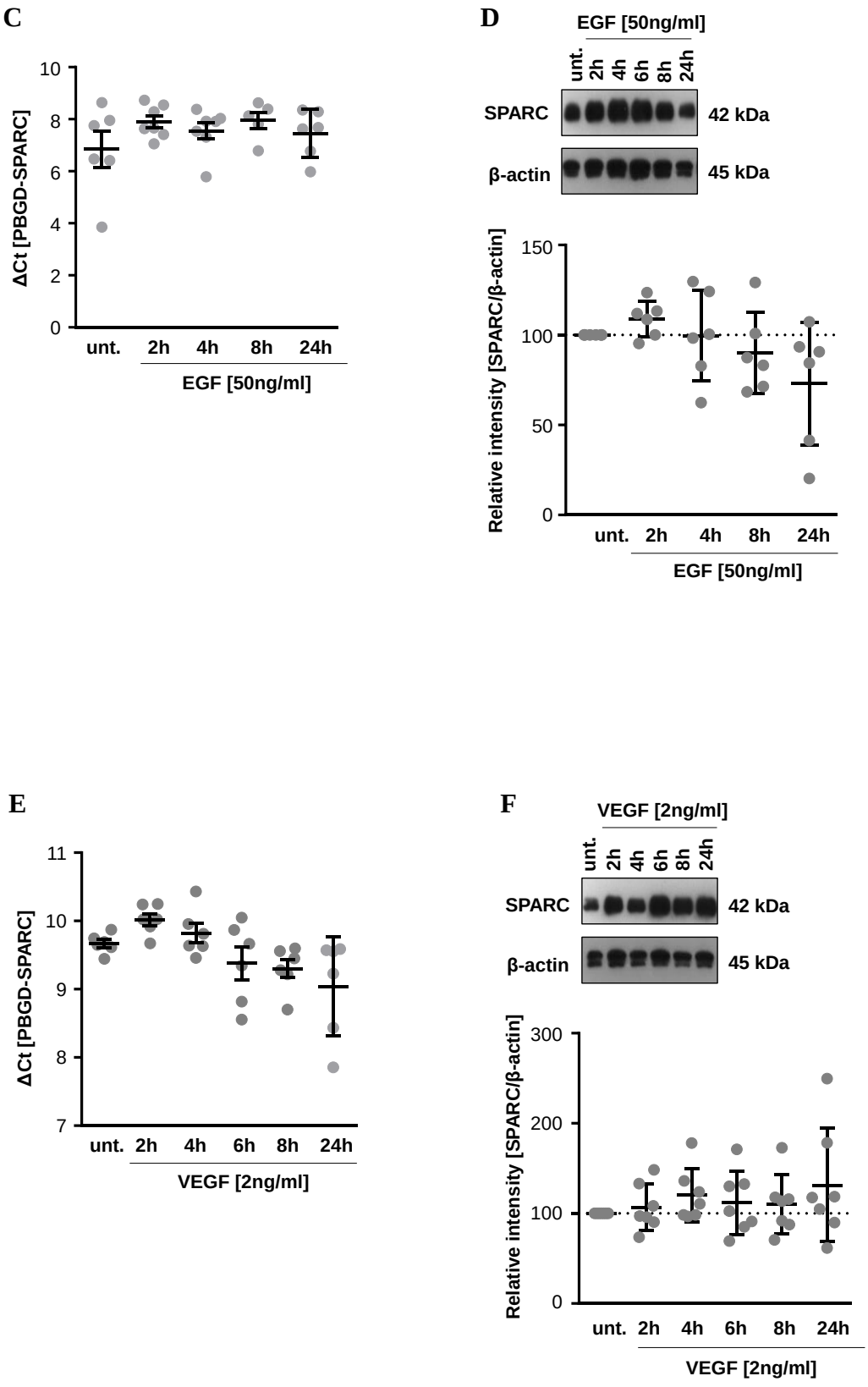
C
ΔCt [PBGD-SPARC]
10
8
6
4
2
0
unt.
2h
4h
8h
24h
EGF [50ng/ml]
D
EGF [50ng/ml]
unt.
2h
4h
6h
8h
24h
SPARC
42 kDa
β-actin
45 kDa
Relative intensity [SPARC/β-actin]
150
100
50
0
unt.
2h
4h
8h
24h
EGF [50ng/ml]
E
ΔCt [PBGD-SPARC]
11
10
9
8
7
unt.
2h
4h
6h
8h
24h
VEGF [2ng/ml]
F
VEGF [2ng/ml]
unt.
2h
4h
6h
8h
24h
SPARC
42 kDa
β-actin
45 kDa
Relative intensity [SPARC/β-actin]
300
200
100
0
unt.
2h
4h
6h
8h
24h
VEGF [2ng/ml]

Figure 12: SPARC expression expression is not regulated via PDGF-BB, EGF and VEGF

A. q(RT)-PCR analyzing SPARC mRNA expression in primary hPASMC stimulated with 5 ng/ml PDGF-BB (n=3-7) for the indicated time points in comparison to control (unt., solvent control). SPARC expression was normalized to PBGD. B. Representative Western blot analysis and densitometry of SPARC expression in PDGF-BB stimulated PASMC. n=7. Control was set to 100%. C. q(RT)-PCR depicting SPARC mRNA expression in primary hPASMC stimulated with 50 ng/ml EGF (n=5-6) for the indicated time points in comparison to control (solvent control). SPARC expression was normalized to PBGD. D. Representative Western blot analysis and densitometry of SPARC expression in EGF stimulated PASMC. n=6. Control was set to 100%. E. q(RT)-PCR showing SPARC mRNA expression in primary hPASMC stimulated with 2 ng/ml VEGF (n=6) for the indicated time points in comparison to control (solvent control). SPARC expression was normalized to PBGD. F. Representative Western blot analysis and densitometry of SPARC expression in VEGF stimulated PASMC. n=7. Control was set to 100%.

3.5 SPARC regulates PASMC proliferation *in vitro*

Since abnormal PASMC function significantly contributes to PH pathogenesis, next, the functional role of SPARC *in vitro* was assessed. In this regard, SPARC was silenced in primary hPASMC by specific siRNA transfection. 24, 48 and 72 h post transfection, SPARC was significantly downregulated on mRNA and protein level, compared to control (siR) (**Figure 13A** and **B**). Since SPARC knockdown was successful, role of SPARC in expression of pro-proliferative proteins was examined. Western blot and q(RT)-PCR depicted attenuated cyclin D1, PCNA and Ki67 levels following SPARC silencing (**Figure 13C - E**). Moreover, knockdown of SPARC significantly impaired PASMC proliferation, assessed by cell counting, 24 and 72 h post silencing (**Figure 13G**).

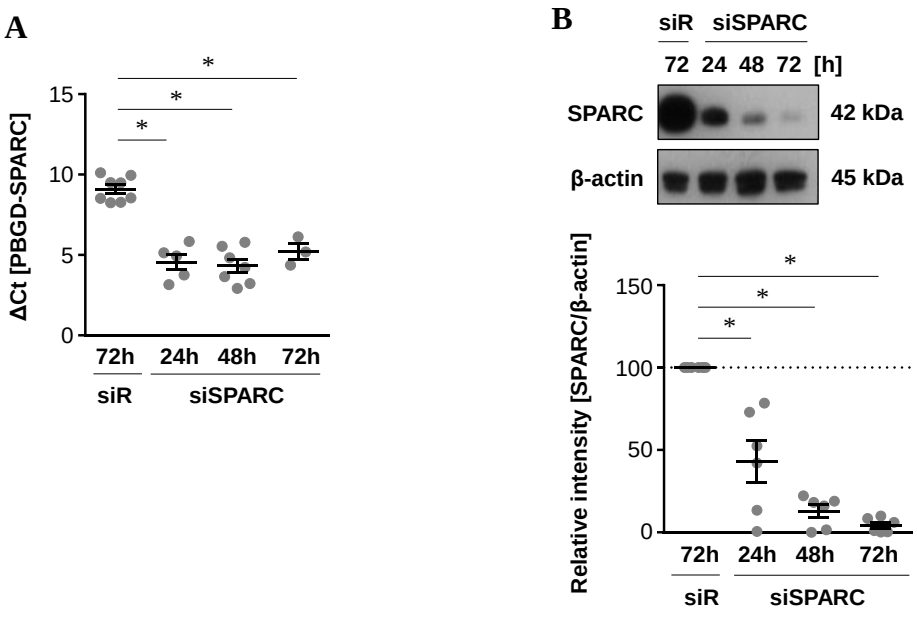

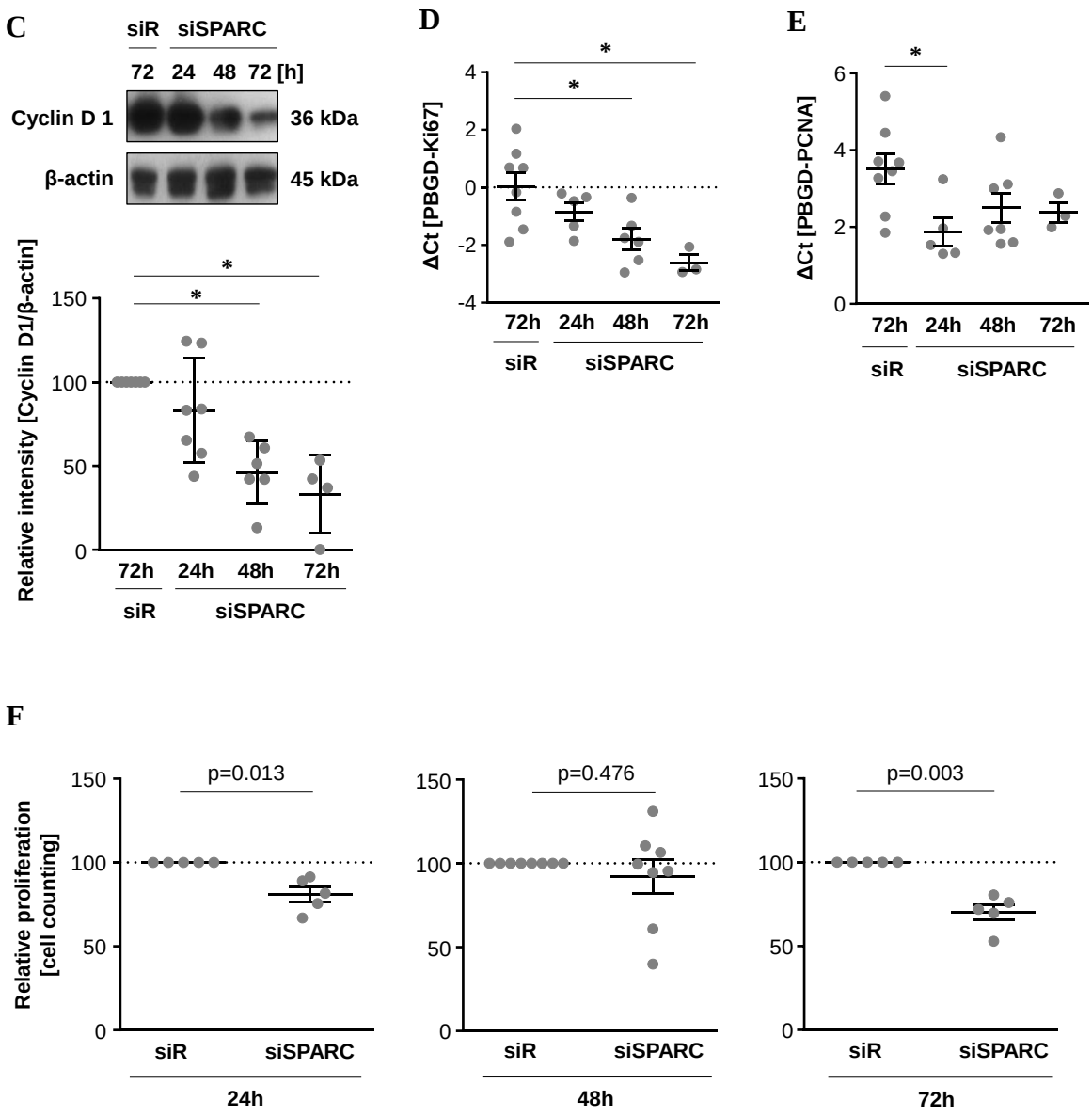

Figure 13: SPARC regulates PASMC proliferation

A. q(RT)-PCR analyzing SPARC mRNA expression in primary hPASMC after siRNA transfection against SPARC (siSPARC) for the indicated time points in comparison to control (siR). n=3-8. SPARC expression was normalized to PBGD. B. Representative Western blot analysis and densitometry after SPARC silencing. n=7. Control was set to 100%. C. Representative Western blot analysis and densitometry for cyclin D1 after SPARC silencing. n=4-7. Control was set to 100%. q(RT)-PCR depicting D. PCNA (n=3-8) and E. Ki67 (n=6-7) mRNA expression. F. Proliferation of primary hPASMC assessed by cell counting after knockdown of SPARC (siSPARC) for 24, 48 and 72 hours in comparison to control. n=5-8. Control was set to 100%. *p<0.05 vs respective control (siR).

3.6 SPARC affects PASMC proliferation via the PI3K/AKT/mTOR signaling pathway

Since SPARC affects PASMC proliferation, next, possible regulatory role of SPARC in pro-proliferative phosphatidylinositol 3-kinase (PI3K)-AKT and extracellular signal-regulated kinase (ERK1/2) signaling pathways was assessed. Western blot analysis showed less phosphorylation of AKT following SPARC silencing (**Figure 14A**), while ERK1/2 phosphorylation was not affected (**Figure 14B**), suggesting that SPARC regulates PASMC proliferation via the PI3K-AKT signaling pathway.

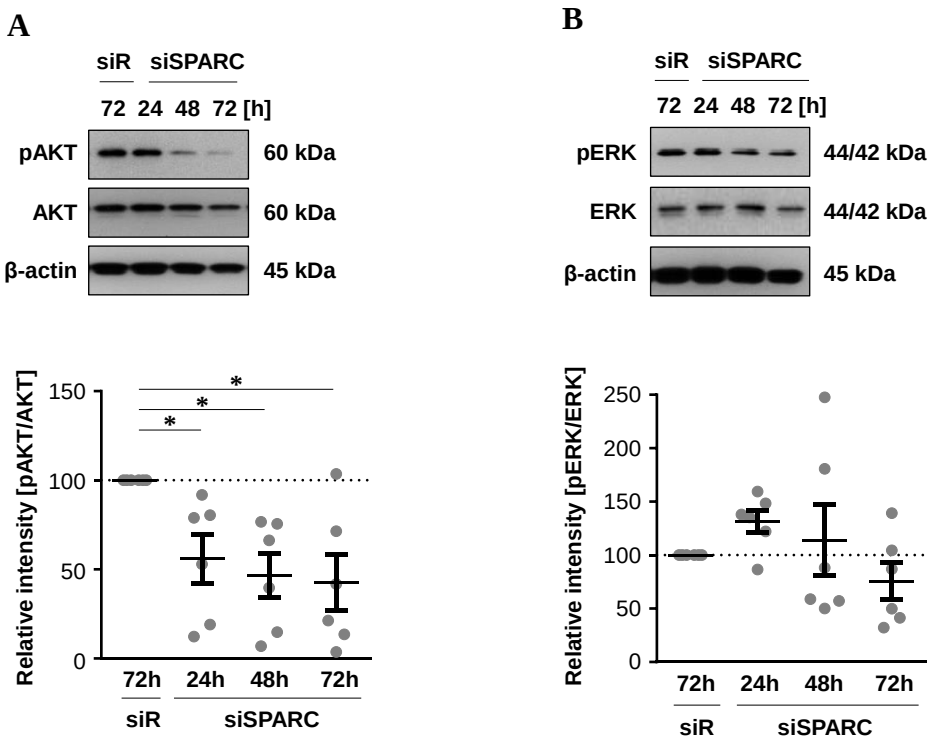

Figure 14: SPARC regulates PASMC proliferation via the PI3K/AKT signaling

A. Representative Western blot analysis and densitometry for AKT phosphorylation after SPARC silencing for the indicated time points. n=7. Control (siR) was set to 100%. B. Representative Western blot analysis and densitometry for ERK phosphorylation after SPARC silencing. n=6. Control was set to 100%. *p<0.05 vs respective control (siR).

Since SPARC silencing negatively affected AKT phosphorylation, next, AKT was inhibited by wortmannin. TGF-β-induced SPARC mRNA expression was reversed following wortmannin application (**Figure 15A**). To further characterize the downstream signaling of SPARC/AKT, we focused on mammalian target of rapamycin (mTOR). mTOR is a downstream effector of AKT signaling[130]. It is implicated in pathogenesis of PH and possesses a role in PASMC proliferation[131]. SPARC silencing attenuated mTOR mRNA expression (**Figure 15B**). However, blocking the mTOR pathway by rapamycin did not affect SPARC mRNA expression **(Figure 15C)**. Moreover, mTOR mRNA level was elevated in lung homogenate derived from IPAH patients compared to donor lungs (**Figure 15D**).

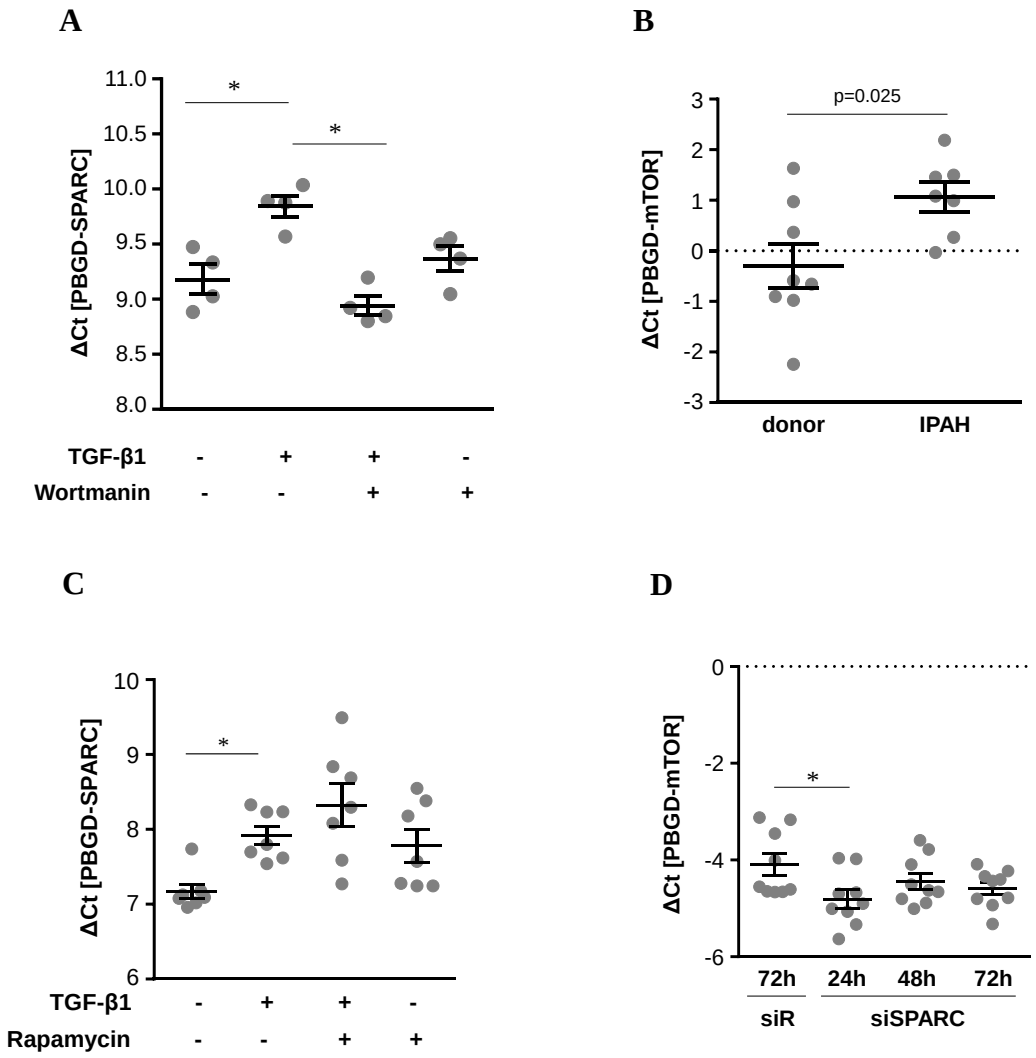

Figure 15: Role of mTOR in SPARC signaling pathway

A. q(RT)-PCR assessing SPARC mRNA expression in TGF-β1-stimulated (4h) primary hPASMC after AKT pathway inhibition by 50 nM wortmannin for 20 h. n=4. B. q(RT)-PCR assessing mTOR mRNA expression after siRNA transfection against SPARC (siSPARC) for the indicated time points in comparison to control (siR). n=9. C. q(RT)-PCR assessing SPARC mRNA expression after mTOR pathway inhibition with 0.5 µM rapamycin for 20h prior to TGF-β1 stimulation for 4 h. n=7. D. q(RT)-PCR depicting mTOR mRNA expression in lung homogenate from donor and idiopathic pulmonary arterial hypertension (IPAH) patients. n=7-8. mTOR expression was normalized to PBGD.*p<0.05 vs respective control (siR).

3.7 ILK is located upstream in the SPARC signaling pathway

Besides signaling pathways located downstream of SPARC, upstream signaling was of interest. It has been shown that integrin linked kinase (ILK) plays a role in PASMC proliferation in PAH[132]. Moreover, it was observed that SPARC binds to ILK in glioma migration, activating proliferation via the PI3K/AKT pathway[133]. To decipher the possible role of ILK in SPARC signaling in primary hPASMC, knockdown experiments were performed, revealing that SPARC silencing did not influence ILK mRNA and protein expression (**Figure 16A** and **B**). However, knockdown of ILK (**Figure 16C** and **D)** led to attenuated SPARC mRNA and protein expression (**Figure 16E** and **F**). In addition, ILK inhibition by Cpd 22 led to diminished SPARC mRNA expression (**Figure 16G)**. Moreover, ILK was more prominent expressed in IPAH patients compared to healthy donors (**Figure 16H**).

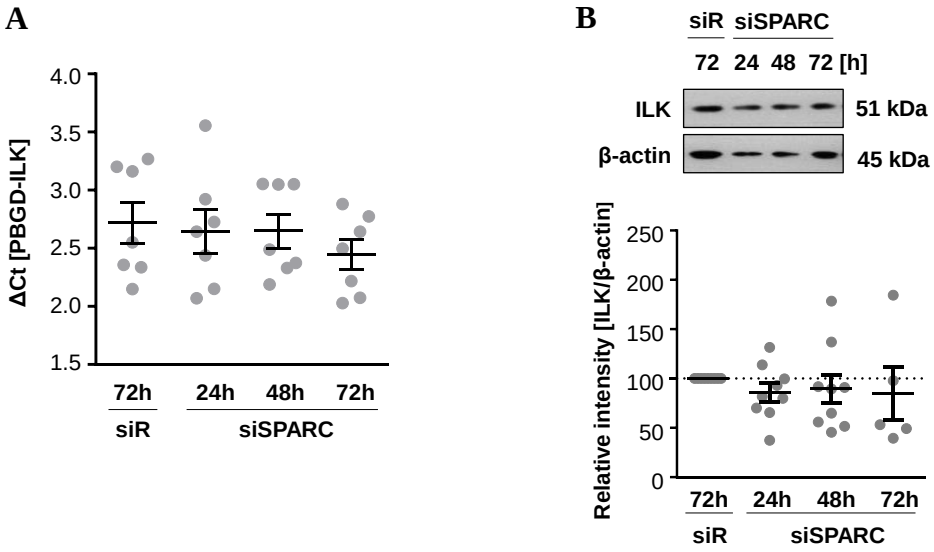

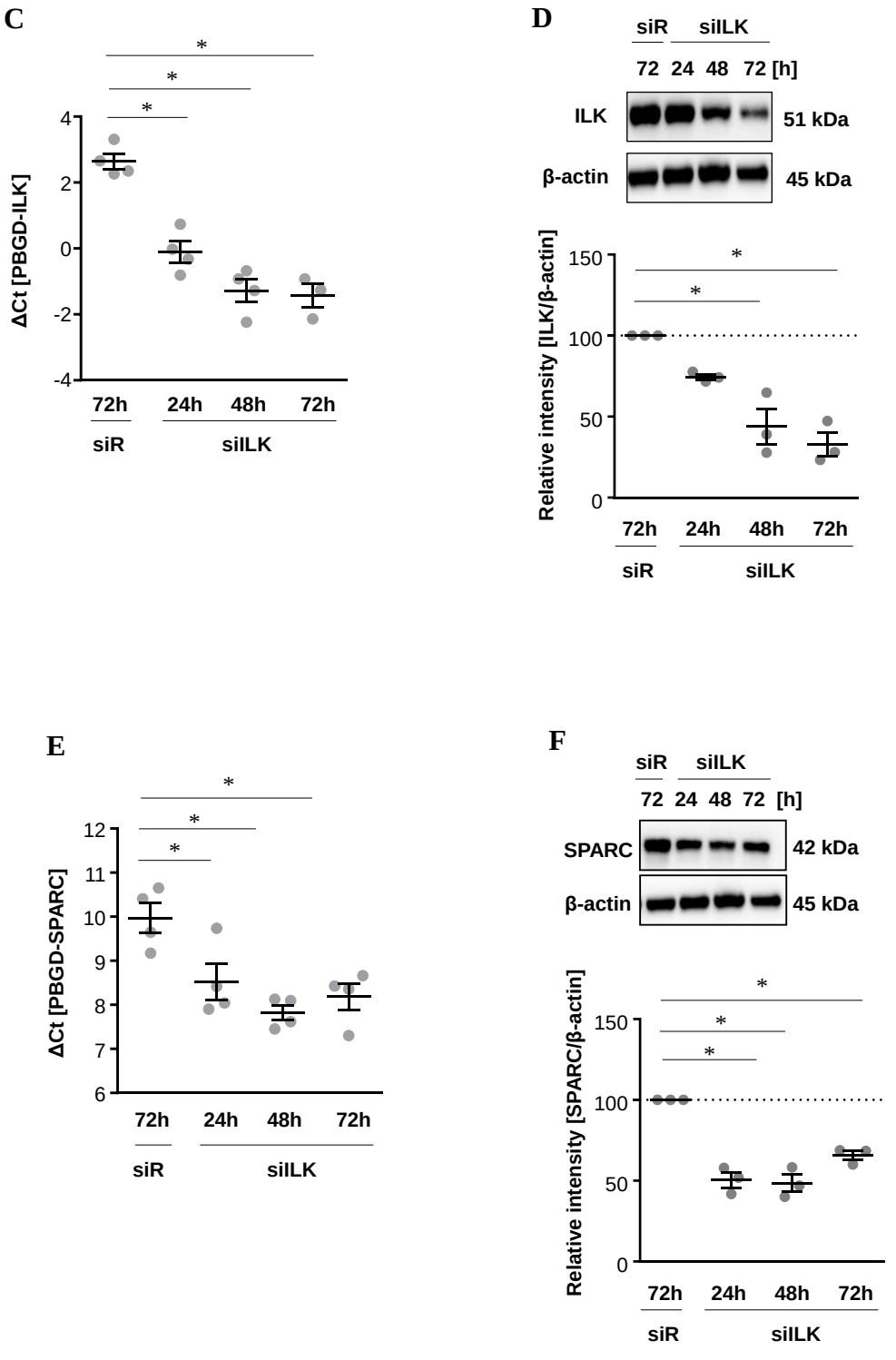
C
ΔCt [PBGD-ILK]
4
2
0
-2
-4
*
*
*
72h
24h
48h
72h
siR
siILK
D
siR
siILK
72 24 48 72 [h]
ILK
51 kDa
β-actin
45 kDa
Relative intensity [ILK/β-actin]
150
100
50
0
*
*
72h
24h
48h
72h
siR
siILK
E
ΔCt [PBGD-SPARC]
12
11
10
9
8
7
6
*
*
*
72h
24h
48h
72h
siR
siILK
F
siR
siILK
72 24 48 72 [h]
SPARC
42 kDa
β-actin
45 kDa
Relative intensity [SPARC/β-actin]
150
100
50
0
*
*
*
72h
24h
48h
72h
siR
siILK

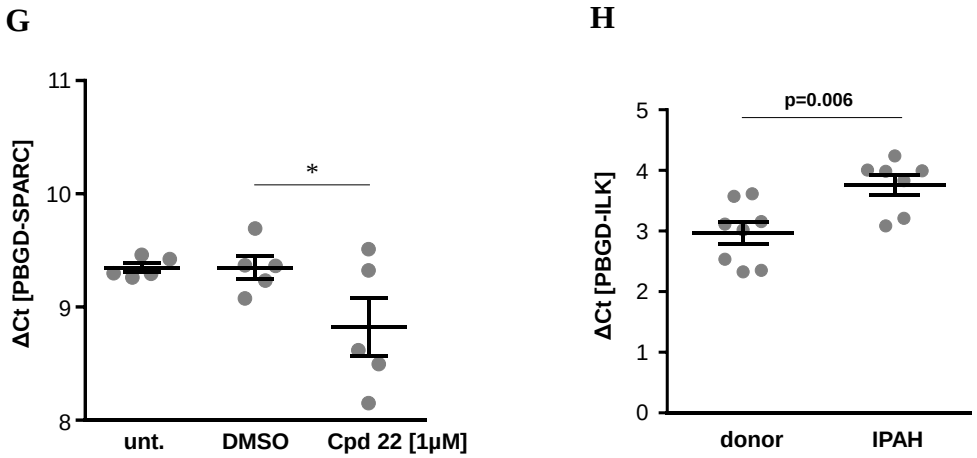

Figure 16: ILK is upstream of SPARC

A. q(RT)-PCR depicting ILK mRNA expression in primary hPASMC after siRNA transfection against SPARC (siSPARC) for the indicated time points in comparison to control (siR). n=7. ILK expression was normalized to PBGD. B. Representative Western blot analysis and densitometry for ILK after SPARC silencing for the indicated time points. n=3. Control (siR) was set to 100%. C. q(RT)-PCR showing ILK mRNA expression after siRNA transfection against ILK (siILK) in comparison to control. n=5. D. Representative Western blot analysis and densitometry for ILK after ILK silencing for the indicated time points. n=3. Control (siR) was set to 100%. E. q(RT)-PCR analyzing SPARC mRNA expression in after siRNA transfection against ILK for the indicated time points in comparison to control. n=4. SPARC expression was normalized to PBGD. F. Representative Western blot analysis and densitometry for SPARC after ILK silencing for the indicated time points. n=3. Control (siR) was set to 100%. G. q(RT)-PCR analyzing SPARC mRNA expression in PASMC after ILK inhibition by Cpd 22 (1 µm) for 24 h in comparison to control (DMSO). n=6. H. q(RT)-PCR analyzing ILK mRNA expression in lung homogenate from donor and idiopathic pulmonary arterial hypertension (IPAH) patients. n=7-8. ILK expression was normalized to PBGD. *p<0.05 vs respective control (siR).

3.8 No *in vivo* effect of SPARC deletion in chronic hypoxia-induced pulmonary hypertension in mice

In order to investigate the *in vivo* function of individual genes, knockout mice can be used. In this regard, homozygous SPARC knockout ($SPARC^{-/-}$) mice and their littermate controls (wild-type, WT) were used to assess the role of SPARC in chronic hypoxia-induced PH. The mice were either exposed to normoxia (21% O_2, 28 days) or chronic hypoxia (10% O_2, 28 days), followed by echocardiography and hemodynamic measurements to evaluate RV remodeling and function. An overview about the time schedule and the different groups is depicted in **(Figure 17A)**. Protein levels from the lung homogenate of WT and $SPARC^{-/-}$ mice showed absence of SPARC in the knockout mice **(Figure 17B)**. Chronic hypoxia did not cause any changes in right ventricular

internal diameter (RVID), cardiac output (CO) and cardiac index (CI), whereas right ventricular wall thickness (RVWT) (**Figure 17C-E**) was enhanced in WT mice. However, right heart catheterization revealed an increase in right ventricular systolic pressure (RVSP) in both WT and SPARC$^{-/-}$ mice. (**Figure 17F**). Moreover, right heart hypertrophy, depicted by the fulton index (RV/(LV+S)) was more pronounced in chronic hypoxic WT and SPARC$^{-/-}$ mice (**Figure 17G**). Left ventricular weight was not affected by genotype and experimental condition. In all parameters assessed, SPARC$^{-/-}$ mice did not differ from WT mice in their response to chronic hypoxia (**Figure 17C-G**).

A

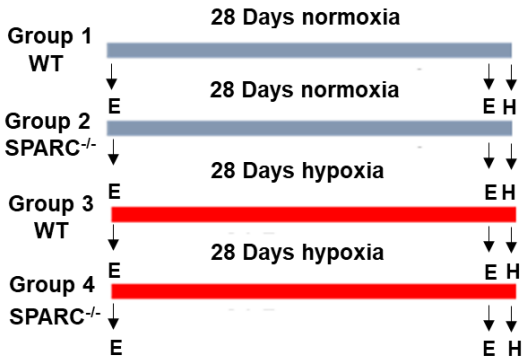

B

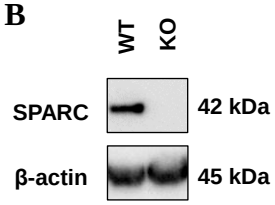

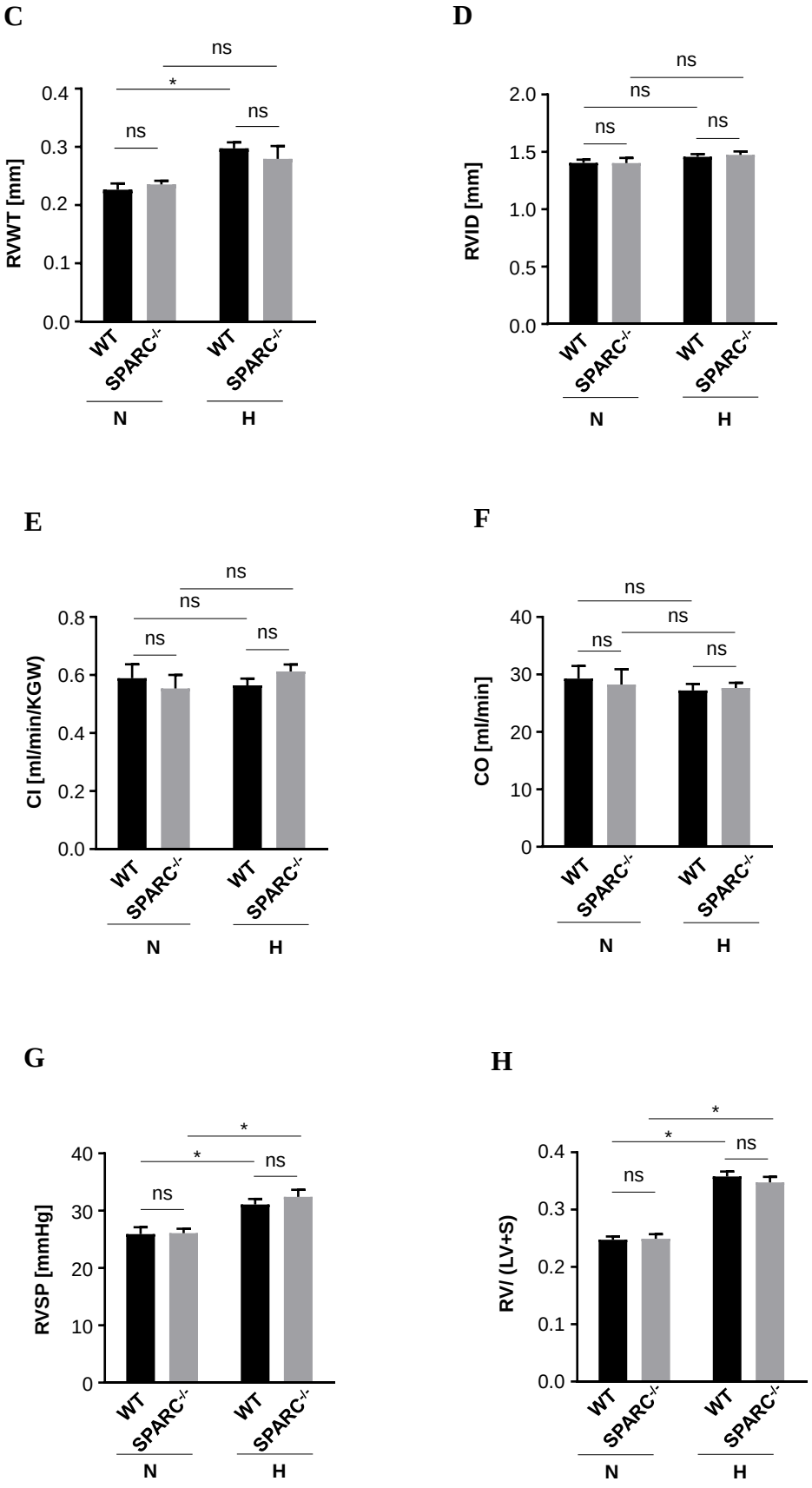
C
RVWT [mm]
0.4
0.3
0.2
0.1
0.0
ns
*
ns
ns
WT
SPARC-/-
WT
SPARC-/-
N
H
D
RVID [mm]
2.0
1.5
1.0
0.5
0.0
ns
ns
ns
ns
WT
SPARC-/-
WT
SPARC-/-
N
H
E
CI [ml/min/KGW)
0.8
0.6
0.4
0.2
0.0
ns
ns
ns
ns
WT
SPARC-/-
WT
SPARC-/-
N
H
F
CO [ml/min]
40
30
20
10
0
ns
ns
ns
ns
WT
SPARC-/-
WT
SPARC-/-
N
H
G
RVSP [mmHg]
40
30
20
10
0
*
*
ns
ns
WT
SPARC-/-
WT
SPARC-/-
N
H
H
RV/ (LV+S)
0.4
0.3
0.2
0.1
0.0
*
*
ns
ns
WT
SPARC-/-
WT
SPARC-/-
N
H

Figure 17: SPARC knockout does not influence echocardiographic and hemodynamic parameters in chronic hypoxic mice

A. Time table of the experimental design. Wild-type (WT) and SPARC$^{-/-}$ mice were kept under normoxic (N, 21% O_2) or chronic hypoxic (H, 10% O_2) conditions for 28 days. E=echocardiography, H=hemodynamic measurement. B. Representative Western blot analysis of SPARC protein expression in lung homogenate of wild-type (WT) and SPARC$^{-/-}$ mice. C. Right ventricular wall thickness (RVWT). n=13. D. Right ventricular internal diameter (RVID). n=8-13. E. Cardiac index (CI). n=13-14. F. Cardiac output (CO). n=13-15. G. Right ventricular systolic pressure (RVSP). n=12-14. H. Fulton index depicted by the mass of the right ventricle (RV) / (mass of the left ventricle (LV) + septum (S)). n=13-15. *p<0.05 vs respective control. ns=not significant different.

PH is characterized by pulmonary vascular remodeling. In this regard, influence of SPARC on muscularization was assessed, revealing that hypoxia significantly reduced the number of small non-muscularized pulmonary vessels in the WT group. Same trend was observed in SPARC$^{-/-}$ mice, however did not reach statistical significance (**Figure 18A**). Moreover, amount of full muscularized vessels trended to increase under hypoxia. Representative pictures for muscularization of small pulmonary vessels are shown in (**Figure 18B)**. In summary, SPARC$^{-/-}$does not affect muscularization of small pulmonary vessels.

A

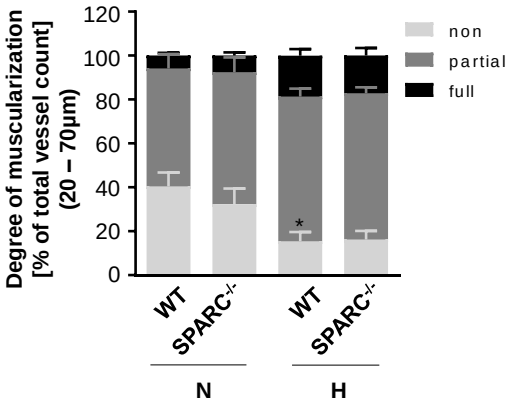

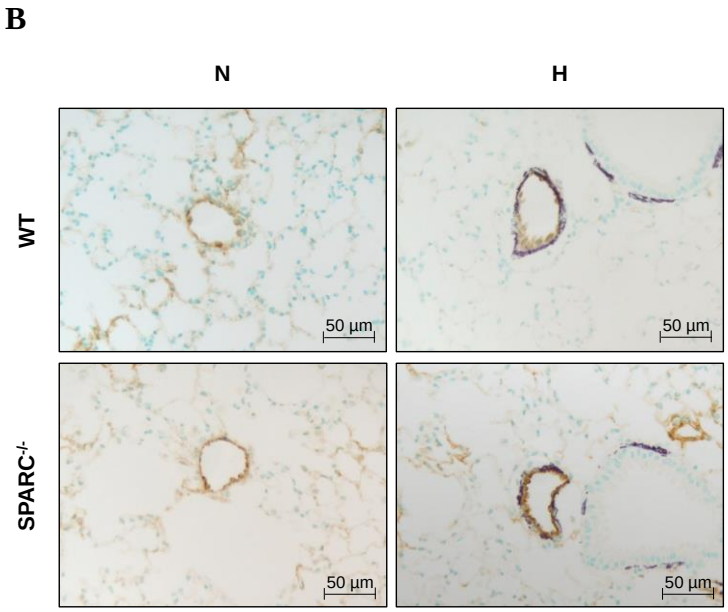

Figure 18: SPARC knockout does not affect pulmonary vascular remodeling

A. Degree of muscularization of small pulmonary vessels in chronic hypoxic (H, 10% O_2, 28 days) wild-type (WT) and SPARC$^{-/-}$ mice. Values are given for non-muscularized, partially muscularized, or fully muscularized vessels (outer diameter, 20–70 µm) from paraffin-embedded lung sections co-stained against α-smooth mucle actin (α-sma) and von Willebrand factor. n=14-15. B. Representative images of the degree of muscularization from one animal per group. *p<0.05 vs respective control (WT N).

3.9 Possible compensatory effect in SPARC$^{-/-}$ mice

SPARC$^{-/-}$ mice did not differ from WT mice in their response to chronic hypoxia. However, a prominent effect of SPARC on PASMC proliferation *in vitro* might point towards a possible compensatory mechanism *in vivo*, in SPARC$^{-/-}$mice. In this regard, expression level of SPARC family members in lung homogenate was assessed. Expression of follistatin-like protein 1 (FSTL1), secreted modular calcium binding protein 1 (SMOC1) and 2 (SMOC2) and SPARC (osteonectin), cwcv and kazal like domains proteoglycan 1 (SPOCK1) did not show any compensatory mechanism in hypoxic SPARC$^{-/-}$ lung homogenate (**Figure 19A-D**).

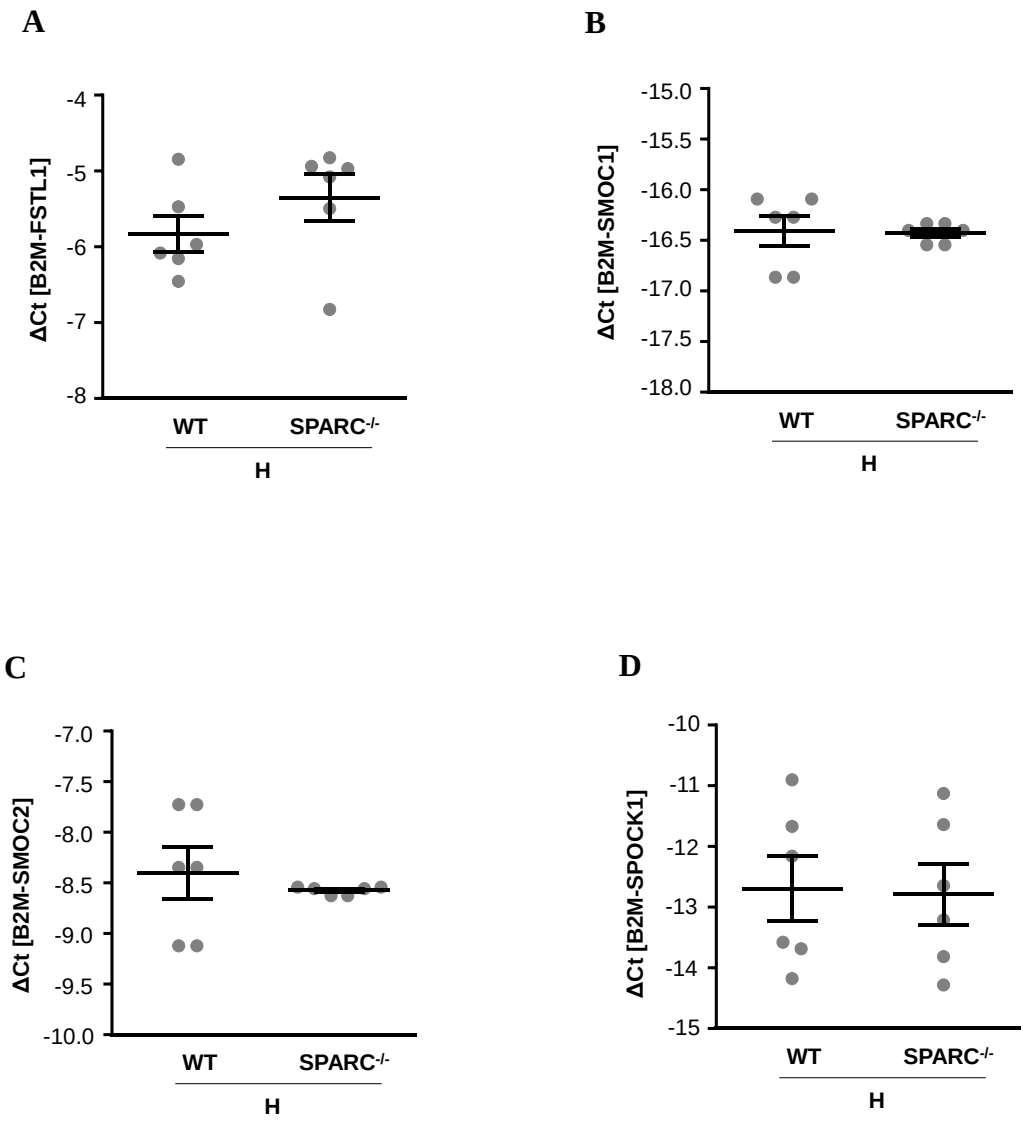

Figure 19: SPARC ablation does not influence expression of SPARC family members in lung homogenate derived from chronic hypoxic mice

q(RT)-PCR analyzing A. FSTL1, B. SMOC1, C. SMOC2 and D. SPOCK1 mRNA expression in lung homogenate from chronic hypoxic (H, 10% O_2, 28 days) wild-type (WT) and SPARC$^{-/-}$ mice. n=5-6. SPARC expression was normalized to B2M.

Since SPARC family member expression was not counter regulated in lung homogenate from hypoxic SPARC$^{-/-}$ mice, possible direct compensatory mechanism on PASMC function was assessed. In this regard, PASMC from SPARC$^{-/-}$ and their littermate controls were isolated and incubated for 24 h under hypoxic conditions. Interestingly, PASMC derived from SPARC$^{-/-}$ mice possessed a higher degree of proliferation than respective cells from WT animals **(Figure 20A)**. Moreover, the level of AKT phosphorylation was enhanced in SPARC$^{-/-}$ mice **(Figure 20B)**.

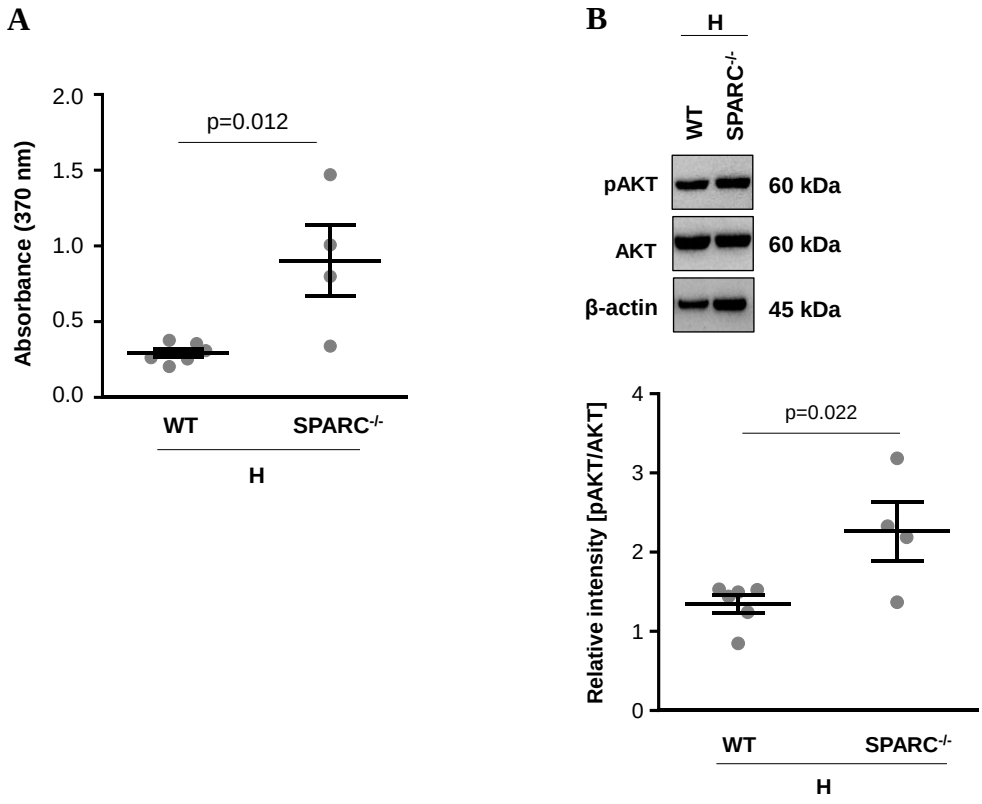

Figure 20: Elevated hypoxia-induced poliferation and AKT phosphorylation in PASMC isolated from SPARC$^{-/-}$ mice

A. Proliferation of WT and SPARC$^{-/-}$ mPASMC following 24 h hypoxic (1% O_2) treatment,assessed by thymidine analogue 5-bromo-2'-deoxyuridine (BrdU) incorporation. The assay was performed in passage 1. n = 4-6. B. Representative Western blot analysis and densitometry for AKT phosphorylation in mPASMC isolated from WT and SPARC$^{-/-}$ mice and incubated for 24 h under hypoxic conditions. n=4-6.

4. Discussion

In general, the major findings of the present thesis are:

1. Laser-microdissection followed by the microarray technique is a powerful tool to identify novel genes regulated in the pathogenesis of PH. In this regard, secreted protein acidic and rich in cysteine (SPARC) was identified as one gene down-regulated in murine vessels following re-oxygenation of chronic hypoxic mice.
2. Up-regulation of SPARC was observed in chronic hypoxic mice as well as in human idiopathic pulmonary arterial hypertension patients.
3. Immunohistochemical staining predominantly localized SPARC to the pulmonary vasculature.
4. Hypoxia-dependent SPARC regulation was confirmed in primary hPASMC.
5. Molecular analysis revealed HIF-2α-dependent SPARC expression under hypoxia.
6. Next to hypoxia, TGF-β1 up-regulated SPARC expression. However, PDGF-BB, EGF, and VEGF stimulation did not affect SPARC expression.
7. Functional importance of SPARC in PASMC proliferation was shown *in vitro*, following SPARC silencing.
8. Regulation of PASMC proliferation occurred via the PI3K/AKT/mTOR pathway.
9. Integrin linked kinase was identified upstream of the SPARC signaling pathway.
10. However, in an *in vivo* approach $SPARC^{-/-}$ mice were not protected from hypoxia-induced PH.
11. As a compensatory mechanism, an increased AKT phosphorylation and PASMC proliferation was observed in $SPARC^{-/-}$ mice under hypoxic conditions.

We suggest SPARC as a novel protein associated with PH and PASMC function.

4.1 Selection of the animal model

In the present thesis, the mouse model of chronic hypoxia-induced PH was used, representing group three (PH secondary to lung disease and/or hypoxia) in the 6th World Symposium classification[30, 33, 134]. In mice, chronic hypoxic exposure (10% O_2) leads to muscularization of small, normally nonmuscular arteries, elevated pulmonary arterial pressure and structural remodeling of the pulmonary vessels, resulting in an increase in pulmonary vascular resistance and right heart hypertrophy[30]. Moreover, the chronic hypoxic mouse model is highly predictable and highly reproducible within a selected strain. However, the three critical points of human PH, obliteration of pulmonary arterioles, non-reversibility and development of the right ventricle failure[108] are not represented in this model. In this regard, there is only a slight increase in pulmonary arterial pressure following chronic hypoxia[135]. Thus, the model of chronic hypoxia-induced PH in mice is a widely used model to investigate milder forms of human PH such as PH associated with residence at high altitude[85]. Further one, chronic hypoxia-induced PH in mice is reversible when the stimulus stops[113, 118] even without therapeutic intervention. As the aim of the present thesis was to screen for novel candidate genes involved in pulmonary vascular remodeling and its reversal following re-oxygenation, the chronic hypoxic mouse model was the ideal/best available model. Availability of SPARC knockout mice additionally indicated for this model.

However, as the chronic hypoxic PH model in mice is a model for less severe forms of PH, in further experiments, it might be recommendable to confirm elevated SPARC levels in PH in other more severe models. In this regard, the MCT-induced PH model is a well characterized and often used model. MCT is a toxic pyrrolizidine alkaloid agent present in the plant *Crotalaria spectabilis*[110]. It is mostly used in rats, while mice are not able to metabolize MCT to its active metabolite dehydromonocrotaline. Metabolization requires a CYP3A isoenzyme, which is lacking in the mouse liver[108]. A single MCT injection in rats induces endothelial damage, vascular inflammation and edema formation, followed by an increase in pulmonary vascular resistance. Finally vascular remodeling, including media hypertrophy, right heart hypertrophy and even right heart failure occurs[82, 108, 109]. However, the response to MCT is variable among species, strains and even animals. The different pathophysiology in this model makes it an attractive and interesting second model for studying SPARC dysregulation in PH.

4.2 Identification of a candidate gene for reverse remodeling

In a previous study, Weisel et al., screened for potential candidates genes contributing to reverse remodeling by using the DNA microarray technique[113]. In this regard, mice were exposed to normoxia, chronic hypoxia or chronic hypoxia with subsequent re-exposure to normoxia for different time points, followed by microarray analysis from lung homogenate. S-adenosylmethionine decarboxylase 1 (AMD-1) was identified as a novel candidate gene for pulmonary vascular remodeling processes. AMD-1 was elevated expressed in chronic hypoxic mice and down-regulated following re-oxygenation of mice. Furthermore, AMD-1 was critically involved in dysregulated PASMC proliferation and apoptosis. In addition, AMD-1 knockout mice possessed less chronic hypoxia-induced PH than respective controls[113].

Going beyond this approach, the present thesis focused on the gene expression alterations in the lung vasculature by using the laser-microdisection/microarray-technique. Laser microdissection of pulmonary vessels will possibly enhance the chance to detect additional relevant new genes/pathways for vascular remodeling which predominantly takes place in small pulmonary arteries[72]. Using the laser microdissection technique allows the isolation and thus the expression analysis of a specific compartment[136, 137]. In contrast, using lung homogenate for microarray analysis will display expression alterations of a complete organ[137]. In this regard, possible gene expression changes occurring specifically in the vascular compartment might be not detectable[137].

The microarray technique is used for large scale screening and expression studies[138]. In this regard, it allows the simultaneous characterization of gene expression alterations of thousands of genes and thus signaling pathways in healthy and disease state[113, 139]. Moreover, the microarray technique can be used for identification of prognostic markers for certain diseases[139]. Thus, while microarrays are useful in a large variety of applications, they have some disadvantages[140]. Firstly, microarrays can lead false positive results with the generation of enormous data masses and with degraded mRNA[138, 140]. Secondly, the use of cDNA microarrays is also very expensive and results are dependent on the purity of RNA[138, 140]. And thirdly, a DNA array can only detect sequences which are specific for the detection[138, 140].

In this regard, mice were exposed to normoxia (21 days), chronic hypoxia (21 days) and chronic hypoxia (21 days) with subsequent re-exposure to normoxia followed by laser-microdissection of pulmonary vessels.

Of all differentially expressed genes, the present thesis focused on SPARC. SPARC, also called osteonectin or basement membrane protein-40 (BM-40), is a 42 kDa multifunction glycoprotein[125]. SPARC is expressed in endothelial cells, vascular smooth muscle cells, macrophages, fibroblasts, and the alveolar epithelium[141-143]. SPARC is involved in regulation of various cellular processes such as cell proliferation, migration and angiogenesis[144] as well as changing cell shape, inhibiting cell-cycle progression, and influencing the synthesis of extracellular matrix (ECM) proteins[145]. Among other functions, SPARC regulates wound healing, responses to injury and tissue remodeling[141]. In this regard, association of SPARC with several cancer forms and pulmonary fibrosis was observed[57, 146].

SPARC was consistently down-regulated in all re-oxygenation time-points investigated. Moreover, it is critically involved in several cellular processes that are dysregulated in PH and is associated with several hyper-proliferative diseases. Thus, it might be a promising novel potential target gene for pulmonary vascular remodeling processes underlying PH. In addition, involvement of several SPARC interaction, partners with what PH pathogenesis are already known for: Signal transducers and activators of transcription-3 (STAT3)[147], transforming growth factor beta-1 (TGF-β1)[80], AKT1[148], MAPK1[149], Caveolin 1 (CAV1)[150], murine double minute 2 (Mdm2)[151]] and integrin linked kinase (ILK)[132].

Since the microarray technique can lead to false results, results should be validated by additional methods. In this regard, SPARC regulation in pulmonary vessels isolated from normoxic, hypoxic and re-oxygenated hypoxic mice was confirmed on mRNA level by q(RT)-PCR. In detail, in both techniques, there were no differences in SPARC regulation between the normoxic and hypoxic group and down-regulation following re-oxygenation.

In further experiments, SPARC regulation in lung homogenate obtained from mice suffering from chronic hypoxia-induced PH as well as from human IPAH patients was analyzed on mRNA and protein level. In addition, functional importance of SPARC was assessed by *in vitro* experiments. Finally, SPARC knockout mice were used to decipher the role of SPARC in PH *in vivo*.

4.3 Characterization of SPARC expression in chronic hypoxia-induced PH and in IPAH patients

In the present thesis, lung homogenate from mice exposed to chronic hypoxia and patients with IPAH was used. Similar to the pulmonary vasculature, there was no induction of SPARC mRNA expression in lung homogenate derived from chronic hypoxic mice. However, SPARC protein expression was enhanced in lungs of chronic hypoxic mice, depicting that RNA and protein regulation not necessarily correlates. In addition, in IPAH patients, both SPARC mRNA and protein levels were enhanced in comparison to donor lungs. Elevated SPARC levels in chronic hypoxic mice as well as IPAH patients might point that there are no species-dependent differences in SPARC regulation.

Involvement of SPARC in hyperproliferatives disease is already known from previous studies. In this regard, it has been showed that, SPARC may contribute to the progression of pulmonary fibrosis[128, 152-154], breast cancer, melanoma and glioblastoma[146]. Enhanced SPARC levels were also observed in heat shock-, heavy metal- or endotoxin-induced tissue injury models in mice, chick embryo and dog[155-158]. Together, the role of SPARC in fibrosis, cancer and injury models points towards an important function of SPARC in hyper-proliferative diseases such as PH, most likely by affecting tissue remodeling processes. In this regard, in the present thesis, SPARC was predominantly localized to the pulmonary vessel wall, the site of the pulmonary vascular remodeling[57]. Vascular specific SPARC expression in the lung was already observed in bleomycin-induced pulmonary fibrosis in mice[152]. In addition, elevated SPARC expression in chronic hypoxic mice was specific for the pulmonary vasculature as there were no changes in expression in the systemic vasculature (aorta).

4.4 Hypoxia as a critical factor of SPARC expression

Elevated SPARC expression in chronic hypoxia-induced PH in mice might point towards hypoxia as a critical factor in SPARC regulation. As SPARC was localized in the medial layer of the vasculature wall and PASMC are critically involved in pulmonary vascular remodeling[72], primary human PASMC were chosen for *in vitro* experiments. In this regard, PASMC were exposed to normoxia, hypoxia or hypoxia with a subsequent re-exposure to normoxia, mimicking the reverse remodeling approach *in vivo*. Hypoxia led to an increase in SPARC expression which was reversed by re-oxygenation of cells. Hypoxia-dependent SPARC expression was already shown in human malignant glioma cells[159].

Since chronic hypoxic mice and hypoxic primary human PASMC possessed enhanced SPARC levels, next potential involvement of hypoxia inducible factors (HIF) in regulation of SPARC expression was assessed. Under normoxic conditions HIF-α is hydroxylated by prolyl hydroxylase domain (PHD) proteins at conserved prolines 402 and 564[160, 161] in the oxygen-dependent degradation domain[162]. However, under hypoxic conditions, HIF-α hydroxylation by PHD is inhibited,[160] causing HIF-α accumulation and translocation to the cell nucleus. In the nucleus, HIF-α dimerizes with the HIF-β subunit, forming together with transcriptional co-activators such as CREB-binding protein and p300, an active transcription factor[129]. Binding of the active transcription factor to hypoxia response elements leads to expression of hypoxia-specific genes[129] which can ensure sufficient O_2 delivery, O_2 transport and metabolic adaptations as well as vascular remodeling[129, 163].

In this regard, HIF levels were enhanced in the pulmonary vasculature of chronic hypoxic mice, in plexiform lesions of IPAH patients as well as in fawn-hooded rats[86, 164, 165].

In the present thesis, HIF-1α silencing did not alter SPARC expression in hypoxic primary hPASMC. However, HIF-2α knockdown impaired SPARC expression in hypoxic cells. HIF-dependent SPARC expression was already shown in human malignant glioma cell lines following HIF-1α silencing[159]. Role of HIF-2α in regulation of SPARC transcription is until now unknown. However, analysis of the SPARC promoter revealed two potential HIF binding sites in the 2000bp promoter region. If HIF-2α directly or indirectly regulates SPARC expression in primary hPASMC has to be addressed in further experiments, such as electrophoretic mobility shift assays (EMSA) or chromatin immunoprecipitation (ChIP).

In addition to HIF, binding of SRY (sex-determining region Y) - box 5 (SOX-5) to the SPARC promoter is known[166]. However, next to HIF and SOX-5, there might be additional not yet identified transcription factors, playing a role in SPARC regulation as well.

Taken together, SPARC expression was increased in IPAH patients and chronic hypoxic mice. *In vitro,* SPARC expression was regulated via the hypoxia/HIF-2α pathway in primary hPASMC. Next to hypoxia, SPARC expression was regulated by TGF-β.

4.5 Effects of growth factor stimulations on SPARC expression

Several growth factors, including TGF-β1[80], PDGF[81, 82], EGF[83]and VEGF[84], have been implicated in the pathogenesis of PH, by influencing abnormal proliferation and migration of pulmonary arterial vascular cells[87].

Thus, next, influence of those growth factors on SPARC expression was assessed. In literature, SPARC interaction with several growth factors, including TGF-β1, VEGF and PDGF is described[146]. In bleomycin-induced lung fibrosis in mice TGF-β increases SPARC expression in mice fibroblasts[128]. Additionally, TGF-β upregulates SPARC expression in human gingival fibroblasts, human dermal fibroblasts, and human pulp cells[167, 168]. Blocking the TGF-β signaling leads to significantly attenuated SPARC levels and degree of fibrosis[128]. EGF and PDGF downregulates SPARC expression in human pulp cells and also in rabbit chondrocytes[168]. Moreover, SPARC binding to VEGF inhibits VEGF-stimulated proliferation of endothelial cells[169].

Experiments in the present thesis in primary hPASMC revealed an induction of SPARC expression following TGF-β1 stimulation, which is in line with the literature in fibroblasts. However, PDGF-BB, EGF and VEGF were not able to induce SPARC expression.

4.6 Functional role of SPARC

Since SPARC expression is up-regulated in PH, next, its possible functional role was of major interest. In this regard, its impact on primary hPASMC proliferation was assessed. Abnormal PASMC proliferation is one of the key features in PH pathogenesis[72]. SPARC mRNA and protein expression was down-regulated by specific siRNA transfection in a time-dependent manner. Indeed, SPARC knockdown negatively affected PASMC proliferation. Impact of SPARC in proliferation was already observed in ovarian cancer cells, gastric cancer cells, glioma cells and melanoma cells[127]. Modulation of hPASMC proliferation most probably occurred via the proliferation markers cyclin D1, Ki67 and PCNA, since those were attenuated following SPARC silencing.

Ki-67 is a nuclear antigen expressed during the G1, S, and G1–M phases of the cell cycle in proliferating cells[170]. PCNA is a highly conserved nuclear protein, which is expressed during cell replication and DNA repair[170]. Next to Ki67 and PCNA, cyclin D1 is one of the key genes controlling cell cycle and thus proliferation by influencing transition of cells between the G1 phase and the S phase[171].

Together, these results clearly indicated that SPARC affects PASMC proliferation. Finally, the involved pathway was of major interest.

4.7 SPARC signaling pathway

PI3K/AKT and extracellular signal–regulated kinase (ERK1/2) signaling pathways are closely connected with pro-proliferative processes in hyperplastic diseases such as fibrosis, cancer and PH[148, 172, 173]. In detail, the PI3K/AKT signaling pathway is known to be involved in vascular development and normal vascular function by influencing proliferation of rat PASMC[148]. In this regard, PI3K/AKT signaling inhibition by triciribine led to impared rat PASMC proliferation[148]. The MAPK pathways consist of ERK1/2, c-Jun NH2-terminal kinase (JNK) and p38 MAPK, regulating cellular proliferation[149]. In this regard, elevated levels of ERK1/2 expression and phosphorylation were observed in proliferating pulmonary vascular SMC from broilers[174].

Consequently, SPARC expression was silenced and the impact on AKT/ERK activation (phosphorylation) was assessed, indicating attenuated phosphorylation of AKT following SPARC silencing. Moreover, inhibition of AKT by wortmannin led to attenuated TGF-β1-induced SPARC expression, indicating a bidirectional regulatory role of SPARC and AKT. However, SPARC silencing did not impair ERK activation. A connection of SPARC with the AKT signaling pathway was already found in a recent publication, revealing less phosphorylation of AKT following SPARC depletion in human melanoma cell lines[175].

In addition to PI3K/AKT, mTOR, an AKT downstream effector, plays a major role in proliferation[176] and PH pathogenesis [177]. In detail, increased levels of mTOR (Ser-2481) phosphorylation and activation were found in hypoxic primary human and rat pulmonary arterial vascular smooth muscle cells (PAVSMC), causing elevated cell proliferation[177]. In this regard, in the present thesis, mTOR dysregulation in IPAH patients was confirmed.

Moreover, SPARC silencing reduced mTOR expression in hPASMC. However, mTOR inhibition by rapamycin did not influence TGF-β-induced SPARC expression, indicating that mTOR is located down-stream of SPARC in the signaling pathway. Taken together, SPARC affects PASMC proliferation most probably via the PI3K/AKT/mTOR signaling pathway **Figure 21**.

After identifying members of the downstream signaling pathway of SPARC, upstream signaling was addressed. ILK is a serine-threonine kinase localized in focal adhesion complexes[178]. Elevated ILK expression and activation occurs in several types of

cancers, including leukemia and glioblastoma[179]. ILK acts as an intracellular adaptor and kinase, linking integrins, (cell-adhesion receptors), and growth factors to a range of signaling pathways[179]. The kinase activity of ILK is modulated by cell–ECM interactions[179]. Intracellular, there is a direct interaction between ILK and actin and α-actinin-binding proteins such as the parvins, affixin and paxillin[180-182]. Moreover, blockage of ILK expression and activity is anti-tumorigenic. Thus, ILK is an attractive target for cancer therapeutics[179]. Previous reports depicted SPARC binding to ILK, leading to human glioblastoma multiform cell migration by inducing the downstream phosphorylation of the AKT and ERK pathways[133].

In the present thesis, first ILK expression was assessed after SPARC silencing, revealing no influence on expression. However, ILK silencing negatively affected SPARC expression, clearly indicating that ILK is located upstream in the SPARC signaling pathway. Cpd 22 is a cell-permeable compound which acts as an ILK inhibitor[183]. Cpd 22 possess a pro-apoptotic role in human prostate and breast cancer cell lines[183]. Similar than ILK silencing, ILK inhibition by Cpd 22 migtates SPARC expression. Next to SPARC and mTOR, ILK is enhanced expressed in IPAH patients. Elevated ILK expression in IPAH patients was already observed in a previous study[132]. However, the connection of ILK to SPARC and AKT/mTOR signaling in hPASMC is to the best of our knowledge new. In this regard, pharmacological intervention of SPARC might be a possible novel treatment strategy for PH pathogenesis.

In head and neck cancer, SPARC expression is a poor prognostic factor for disease outcome[184]. However, SPARC might favor tumor response to nab-paclitaxel treatment in a clinical setting in those tumors. In detail, SPARC has been suggested as an important factor that affects drug accumulation. Via its albumin binding site and its high abundance in several tumor forms such as neck and head tumor, SPARC gathers the albumin-bound drug, nab-paclitaxel to tumor tissue[184-186]. However, further verification and several larger ongoing clinical studies are required in multiple tumor types for approving SPARC as a predictive biomarker for nab-paclitaxel treatment[184].

4.8 *In vivo* relevance of SPARC

Since SPARC affects PASMC function *in vitro*, SPARC might possess an *in vivo* function as well. In this regard, global SPARC$^{-/-}$ mice and their littermate controls (wild-type, WT) were exposed to chronic hypoxia for 28 days. Following, echocardiography, hemodynamic measurements and muscularization were assessed. The RV has an important role in the determination of functional state and prognosis in PH[134]. Under physiological conditions the RV has a very thin walled crescent shaped structure and is designed to pump blood through a low pressure and high flow pulmonary vascular system[187]. However, under pathophysiological conditions such as chronic hypoxia, pulmonary vascular resistance and pressure increases due to narrowing of the pulmonary vascular lumen, leading to pressure overload of the right ventricle. An adaption mechanism leads to right heart hypertrophy[188]. However, at a certain time point, hypertrophy is no longer compensated and right ventricular failure might occur[189].

In the present thesis, RV remodeling and function is depicted by RVWT, RVID, CO and CI. RVID, CO and CI were regulated neither by hypoxia nor by genotype. RVWT was increased in WT mice following chronic hypoxia, but did not reach statistical significance in SPARC$^{-/-}$ mice. In conclusion, echocardiography parameters assessed indicate same degree of RV function and remodeling in the WT and knockout group. Elevated RVSP and fulton index in chronic hypoxic WT mice and decreased amount of non-muscularized vessels were already observed in numerous previous studies[108, 113, 190]. Taken together, echocardiography and hemodynamic data indicate that possible hemodynamic changes occurred prior to changes in the heart.

Moreover, remarkably there was;

1) An obvious variability in the single experimental groups in echocardiographic and hemodynamic values assessed.
2) An upward shift in already under baseline conditions (normoxia), especially for RVSP.

SPARC$^{-/-}$ mice used for the *in vivo* experiments in the present thesis possessed a mixed genetic background, consisting of C57BL/6 and 129Sv[191, 192]. Since littermate controls were used, the control was as similar to the experimental group as feasibly and other possible confounders could be excluded.

Normally, RVSP in normoxic C57BL6/J mice ranges between 10-20 mmHg, whereas in hypoxic C57BL6/J mice it is between 14-26 mmHg[108]. Moreover, RVSP in normoxic 129Sv mice ranges between 27-30 mmHg, whereas in hypoxic 129Sv mice it is 42-45 mmHg[193]. Results in the present thesis showed RVSP 20-30 mmHg in normoxic and 30-40 mmHg in hypoxic WT mice.

Moreover, due to animal availability, the experimental groups contained higher numbers of females than males, which in addition can cause variations in experimental groups. In detail, previous studies observed that female gender and/or estrogens can be protective in experimental models of PH, such as the hypoxic and monocrotaline models[194].

Taken together all those factors might cause that SPARC$^{-/-}$ mice did not differ to WT mice in their response to chronic hypoxia, neither in RV remodeling and function, nor in hemodynamic data, fulton index and degree of muscularization of small pulmonary vessels. However, additional reasons might be the occurance of compensatory mechanisms in global SPARC$^{-/-}$ mice or the usage of the wrong model. Possibly, SPARC$^{-/-}$ does not affect pulmonary vascular remodeling but reverse remodeling.

4.9 SPARC family members

SPARC is a member of a gene family possessing structural similarities in one or more protein domains[195]. The family members are: secreted modular calcium binding protein (SMOC) 1 and 2, follistatin like protein 1 (FSTL-1), testican 1 (SPARC/osteonectin, CWCV, and Kazal-like domains proteoglycans, SPOCK)[196]. SMOC1 binds tenascin C[197] which is involved in PH pathogenesis[72]. SMOC2 is highly expressed in heart and muscle[198] and has a role in proliferation in human hepatocellular carcinoma cells[199]. FSTL-1 has a role in respiratory distress and multiple defects in lung development[200]. SPOCK1 is involved in the development and progression of tumors[201].

Since SPARC$^{-/-}$ mice are not protected from chronic hypoxia-induced PH and SPARC family members are involved in hyperproliferative diseases and/or lung pathologies, next screening of possible compensatory mechanisms in SPARC$^{-/-}$ mice were performed. In this regard, expression levels of SPARC family members was assessed in WT and SPARC$^{-/-}$ mouse lung homogenate. However, degree of expression for FSTL-1, SMOC1, SMOC2 and SPOCK1 did not differ between WT and SPARC$^{-/-}$, revealing no compensatory expression in SPARC family members in SPARC$^{-/-}$ mice.

4.10 Possible compensatory mechanisms

In the present thesis SPARC regulates PASMC proliferation via the PI3K/AKT/mTOR pathway. However SPARC$^{-/-}$ mice did not differ from WT mice in their response to chronic hypoxia, neither in RV remodeling and function, nor in hemodynamic data, fulton index and degree of muscularization of small pulmonary vessels. Moreover, as a compensatory mechanism, degree of expression for SPARC family members also did not differ between WT and SPARC$^{-/-}$. Taken together, other possible compensatory mechanisms might be the reason for the *in vivo* results in the present thesis.

Indeed, a direct compensatory mechanism on PASMC function was observed *in vitro*. PASMC isolated from SPARC$^{-/-}$ mice and incubated under hypoxic conditions possessed a higher level of AKT phosphorylation and proliferation than respective cells from WT animals. Compensatory upregulation of those two processes might explain why WT and SPARC$^{-/-}$ mice did not differ in their response to chronic hypoxia **Figure 21.**

For the *in vivo* studies, global SPARC$^{-/-}$ mice and littermate controls were used. A global KO leads to a permanent deletion of a specific gene in the whole animal, in every cell of the organism[202]. In future, conditional KO mice might be more beneficial while in this model the gene of interest is temporally controllable at a given time-point in preferable adult animals prior to start of the experiment with the usage of external inducer-agents such as tamoxifen or tetracycline[203]. Finally, inducible cell type specific SPARC$^{-/-}$ mice might help to decipher the role of SPARC *in vivo* in a specific cell type.

Next to the conventional KO, SPARC$^{-/-}$ mice can be induced via clustered regularly interspaced short palindromic repeats (CRISPR)/CRISPR-associated genes (CRISPR/Cas) and adeno associated virus (AAV)[202, 203].

CRISPR/Cas is a new system which allows editing of the mice genome much faster than previously used techniques. Moreover, in this system multiple mutations can be made in a single experiment. Until now, it is the easiest method for obtaining a viable knockdown mouse model, which can be used for experiments[204, 205].

Selective gene silencing by RNA interference (RNAi) is another possible approach. Short hairpin RNA (shRNA) is an artificial RNA molecule which targets a specific gene, causing stable gene silencing[206, 207]. Additionally, viral vectors have been used as the delivery method in many studies[207]. It has been observed that, shRNA delivery by AAV

systems are more efficient in gene silencing than alternative methods such as retroviral or lentiviral systems[207].

In conclusion, experiments using time-point specific (conditional) and/or cell type specific SPARC$^{-/-}$ mice will be needed to avoid the occurrence of compensatory mechanisms and to assess the role of SPARC *in vivo.* Finally, a therapeutic intervention can be taken in consideration for treatment of patients.

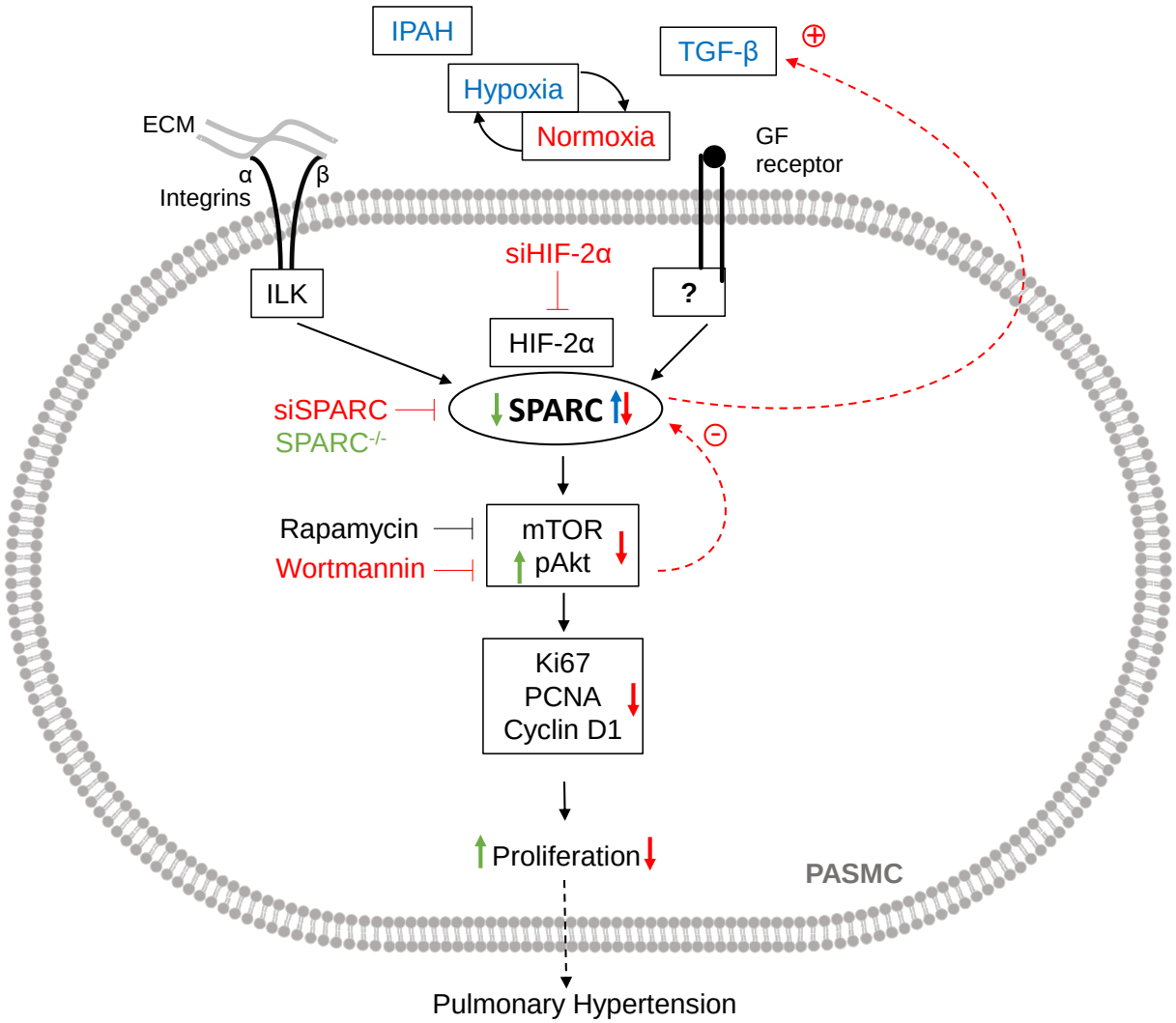

Figure 21: Proposed functional role of SPARC in PASMC

SPARC is elevated expressed in IPAH patients, in chronic hypoxic mice and in primary hPASMC following TGF-β1 stimulation or hypoxic treatment. Hypoxia-induced SPARC expression is regulated via HIF-2α. Re-oxygenation of PASMC reversed enhanced SPARC expression under hypoxic conditions. Silencing of SPARC inhibits PASMC proliferation via the PI3K/AKT/mTOR signaling pathway. ILK is located upstream in the SPARC signaling

pathway. SPARC$^{-/-}$ are not protected from chronic hypoxia-induced PH, possibly because of enhanced AKT phosphorylation and PASMC proliferation in hypoxic SPARC$^{-/-}$ PASMC.

AKT: Protein kinase B, ECM: extracellular matrix, GF: growth factor, HIF: hypoxia inducible factor, ILK: integrin linked kinase, IPAH: idiopathic pulmonary arterial hypertension, mTOR: the mammalian target of rapamycin, PASMC: pulmonary arterial smooth muscle cells, PCNA: proliferating-cell-nuclear-antigen, SPARC: secreted protein acidic and rich in cysteine, TGF-β1: transforming growth factor beta.

5. Summary

Pulmonary hypertension (PH) is a life-threatening disease, characterized by excessive pulmonary vascular remodeling, leading to elevated pulmonary arterial pressure and right heart hypertrophy. PH is caused among others by chronic hypoxia, vasoconstrictor/vasodilator and/or growth factor imbalance leading to pulmonary arterial smooth muscle cell (PASMC) dysregulation. Upon re-exposure to normoxia, hypoxia-induced PH in mice is reversible.

Until now, research in the field of PH concentrates mostly on the onset and development of PH. In this thesis, we aim to identify novel candidate genes for pulmonary vascular remodeling and its reversal specifically in the pulmonary vasculature.

Reverse remodeling was investigated in adult mice (C57BL/6J) either exposed to normoxia (21% O_2), chronic hypoxia (10% O_2), or chronic hypoxia with subsequent re-exposure to normoxia for 1, 3, 7, 14 days. Pulmonary vessels were laser-microdissected followed by RNA isolation and microarray analysis. In addition, the functional role of the candidate gene was confirmed *in vitro* in human primary PASMC and *in vivo* in respective knockout mice.

In laser-microdissected murine pulmonary vessels, secreted protein acidic and rich in cysteine (SPARC) was identified as one gene consistently down-regulated in all re-oxygenation time points investigated. Up-regulation of SPARC specifically in the pulmonary vasculature was observed in chronic hypoxic mice and in idiopathic pulmonary arterial hypertension patients. Furthermore, TGF-β1 or hypoxia-HIF-2α signaling pathway induced SPARC expression. In *in vitro* studies, SPARC silencing in primary human PASMC led to reduced proliferation and diminished PI3K/AKT/mTOR activation. However, SPARC *in vivo* knockout did not attenuate chronic hypoxia-induced PH, possibly due to elevated AKT activation and PASMC proliferation under hypoxic conditions in SPARC knockout PASMC.

In summary, SPARC was identified as a novel gene involved in dysregulation of primary human PASMC proliferation. Moreover, to the best to our knowledge this is the first evidence about its associated with the human PH disease.

6. List of Figures

7. List of Tables

8. **Abbreviations**

α-sma	Alpha smooth muscle actin
ALK1	Activin receptor-like kinase 1
AKT	Serin/Threonin Protein-Kinase Akt
AMD-1	S-adenosylmethionine decarboxylase 1
APS	Ammoniumpersulfat
ATP	Adenosine triphosphate
BCA	Bicinchoninic acid assay
bFGF	Basic fibroblast growth factor
B2M	β2-Microglobulin
BM-40	Basement membrane protein-40
BMPR2	Bone Morphogenetic protein receptor, type 2
Bp	Basepairs
BSA	Bovines Serum-Albumin
°C	Celsius
CAV1	Caveolin-1
cDNA	Complementary DNA
cGMP	Cyclic guanosine monophosphate
CI	Cardiac index
CH	Chronic hypoxia
CHD	Congenital heart disease
ChIP	Chromatin immunoprecipitation
CO	Cardiac output

CO_2	Carbondioxide
COPD	Chronic obstructive pulmonary disease
CTEPH	Chronic thromboembolic pulmonary hypertension
d	Day
DNA	Deoxyribonucleicacid
dNTP	Deoxyribonucleotidtriphosphate
DPBS	Dulbecco's phosphate-buffered saline
EC	Endothelial cells
ECM	Extracellular matrix components
EDTA	Ethylenediaminetetraacetic acid
EGF	Epidermal growth factor
EF	Ejection fraction
EMSA	Electrophoretic mobility shift assays
ENG	Endoglin
Erk1/2	Extracellular signal-regulated Kinases 1 and 2
ET-1	Endotelin 1
FBS	Fetal bovine serum
FDA	Food and Drug Administration
FiO_2	Fraction of inspired oxygen
FOXO1	Forkhead box O1
FP	Forward Primer
FSTL1	Follistatin like protein 1
g	Gram

GF	Growth factor
h	Hours
H	Hypoxia
HCl	Hydrochloric acid
HIF	Hypoxia-inducible factor
HIF-1α	Hypoxia-inducible factor 1 alpha
HIF-2α	Hypoxia-inducible factor 2 alpha
HIV	Human immunodeficiency virus
H_2O	Water
H_2O_2	Hydrogen peroxide
hPASMC	human PASMC
HPV	Hypoxic pulmonary vasoconstriction
HR	Heart rate
IgG	Immunoglobulin g
ILD	Interstitial lung disease
ILK	Integrin linked kinase
IPAH	Idiopathic pulmonary hypertension
JNK	c-Jun NH2-terminal kinase
K^+	Potassium
kDa	Kilodalton
kg	Kilogram
KH_2PO_4	Monopotassium phosphate
KCNK3	Potassium channel super family K member-3
KLF4	Krüppel-like factor 4

KO	Knock out
LV	Left ventricle
µ	Micro (10^{-6})
µg	Microgram
µl	Microliter
m	Mili (10^{-3})
m^2	Square meters
M	Molar (Mol per Liter)
MAPK	Mitogen-activated Protein-Kinase
MCT	Monocrotaline
Mdm2	Murine double minute 2
mg	Milligram
min	Minute
mM	Milimolar
mmHg	Milimeter mercury
mPAP	Mean pulmonary arterial pressure
mPASMC	Mouse PASMC
MRI	Magnetic resonance imaging
mRNA	Messenger RNA
mTOR	The mammalian target of rapamycin
mTORC1	mTOR complex 1
mTORC2	mTOR complex 2
n	Number of experiments
N	Normoxia
N_2	Nitrogen

Na^+	Sodium
NaCl	Sodium chloride
Na_2HPO_4	Disodium phosphate
Na_3VO_4	Sodium ortho vanadate
NC	Negative control
Nfatc2	Nuclear factor of activated T-cells, cytoplasmic, calcineurin-dependent 2
nm	Nanometer
NO	Nitric Oxide
O_2	Oxygen
OSA	Obstructive sleep apnea
OPN	Osteopontin
2-Propanol	Isopropylalcohol
PAGE	Polyacrylamide gel electrophoresis
PA	Pulmonary artery
PAH	Pulmonary Arterial Hypertension
PASMC	Pulmonary arterial smooth muscle cells
PBGD	Porphobilinogen Deaminase
PBS	Phosphate Buffered Saline
PCNA	Proliferating Cell Nuclear Antigen
PCR	Polymerase chain reaction
PCH	Pulmonary capillary hemangiomatosis
PDE-5	Phosphodiesterase 5
PDGF	Platelet-derived growth factor
PAEC	Pulmonary arterial endothelial cells

PH	Pulmonary Hypertension
PHD	Prolyl hydroxylase domain
PI3K	Phosphatidylinositol 3-kinase
pmol	Pikomol
POPH	Portopulmonary hypertension
PO_2	Partial pressure of O_2
PPH	Primary pulmonary hypertension
PPHN	Persistent pulmonary hypertension of the newborn
PPARG1	Peroxisome proliferator–activated receptor γ 1
PVDF	Polyvinylidenfluoride
PVOD	Pulmonary veno-occlusive disease
PVR	Pulmonary vascular resistance
RIPA	Radioimmunoprecipitation assay buffer
ROCK	Rho-Kinase
RP	Reverse Primer
RNA	Ribonucleicacid
rpm	rounds per minute
RV	Right ventricle
RVID	Right ventricular internal diameter
RVF	Right ventricle failure
RVH	Right ventricular hypertrophy
RVP	Right ventricular pressure
RVWT	Right ventricular wall thickness

s	Seconds
SAP	Systemic arterial pressure
Sch-PAH	Schistosomiasis-associated PAH
SDS	Sodium dodecyl sulfate
SDS-PAGE	Sodium dodecyl sulfate-Polyacrylamide gel electrophoresis
SERT	Serotonin receptor
siRNA	small-interfering RNA
SEM	Standard error of the mean
SLUG	Snail family zinc finger 2
SMA	Smooth muscle actin
SMAD 9	Decapentaplegic 9
SMC	Smooth muscle cells
SMOC1	Secreted modular calcium binding protein 1
SMOC2	Secreted modular calcium binding protein 2
SOX-5	SRY (sex-determining region Y) - box 5
SPARC	Secreted protein acidic and rich in cysteine
SPOCK1	SPARC/osteonectin, CWCV, and Kazal-like domains proteoglycans 1
STAT3	Signal transducers and activators of transcription 3
SVR	Systemic vascular resistance
Tab.	Table
TAPSE	Tricuspid annular plane systolic excursion

TBE	TRIS-Borat-EDTA
TBS-T	Tris Buffer Saline with 0,1% Tween20
TEMED	Tetramethylethylenediamine
TGFβ	Transforming growth factor beta
TF	Transcription factors
TRIS	Tris(hydroxymethyl)-aminomethane
TSP1	Thrombospondin 1
U	Unit
q(RT)-PCR	Quantitative real-time polymerase chain reaction
V	Voltage
VEGF	Vascular endothelial growth factor
VIP	Vasoactive Intestinal Peptide
v/v	Volume per Volume
vWF	von Willebrand factor
Watt	Watt
WB	Western Blot
w/v	Weight per Volume
WT	Wild-type
5-HTT	5-Hydroxytryptamintran
6MWD	6-minute walk distance

9. **Declaration**

I declare that I have completed this thesis on my own, without unauthorized outside help and only with the assistance acknowledged therein. I have properly acknowledged and referenced all the passages which are derived literally or analogously from published or unpublished work and all information that relates to verbal communications. I have the principles of good scientific practice such as these in the ``Statute of Justus Liebig University Giessen to ensure good scientific practice`` in my work and in my thesis.

Giessen, 2019

10. Acknowledgement

First of all, I would like to thank my supervisor Professor Norbert Weissmann for providing me the opportunity to work in his research group, for his guidance, encouraging support and undying efforts throughout my doctoral studies that made the completion of my PhD degree possible.

I am really grateful to my Postdoc, Dr. Christine Veith-Berger for supporting me from beginning till the end, for being such a great mentor and a great friend. Her ideas are always valuable and without her, this work would not have been possible. Thank you.

I would like to especially thank Prof. Dr. med. Werner Seeger and Dr. med. Rory E. Morty and administrative members for accepting me in my first graduate program "Molecular Biology and Medicine of the Lung "(MBML). Special thanks to Dr. med. Rory E. Morty for always being helpful and supportive through the MBML lectures.

Furthermore, I am truly thankful to my second PhD program "International Giessen Graduate Centre for the Life Sciences" (GGL) for organizing useful diverse courses and special thanks to Professor Eveline Baumgart-Vogt and Dr. Lorna Lück from GGL.

I want to thank all the people at ECCPS who contributed to this thesis in some way. The staff and my colleagues alike deserve a special mention for the help and support that I received throughout the entire period of my education here. Especially to our technicians, Ingrid B. Müller for molecular biology, Karin Quanz for hemodynamics, Carmen Homberger and Nils Schupp for cell culture, Ewa Bieniek for histology without them it would be really hard. Special thanks to Dr. Oleg Pak and Dr. Friederike Weisel for microarray, Dr. Simone Kraut for echocardiography, Katharina Schäfer for lung flushing and Dr. Monika Brosien for cell isolation from mice. I would like to also thank to Djuro Kosanovic, Aleksander Petrovic, Mira Yasemin Gökyildirim, Stefan Hadzic, Cheng Yu Wu, Claudia Garcia, Magdalena Wujak, Inna Tschipakow, Marija Gredic and Ilker Kanbagli for being really good friends and supportive in everything.

Finally, I would like to especially acknowledge my dear husband Ege Özcan for helping and supporting me for every step in my life and also with the research whenever I needed it. Without his endless support it would not have been possible to complete my degree. I am heartily thankful to my parents Pınar and Merih Vartürk for being such supportive to my every decision. I am very grateful to them. They gave me all these best

opportunities beside love and emotional support. I am very lucky to have such a great big family.

11. References

1. https://emedicine.medscape.com/article/1884995-overview.
2. https://www.britannica.com/science/lung.
3. Blaivas AJ. Anatomy and function of the respiratory system. *Penn State Hershey Medical Center*. 2017.
4. Kacmarek RM. Essentials of Respiratory Care. *Elsevier Health Sciences, Elsevier eBook on VitalSource*. 2013.
5. Whittemore S. The Respiratory System. *Chelsea House Publishers*. 2004.
6. https://www.wyzant.com/resources/lessons/science/biology/cellular-respiration.
7. Khakh BS and Burnstock G. The double life of ATP. *Scientific American*. 2009;301:84-90, 92.
8. https://opentextbc.ca/biology/chapter/11-3-circulatory-and-respiratory-systems/.
9. Spaeth EE and Friedlander SK. The diffusion of oxygen, carbon dioxide, and inert gas in flowing blood. *Biophysical Journal*. 1967;7:827-851.
10. Gluecker T, Capasso P, Schnyder P, Gudinchet F, Schaller MD, Revelly JP, Chiolero R, Vock P and Wicky S. Clinical and radiologic features of pulmonary edema. *Radiographics*. 1999;19:1507-1533.
11. Gehr P, Bachofen M and Weibel ER. The normal human lung: ultrastructure and morphometric estimation of diffusion capacity. *Respiratory Physiology*. 1978;32:121-140.
12. Whittemore S. The Circulatory System. *Chelsea House Publishers*. 2004.
13. Von Euler U and Liljestrand G. Observations on the pulmonary arterial blood pressure in the cat. *Acta Physiologica*. 1946;12:301-320.
14. Theissen IL and Meissner A. [Hypoxic pulmonary vasoconstriction]. *Anaesthesist*. 1996;45:643-652.
15. Lumb AB and Slinger P. Hypoxic pulmonary vasoconstriction: physiology and anesthetic implications. *Anesthesiology*. 2015;122:932-946.
16. Aaronson PI, Robertson TP, Knock GA, Becker S, Lewis TH, Snetkov V and Ward JP. Hypoxic pulmonary vasoconstriction: mechanisms and controversies. *The Journal of Physiology*. 2006;570:53-58.
17. Sommer N, Dietrich A, Schermuly RT, Ghofrani HA, Gudermann T, Schulz R, Seeger W, Grimminger F and Weissmann N. Regulation of hypoxic pulmonary

vasoconstriction: basic mechanisms. *The European Respiratory Journal*. 2008;32:1639-1651.

18. Sommer N, Strielkov I, Pak O and Weissmann N. Oxygen sensing and signal transduction in hypoxic pulmonary vasoconstriction. *The European Respiratory Journal*. 2016;47:288-303.

19. Simonneau G, Gatzoulis MA, Adatia I, Celermajer D, Denton C, Ghofrani A, Gomez Sanchez MA, Krishna Kumar R, Landzberg M, Machado RF, Olschewski H, Robbins IM and Souza R. Updated clinical classification of pulmonary hypertension. *Journal of the American College of Cardiology*. 2013;62:34-41.

20. Galie N, Humbert M, Vachiery JL, Gibbs S, Lang I, Torbicki A, Simonneau G, Peacock A, Vonk Noordegraaf A, Beghetti M, Ghofrani A, Gomez Sanchez MA, Hansmann G, Klepetko W, Lancellotti P, Matucci M, McDonagh T, Pierard LA, Trindade PT, Zompatori M and Hoeper M. 2015 ESC/ERS Guidelines for the diagnosis and treatment of pulmonary hypertension: The Joint Task Force for the Diagnosis and Treatment of Pulmonary Hypertension of the European Society of Cardiology (ESC) and the European Respiratory Society (ERS): Endorsed by: Association for European Paediatric and Congenital Cardiology (AEPC), International Society for Heart and Lung Transplantation (ISHLT). *The European Respiratory Journal*. 2015;46:903-975.

21. Badesch DB, Champion HC, Sanchez MA, Hoeper MM, Loyd JE, Manes A, McGoon M, Naeije R, Olschewski H, Oudiz RJ and Torbicki A. Diagnosis and assessment of pulmonary arterial hypertension. *Journal of the American College of Cardiology*. 2009;54:55-66.

22. Simonneau G, Robbins IM, Beghetti M, Channick RN, Delcroix M, Denton CP, Elliott CG, Gaine SP, Gladwin MT, Jing ZC, Krowka MJ, Langleben D, Nakanishi N and Souza R. Updated clinical classification of pulmonary hypertension. *Journal of the American College of Cardiology*. 2009;54:43-54.

23. www.heart.org.

24. Archer SL, Weir EK and Wilkins MR. Basic science of pulmonary arterial hypertension for clinicians: new concepts and experimental therapies. *Circulation*. 2010;121:2045-2066.

25. Chin KM and Rubin LJ. Pulmonary arterial hypertension. *Journal of the American College of Cardiology*. 2008;51:1527-1538.

26. Sun XG, Hansen JE, Oudiz RJ and Wasserman K. Pulmonary function in primary pulmonary hypertension. *Journal of the American College of Cardiology*. 2003;41:1028-1035.

27. Hinderliter AL, Willis PWt, Long W, Clarke WR, Ralph D, Caldwell EJ, Williams W, Ettinger NA, Hill NS, Summer WR, de Biosblanc B, Koch G, Li S, Clayton LM, Jobsis MM and Crow JW. Frequency and prognostic significance of pericardial effusion in primary pulmonary hypertension. PPH Study Group. Primary pulmonary hypertension. *American Journal of Cardiology*. 1999;84:481-484.

28. Rich JD and Rich S. Clinical diagnosis of pulmonary hypertension. *Circulation*. 2014;130:1820-1830.

29. Simonneau G, Galie N, Rubin LJ, Langleben D, Seeger W, Domenighetti G, Gibbs S, Lebrec D, Speich R, Beghetti M, Rich S and Fishman A. Clinical classification of pulmonary hypertension. *Journal of the American College of Cardiology*. 2004;43:5-12.

30. Stenmark KR, Meyrick B, Galie N, Mooi WJ and McMurtry IF. Animal models of pulmonary arterial hypertension: the hope for etiological discovery and pharmacological cure. *American Journal of Physiology-Lung Cellular and Molecular Physiology*. 2009;297:1013-1032.

31. Fishman AP. Clinical classification of pulmonary hypertension. *Clinics in Chest Medicine*. 2001;22:385-391.

32. Montani D, Price LC, Dorfmuller P, Achouh L, Jais X, Yaici A, Sitbon O, Musset D, Simonneau G and Humbert M. Pulmonary veno-occlusive disease. *The European Respiratory Journal*. 2009;33:189-200.

33. Simonneau G, Montani D, Celermajer DS, Denton CP, Gatzoulis MA, Krowka M, Williams PG and Souza R. Haemodynamic definitions and updated clinical classification of pulmonary hypertension. *The European Respiratory Journal*. 2019;53.

34. Harrison RE, Flanagan JA, Sankelo M, Abdalla SA, Rowell J, Machado RD, Elliott CG, Robbins IM, Olschewski H, McLaughlin V, Gruenig E, Kermeen F, Halme M, Raisanen-Sokolowski A, Laitinen T, Morrell NW and Trembath RC. Molecular and functional analysis identifies ALK-1 as the predominant cause of pulmonary hypertension related to hereditary haemorrhagic telangiectasia. *Journal of Medical Genetics*. 2003;40:865-871.

35. Chaouat A, Coulet F, Favre C, Simonneau G, Weitzenblum E, Soubrier F and Humbert M. Endoglin germline mutation in a patient with hereditary haemorrhagic

telangiectasia and dexfenfluramine associated pulmonary arterial hypertension. *Thorax*. 2004;59:446-448.

36. Nasim MT, Ogo T, Ahmed M, Randall R, Chowdhury HM, Snape KM, Bradshaw TY, Southgate L, Lee GJ, Jackson I, Lord GM, Gibbs JS, Wilkins MR, Ohta-Ogo K, Nakamura K, Girerd B, Coulet F, Soubrier F, Humbert M, Morrell NW, Trembath RC and Machado RD. Molecular genetic characterization of SMAD signaling molecules in pulmonary arterial hypertension. *Human Mutation*. 2011;32:1385-1389.

37. Austin ED, Ma L, LeDuc C, Berman Rosenzweig E, Borczuk A, Phillips JA, 3rd, Palomero T, Sumazin P, Kim HR, Talati MH, West J, Loyd JE and Chung WK. Whole exome sequencing to identify a novel gene (caveolin-1) associated with human pulmonary arterial hypertension. *Circulation-Cardiovascular Genetics*. 2012;5:336-343.

38. Ma L, Roman-Campos D, Austin ED, Eyries M, Sampson KS, Soubrier F, Germain M, Tregouet DA, Borczuk A, Rosenzweig EB, Girerd B, Montani D, Humbert M, Loyd JE, Kass RS and Chung WK. A novel channelopathy in pulmonary arterial hypertension. *The New England Journal of Medicine*. 2013;369:351-361.

39. Fishman AP. Aminorex to fen/phen: an epidemic foretold. *Circulation*. 1999;99:156-161.

40. Hachulla E, Gressin V, Guillevin L, Carpentier P, Diot E, Sibilia J, Kahan A, Cabane J, Frances C, Launay D, Mouthon L, Allanore Y, Tiev KP, Clerson P, de Groote P and Humbert M. Early detection of pulmonary arterial hypertension in systemic sclerosis: a French nationwide prospective multicenter study. *Arthritis and Rheumatology*. 2005;52:3792-3800.

41. Mukerjee D, St George D, Coleiro B, Knight C, Denton CP, Davar J, Black CM and Coghlan JG. Prevalence and outcome in systemic sclerosis associated pulmonary arterial hypertension: application of a registry approach. *Annals of the Rheumatic Diseases*. 2003;62:1088-1093.

42. Tyndall AJ, Bannert B, Vonk M, Airo P, Cozzi F, Carreira PE, Bancel DF, Allanore Y, Muller-Ladner U, Distler O, Iannone F, Pellerito R, Pileckyte M, Miniati I, Ananieva L, Gurman AB, Damjanov N, Mueller A, Valentini G, Riemekasten G, Tikly M, Hummers L, Henriques MJ, Caramaschi P, Scheja A, Rozman B, Ton E, Kumanovics G, Coleiro B, Feierl E, Szucs G, Von Muhlen CA, Riccieri V, Novak S, Chizzolini C, Kotulska A, Denton C, Coelho PC, Kotter I, Simsek I, de la Pena Lefebvre PG, Hachulla E, Seibold JR, Rednic S, Stork J, Morovic-Vergles J and Walker UA.

Causes and risk factors for death in systemic sclerosis: a study from the EULAR Scleroderma Trials and Research (EUSTAR) database. *Annals of the Rheumatic Diseases*. 2010;69:1809-1815.

43. Sitbon O, Lascoux-Combe C, Delfraissy JF, Yeni PG, Raffi F, De Zuttere D, Gressin V, Clerson P, Sereni D and Simonneau G. Prevalence of HIV-related pulmonary arterial hypertension in the current antiretroviral therapy era. *American Journal of Respiratory and Critical Care Medicine*. 2008;177:108-113.

44. Nunes H, Humbert M, Sitbon O, Morse JH, Deng Z, Knowles JA, Le Gall C, Parent F, Garcia G, Herve P, Barst RJ and Simonneau G. Prognostic factors for survival in human immunodeficiency virus-associated pulmonary arterial hypertension. *American Journal of Respiratory and Critical Care Medicine*. 2003;167:14331-14339.

45. Herve P, Lebrec D, Brenot F, Simonneau G, Humbert M, Sitbon O and Duroux P. Pulmonary vascular disorders in portal hypertension. *The European Respiratory Journal*. 1998;11:1153-1166.

46. Rodriguez-Roisin R, Krowka MJ, Herve P, Fallon MB and Committee ERSTFP-HVDS. Pulmonary-Hepatic vascular Disorders (PHD). *The European Respiratory Journal*. 2004;24:861-880.

47. Hadengue A, Benhayoun MK, Lebrec D and Benhamou JP. Pulmonary hypertension complicating portal hypertension: prevalence and relation to splanchnic hemodynamics. *Gastroenterology*. 1991;100:520-528.

48. Krowka MJ, Swanson KL, Frantz RP, McGoon MD and Wiesner RH. Portopulmonary hypertension: Results from a 10-year screening algorithm. *Hepatology*. 2006;44:1502-1510.

49. Gan HL, Zhang JQ, Zhou QW, Feng L, Chen F and Yang Y. Patients with congenital systemic-to-pulmonary shunts and increased pulmonary vascular resistance: what predicts postoperative survival? *PloS one*. 2014;9:e83976.

50. Nair J and Lakshminrusimha S. Update on PPHN: mechanisms and treatment. *Seminars in Perinatology*. 2014;38:78-91.

51. Oudiz RJ. Pulmonary hypertension associated with left-sided heart disease. *Clinics in Chest Medicine*. 2007;28:233-241.

52. Kosanovic D, Herrera EA, Sydykov A, Orfanos SE and El Agha E. Pulmonary Hypertension due to Lung Diseases and/or Hypoxia: What Do We Actually Know? *Canadian Respiratory Journal*. 2017;2017:9598089.

53. Minai OA, Chaouat A and Adnot S. Pulmonary hypertension in COPD: epidemiology, significance, and management: pulmonary vascular disease: the global perspective. *Chest*. 2010;137:39-51.

54. Memon HA, Lin CH and Guha A. Chronic Thromboembolic Pulmonary Hypertension: Pearls and Pitfalls of Diagnosis. *Methodist DeBakey Cardiovascular Journal*. 2016;12:199-204.

55. Handa T, Nagai S, Miki S, Fushimi Y, Ohta K, Mishima M and Izumi T. Incidence of pulmonary hypertension and its clinical relevance in patients with sarcoidosis. *Chest*. 2006;129:1246-1252.

56. Mayer E, Kriegsmann J, Gaumann A, Kauczor HU, Dahm M, Hake U, Schmid FX and Oelert H. Surgical treatment of pulmonary artery sarcoma. *The Journal of Thoracic and Cardiovascular Surgery*. 2001;121:77-82.

57. Shimoda LA and Laurie SS. Vascular remodeling in pulmonary hypertension. *Journal of Molecular Medicine*. 2013;91:297-309.

58. Jeffery TK and Wanstall JC. Comparison of pulmonary vascular function and structure in early and established hypoxic pulmonary hypertension in rats. *Canadian Journal of Physiology and Pharmacology*. 2001;79:227-237.

59. Stenmark KR, Nozik-Grayck E, Gerasimovskaya E, Anwar A, Li M, Riddle S and Frid M. The adventitia: Essential role in pulmonary vascular remodeling. *Comprehensive Physiology*. 2011;1:141-161.

60. Firth AL, Mandel J and Yuan JX. Idiopathic pulmonary arterial hypertension. *Disease Models and Mechanisms*. 2010;3:268-273.

61. Dingemans KP and Wagenvoort CA. Pulmonary arteries and veins in experimental hypoxia. An ultrastructural study. *The American Journal of Pathology*. 1978;93:353-368.

62. Meyrick B, Gamble W and Reid L. Development of Crotalaria pulmonary hypertension: hemodynamic and structural study. *American Journal of Physiology*. 1980;239:692-702.

63. Budhiraja R, Tuder RM and Hassoun PM. Endothelial dysfunction in pulmonary hypertension. *Circulation*. 2004;109:159-165.

64. Ranchoux B, Harvey LD, Ayon RJ, Babicheva A, Bonnet S, Chan SY, Yuan JX and Perez VJ. Endothelial dysfunction in pulmonary arterial hypertension: an evolving landscape (2017 Grover Conference Series). *Pulmonary Circulation*. 2018;8:2045893217752912.

65. Voelkel NF and Tuder RM. Cellular and molecular biology of vascular smooth muscle cells in pulmonary hypertension. *Pulmonary Pharmacology and Therapeutics*. 1997;10:231-241.

66. Heath D, Smith P and Gosney J. Ultrastructure of early plexogenic pulmonary arteriopathy. *Histopathology*. 1988;12:41-52.

67. Stewart S. Pathology of adult pulmonary hypertension. *Clinical Pulmonary Hypertension* 1995:43-79.

68. Cool CD, Stewart JS, Werahera P, Miller GJ, Williams RL, Voelkel NF and Tuder RM. Three-dimensional reconstruction of pulmonary arteries in plexiform pulmonary hypertension using cell-specific markers. Evidence for a dynamic and heterogeneous process of pulmonary endothelial cell growth. *The American Journal of Pathology*. 1999;155:411-419.

69. Rabinovitch M. Molecular pathogenesis of pulmonary arterial hypertension. *Journal of Clinical Investigation*. 2012;122:4306-4313.

70. De Meyer GR and Bult H. Mechanisms of neointima formation--lessons from experimental models. *Vascular Medicine*. 1997;2:179-189.

71. Humbert M, Montani D, Perros F, Dorfmuller P, Adnot S and Eddahibi S. Endothelial cell dysfunction and cross talk between endothelium and smooth muscle cells in pulmonary arterial hypertension. *Vascular Pharmacology*. 2008;49:113-118.

72. Rabinovitch M. Molecular pathogenesis of pulmonary arterial hypertension. *Journal of Clinical Investigation*. 2008;118:2372-2379.

73. Yue B. Biology of the extracellular matrix: an overview. *Journal of Glaucoma*. 2014;23:20-23.

74. Bornstein P and Sage EH. Matricellular proteins: extracellular modulators of cell function. *Current Opinion in Cell Biology*. 2002;14:608-616.

75. Jones PL, Cowan KN and Rabinovitch M. Tenascin-C, proliferation and subendothelial fibronectin in progressive pulmonary vascular disease. *The Journal of Pathology*. 1997;150:1349-1360.

76. Sage EH and Bornstein P. Extracellular proteins that modulate cell-matrix interactions. SPARC, tenascin, and thrombospondin. *The Journal of Biological Chemistry*. 1991;266:14831-14834.

77. Lau LF and Lam SC. The CCN family of angiogenic regulators: the integrin connection. *Experimental Cell Research*. 1999;248:44-57.

78. Mao JR, Taylor G, Dean WB, Wagner DR, Afzal V, Lotz JC, Rubin EM and Bristow J. Tenascin-X deficiency mimics Ehlers-Danlos syndrome in mice through alteration of collagen deposition. *Nature Genetics*. 2002;30:421-425.

79. Roberts DD. Emerging functions of matricellular proteins. *Cellular and Molecular Life Sciences*. 2011;68:3133-3136.

80. Botney MD, Bahadori L and Gold LI. Vascular remodeling in primary pulmonary hypertension. Potential role for transforming growth factor-beta. *The American Journal of Pathology*. 1994;144:286-295.

81. Humbert M, Monti G, Fartoukh M, Magnan A, Brenot F, Rain B, Capron F, Galanaud P, Duroux P, Simonneau G and Emilie D. Platelet-derived growth factor expression in primary pulmonary hypertension: comparison of HIV seropositive and HIV seronegative patients. *The European Respiratory Journal*. 1998;11:554-559.

82. Schermuly RT, Dony E, Ghofrani HA, Pullamsetti S, Savai R, Roth M, Sydykov A, Lai YJ, Weissmann N, Seeger W and Grimminger F. Reversal of experimental pulmonary hypertension by PDGF inhibition. *Journal of Clinical Investigation*. 2005;115:2811-2821.

83. Merklinger SL, Jones PL, Martinez EC and Rabinovitch M. Epidermal growth factor receptor blockade mediates smooth muscle cell apoptosis and improves survival in rats with pulmonary hypertension. *Circulation*. 2005;112:423-431.

84. Sakao S, Taraseviciene-Stewart L, Cool CD, Tada Y, Kasahara Y, Kurosu K, Tanabe N, Takiguchi Y, Tatsumi K, Kuriyama T and Voelkel NF. VEGF-R blockade causes endothelial cell apoptosis, expansion of surviving CD34+ precursor cells and transdifferentiation to smooth muscle-like and neuronal-like cells. *FASEB journal : official publication of the Federation of American Societies for Experimental Biology*. 2007;21:3640-3652.

85. Benisty JI, McLaughlin VV, Landzberg MJ, Rich JD, Newburger JW, Rich S and Folkman J. Elevated basic fibroblast growth factor levels in patients with pulmonary arterial hypertension. *Chest*. 2004;126:1255-1261.

86. Tuder RM, Chacon M, Alger L, Wang J, Taraseviciene-Stewart L, Kasahara Y, Cool CD, Bishop AE, Geraci M, Semenza GL, Yacoub M, Polak JM and Voelkel NF. Expression of angiogenesis-related molecules in plexiform lesions in severe pulmonary hypertension: evidence for a process of disordered angiogenesis. *The Journal of Pathology*. 2001;195:367-374.

87. Hassoun PM, Mouthon L, Barbera JA, Eddahibi S, Flores SC, Grimminger F, Jones PL, Maitland ML, Michelakis ED, Morrell NW, Newman JH, Rabinovitch M, Schermuly R, Stenmark KR, Voelkel NF, Yuan JX and Humbert M. Inflammation, growth factors, and pulmonary vascular remodeling. *Journal of the American College of Cardiology*. 2009;54:10-19.

88. Pullamsetti SS, Perros F, Chelladurai P, Yuan J and Stenmark K. Transcription factors, transcriptional coregulators, and epigenetic modulation in the control of pulmonary vascular cell phenotype: therapeutic implications for pulmonary hypertension (2015 Grover Conference series). *Pulmonary Circulation*. 2016;6:448-464.

89. Semenza GL. Regulation of oxygen homeostasis by hypoxia-inducible factor 1. *Physiology*. 2009;24:97-106.

90. Hubbi ME, Gilkes DM, Hu H, Kshitiz, Ahmed I and Semenza GL. Cyclin-dependent kinases regulate lysosomal degradation of hypoxia-inducible factor 1alpha to promote cell-cycle progression. *Proceedings of the National Academy of Sciences of the United States of America*. 2014;111:3325-3334.

91. Tsai H, Sung YK and de Jesus Perez V. Recent advances in the management of pulmonary arterial hypertension. *F1000Research*. 2016;5:2755.

92. https://phassociation.org/patients/treatments.

93. Medarov BI and Judson MA. The role of calcium channel blockers for the treatment of pulmonary arterial hypertension: How much do we actually know and how could they be positioned today? *Respiratory Medicine*. 2015;109:557-564.

94. Enderby CY and Burger C. Medical treatment update on pulmonary arterial hypertension. *Therapeutic Advances in Chronic Disease*. 2015;6:264-272.

95. Humbert M, Sitbon O and Simonneau G. Treatment of pulmonary arterial hypertension. *The New England Journal of Medicine*. 2004;351:1425-1436.

96. Tuder RM, Radisavljevic Z, Shroyer KR, Polak JM and Voelkel NF. Monoclonal endothelial cells in appetite suppressant-associated pulmonary hypertension. *American Journal of Respiratory and Critical Care Medicine*. 1998;158:1999-2001.

97. Sandoo A, Veldhuijzen van Zanten JJ, Metsios GS, Carroll D and Kitas GD. Vascular function and morphology in rheumatoid arthritis: a systematic review. *Rheumatology*. 2011;50:2125-2139.

98. Nadeau V, Potus F, Boucherat O, Paradis R, Tremblay E, Iglarz M, Paulin R, Bonnet S and Provencher S. Dual ETA/ETB blockade with macitentan improves both

vascular remodeling and angiogenesis in pulmonary arterial hypertension. *Pulmonary Circulation*. 2018;8:2045893217741429.

99. Kim FY, Barnes EA, Ying L, Chen C, Lee L, Alvira CM and Cornfield DN. Pulmonary artery smooth muscle cell endothelin-1 expression modulates the pulmonary vascular response to chronic hypoxia. *American Journal of Physiology-Lung Cellular and Molecular Physiology*. 2015;308:368-377.

100. Tonelli AR, Alnuaimat H and Mubarak K. Pulmonary vasodilator testing and use of calcium channel blockers in pulmonary arterial hypertension. *Respiratory Medicine*. 2010;104:481-496.

101. Ghofrani HA, Voswinckel R, Gall H, Schermuly R, Weissmann N, Seeger W and Grimminger F. Riociguat for pulmonary hypertension. *Future Cardiology*. 2010;6:155-166.

102. Mergia E, Friebe A, Dangel O, Russwurm M and Koesling D. Spare guanylyl cyclase NO receptors ensure high NO sensitivity in the vascular system. *Journal of Clinical Investigation*. 2006;116:1731-1737.

103. Vermeersch P, Buys E, Pokreisz P, Marsboom G, Ichinose F, Sips P, Pellens M, Gillijns H, Swinnen M, Graveline A, Collen D, Dewerchin M, Brouckaert P, Bloch KD and Janssens S. Soluble guanylate cyclase-alpha1 deficiency selectively inhibits the pulmonary vasodilator response to nitric oxide and increases the pulmonary vascular remodeling response to chronic hypoxia. *Circulation*. 2007;116:936-943.

104. Nimmegeers S, Sips P, Buys E, Decaluwe K, Brouckaert P and Van de Voorde J. Role of the soluble guanylyl cyclase alpha1-subunit in mice corpus cavernosum smooth muscle relaxation. *International Journal of Impotence Research*. 2008;20:278-284.

105. Taichman DB, Ornelas J, Chung L, Klinger JR, Lewis S, Mandel J, Palevsky HI, Rich S, Sood N, Rosenzweig EB, Trow TK, Yung R, Elliott CG and Badesch DB. Pharmacologic therapy for pulmonary arterial hypertension in adults: CHEST guideline and expert panel report. *Chest*. 2014;146:449-475.

106. Savarese G, Costanzo P, Cleland JG, Vassallo E, Ruggiero D, Rosano G and Perrone-Filardi P. A meta-analysis reporting effects of angiotensin-converting enzyme inhibitors and angiotensin receptor blockers in patients without heart failure. *Journal of the American College of Cardiology*. 2013;61:131-142.

107. Dupuis J and Weissmann N. Chapter 30 Animal Models of Pulmonary Hypertension. *Text Book of Pulmonary Vascular Disease, Springer*. 2010:453-459.

108. Gomez-Arroyo J, Saleem SJ, Mizuno S, Syed AA, Bogaard HJ, Abbate A, Taraseviciene-Stewart L, Sung Y, Kraskauskas D, Farkas D, Conrad DH, Nicolls MR and Voelkel NF. A brief overview of mouse models of pulmonary arterial hypertension: problems and prospects. *American Journal of Physiology -Lung Cellular and Molecular Physiology* 2012;302:977-991.

109. Nogueira-Ferreira R. Animal Models for the Study of Pulmonary Hypertension: Potential and Limitations. *Cardiology and Cardiovascular Medicine*. 2016;1.

110. Maarman G, Lecour S, Butrous G, Thienemann F and Sliwa K. A comprehensive review: the evolution of animal models in pulmonary hypertension research; are we there yet? *Pulmonary Circulation*. 2013;3:739-756.

111. Blumberg FC, Lorenz C, Wolf K, Sandner P, Riegger GA and Pfeifer M. Increased pulmonary prostacyclin synthesis in rats with chronic hypoxic pulmonary hypertension. *Cardiovascular Research*. 2002;55:171-7.

112. Zhao S. A rat model of sustained hypobaric hypoxia-induced pulmonary hypertension. *International Journal of Clinical and Experimental Medicine*. 2017;10.

113. Weisel FC, Kloepping C, Pichl A, Sydykov A, Kojonazarov B, Wilhelm J, Roth M, Ridge KM, Igarashi K, Nishimura K, Maison W, Wackendorff C, Klepetko W, Jaksch P, Ghofrani HA, Grimminger F, Seeger W, Schermuly RT, Weissmann N and Kwapiszewska G. Impact of S-adenosylmethionine decarboxylase 1 on pulmonary vascular remodeling. *Circulation*. 2014;129:1510-1523.

114. Arias-Stella J and Saldana M. The Terminal Portion of the Pulmonary Arterial Tree in People Native to High Altitudes. *Circulation*. 1963;28:915-925.

115. Grover RF, Vogel JH, Voigt GC and Blount SG, Jr. Reversal of high altitude pulmonary hypertension. *The American Journal of Cardiology*. 1966;18:928-932.

116. Abraham AS, Kay JM, Cole RB and Pincock AC. Haemodynamic and pathological study of the effect of chronic hypoxia and subsequent recovery of the heart and pulmonary vasculature of the rat. *Cardiovascular Research*. 1971;5:95-102.

117. Heath D, Edwards C, Winson M and Smith P. Effects on the right ventricle, pulmonary vasculature, and carotid bodies of the rat of exposure to, and recovery from, simulated high altitude. *Thorax*. 1973;28:24-28.

118. Hislop A and Reid L. Changes in the pulmonary arteries of the rat during recovery from hypoxia-induced pulmonary hypertension. *British Journal of Experimental Pathology*. 1977;58:653-662.

119. J.G. B. Heart Anatomy *Anatomy and Physiology*. 2013:787–846.

120. R Development Core Team R Foundation for Statistical Computing. R: A language and environment for statistical computing. *Vienna, Austria ISBN 3-900051-07-0, URL http://wwwR-projectorg*. 2007.

121. Smyth GKG, V. Carey, S. Dudoit, R. Irizarry, W. Huber (eds.), . Limma: linear models for microarray data. In: Bioinformatics and Computational Biology Solutions using R and Bioconductor, R. . *Springer*. 2005:397-420.

122. Gentleman RC, Carey VJ, Bates DM, Bolstad B, Dettling M, Dudoit S, Ellis B, Gautier L, Ge Y, Gentry J, Hornik K, Hothorn T, Huber W, Iacus S, Irizarry R, Leisch F, Li C, Maechler M, Rossini AJ, Sawitzki G, Smith C, Smyth G, Tierney L, Yang JY and Zhang J. Bioconductor: open software development for computational biology and bioinformatics. *Genome Biology*. 2004;5:80.

123. Smyth GK and Speed T. Normalization of cDNA microarray data. *Methods*. 2003;31:265-273.

124. Smyth GK. Linear models and empirical bayes methods for assessing differential expression in microarray experiments. *Statistical Applications in Genetics and Molecular Biology* 2004;3.

125. Bradshaw AD and Sage EH. SPARC, a matricellular protein that functions in cellular differentiation and tissue response to injury. *The Journal of Clinical Investigation*. 2001;107:1049-1054.

126. Koukourakis MI, Giatromanolaki A, Brekken RA, Sivridis E, Gatter KC, Harris AL and Sage EH. Enhanced expression of SPARC/osteonectin in the tumor-associated stroma of non-small cell lung cancer is correlated with markers of hypoxia/acidity and with poor prognosis of patients. *Cancer Research*. 2003;63:5376-5380.

127. Chen J, Wang M, Xi B, Xue J, He D, Zhang J and Zhao Y. SPARC is a key regulator of proliferation, apoptosis and invasion in human ovarian cancer. *PloS One*. 2012;7:e42413.

128. Shibata S and Ishiyama J. Secreted protein acidic and rich in cysteine (SPARC) is upregulated by transforming growth factor (TGF)-beta and is required for TGF-beta-induced hydrogen peroxide production in fibroblasts. *Fibrogenesis & Tissue Repair*. 2013;6:6.

129. Veith C, Schermuly RT, Brandes RP and Weissmann N. Molecular mechanisms of hypoxia-inducible factor-induced pulmonary arterial smooth muscle cell alterations in pulmonary hypertension. *The Journal of Physiology*. 2016;594:1167-1177.

130. Lawrence J and Nho R. The Role of the Mammalian Target of Rapamycin (mTOR) in Pulmonary Fibrosis. *International Journal of Molecular Sciences*. 2018;19.

131. Houssaini A and Adnot S. mTOR: A Key to Both Pulmonary Vessel Remodeling and Right Ventricular Function in Pulmonary Arterial Hypertension? *American Journal of Respiratory Cell and Molecular Biology*. 2017;57:509-511.

132. Kudryashova TV, Goncharov DA, Pena A, Kelly N, Vanderpool R, Baust J, Kobir A, Shufesky W, Mora AL, Morelli AE, Zhao J, Ihida-Stansbury K, Chang B, DeLisser H, Tuder RM, Kawut SM, Sillje HH, Shapiro S, Zhao Y and Goncharova EA. HIPPO-Integrin-linked Kinase Cross-Talk Controls Self-Sustaining Proliferation and Survival in Pulmonary Hypertension. *American Journal of Respiratory and Critical Care Medicine*. 2016;194:866-877.

133. Alam R, Schultz CR, Golembieski WA, Poisson LM and Rempel SA. PTEN suppresses SPARC-induced pMAPKAPK2 and inhibits SPARC-induced Ser78 HSP27 phosphorylation in glioma. *Neuro Oncology*. 2013;15:451-461.

134. Ryan J, Bloch K and Archer SL. Rodent models of pulmonary hypertension: harmonisation with the world health organisation's categorisation of human PH. *International Journal of Clinical Practice Supplement*. 2011:15-34.

135. van Suylen RJ, Smits JF and Daemen MJ. Pulmonary artery remodeling differs in hypoxia- and monocrotaline-induced pulmonary hypertension. *American Journal of Respiratory and Critical Care Medicine*. 1998;157:1423-1428.

136. Legres LG, Janin A, Masselon C and Bertheau P. Beyond laser microdissection technology: follow the yellow brick road for cancer research. *American Journal of Cancer Research*. 2014;4:1-28.

137. Kwapiszewska G, Wilhelm J, Wolff S, Laumanns I, Koenig IR, Ziegler A, Seeger W, Bohle RM, Weissmann N and Fink L. Expression profiling of laser-microdissected intrapulmonary arteries in hypoxia-induced pulmonary hypertension. *Respiratory Research*. 2005;6:109.

138. Russo G, Zegar C and Giordano A. Advantages and limitations of microarray technology in human cancer. *Oncogene*. 2003;22:6497-6507.

139. Simon R, Radmacher MD, Dobbin K and McShane LM. Pitfalls in the use of DNA microarray data for diagnostic and prognostic classification. *Journal of the National Cancer Institute*. 2003;95:14-18.

140. Bumgarner R. DNA microarrays: Types, Applications and their future. *Current Protocols in Molecular Biology*. 2013

141. Lane TF and Sage EH. The biology of SPARC, a protein that modulates cell-matrix interactions. *FASEB journal : official publication of the Federation of American Societies for Experimental Biology*. 1994;8:163-173.

142. Madtes DK, Rubenfeld G, Klima LD, Milberg JA, Steinberg KP, Martin TR, Raghu G, Hudson LD and Clark JG. Elevated transforming growth factor-alpha levels in bronchoalveolar lavage fluid of patients with acute respiratory distress syndrome. *American Journal of Respiratory and Critical Care Medicine*. 1998;158:424-430.

143. Reed MJ, Puolakkainen P, Lane TF, Dickerson D, Bornstein P and Sage EH. Differential expression of SPARC and thrombospondin 1 in wound repair: immunolocalization and in situ hybridization. *Journal of Histochemistry and Cytochemistry*. 1993;41:1467-1477.

144. Kos K and Wilding JP. SPARC: a key player in the pathologies associated with obesity and diabetes. *Nature Reviews Endocrinology*. 2010;6:225-235.

145. Bradshaw AD, Puolakkainen P, Dasgupta J, Davidson JM, Wight TN and Helene Sage E. SPARC-null mice display abnormalities in the dermis characterized by decreased collagen fibril diameter and reduced tensile strength. *Journal of Investigative Dermatology*. 2003;120:949-955.

146. Alachkar H, Santhanam R, Maharry K, Metzeler KH, Huang X, Kohlschmidt J, Mendler JH, Benito JM, Hickey C, Neviani P, Dorrance AM, Anghelina M, Khalife J, Tarighat SS, Volinia S, Whitman SP, Paschka P, Hoellerbauer P, Wu YZ, Han L, Bolon BN, Blum W, Mrozek K, Carroll AJ, Perrotti D, Andreeff M, Caligiuri MA, Konopleva M, Garzon R, Bloomfield CD and Marcucci G. SPARC promotes leukemic cell growth and predicts acute myeloid leukemia outcome. *Journal of Clinical Investigation*. 2014;124:1512-1524.

147. Paulin R, Meloche J, Courboulin A, Lambert C, Haromy A, Courchesne A, Bonnet P, Provencher S, Michelakis ED and Bonnet S. Targeting cell motility in pulmonary arterial hypertension. *The European Respiratory Journal*. 2014;43:531-544.

148. Garat CV, Crossno JT, Jr., Sullivan TM, Reusch JE and Klemm DJ. Inhibition of phosphatidylinositol 3-kinase/Akt signaling attenuates hypoxia-induced pulmonary artery remodeling and suppresses CREB depletion in arterial smooth muscle cells. *Journal of Cardiovascular Pharmacology*. 2013;62:539-548.

149. Roux PP and Blenis J. ERK and p38 MAPK-activated protein kinases: a family of protein kinases with diverse biological functions. *Microbiology and Molecular Biology Reviews*. 2004;68:320-344.

150. Huang J, Wolk JH, Gewitz MH and Mathew R. Caveolin-1 expression during the progression of pulmonary hypertension. *Experimental Biology and Medicine*. 2012;237:956-965.

151. Mouraret N, Marcos E, Abid S, Gary-Bobo G, Saker M, Houssaini A, Dubois-Rande JL, Boyer L, Boczkowski J, Derumeaux G, Amsellem V and Adnot S. Activation of lung p53 by Nutlin-3a prevents and reverses experimental pulmonary hypertension. *Circulation*. 2013;127:1664-1676.

152. Wong SL and Sukkar MB. The SPARC protein: an overview of its role in lung cancer and pulmonary fibrosis and its potential role in chronic airways disease. *British Journal of Pharmacology*. 2017;174:3-14.

153. Wang JC, Lai S, Guo X, Zhang X, de Crombrugghe B, Sonnylal S, Arnett FC and Zhou X. Attenuation of fibrosis in vitro and in vivo with SPARC siRNA. *Arthritis Research and Therapy* 2010;12:R60.

154. Chang W, Wei K, Jacobs SS, Upadhyay D, Weill D and Rosen GD. SPARC suppresses apoptosis of idiopathic pulmonary fibrosis fibroblasts through constitutive activation of beta-catenin. *The Journal of Biological Chemistry*. 2010;285:8196-8206.

155. Sage H, Tupper J and Bramson R. Endothelial cell injury in vitro is associated with increased secretion of an Mr 43,000 glycoprotein ligand. *Journal of Cellular Physiology*. 1986;127:373-387.

156. Sage H, Decker J, Funk S and Chow M. SPARC: a Ca2+-binding extracellular protein associated with endothelial cell injury and proliferation. *Journal of Molecular and Cellular Cardiology*. 1989;21 Suppl 1:13-22.

157. Neri M, Descalzi-Cancedda F and Cancedda R. Heat-shock response in cultured chick embryo chondrocytes. Osteonectin is a secreted heat-shock protein. *European Journal of Biochemistry*. 1992;205:569-574.

158. Sauk JJ, Norris K, Kerr JM, Somerman MJ and Young MF. Diverse forms of stress result in changes in cellular levels of osteonectin/SPARC without altering mRNA levels in osteoligament cells. *Calcified Tissue International*. 1991;49:58-62.

159. Seno T, Harada H, Kohno S, Teraoka M, Inoue A and Ohnishi T. Downregulation of SPARC expression inhibits cell migration and invasion in malignant gliomas. *International Journal of Oncology*. 2009;34:707-715.

160. Epstein AC, Gleadle JM, McNeill LA, Hewitson KS, O'Rourke J, Mole DR, Mukherji M, Metzen E, Wilson MI, Dhanda A, Tian YM, Masson N, Hamilton DL, Jaakkola P, Barstead R, Hodgkin J, Maxwell PH, Pugh CW, Schofield CJ and Ratcliffe

PJ. C. elegans EGL-9 and mammalian homologs define a family of dioxygenases that regulate HIF by prolyl hydroxylation. *Cell*. 2001;107:43-54.

161. Ivan M, Kondo K, Yang H, Kim W, Valiando J, Ohh M, Salic A, Asara JM, Lane WS and Kaelin WG, Jr. HIFalpha targeted for VHL-mediated destruction by proline hydroxylation: implications for O2 sensing. *Science*. 2001;292:464-468.

162. Huang LE, Gu J, Schau M and Bunn HF. Regulation of hypoxia-inducible factor 1alpha is mediated by an O2-dependent degradation domain via the ubiquitin-proteasome pathway. *Proceedings of the National Academy of Sciences of the United States of America*. 1998;95:7987-7992.

163. Semenza GL, Nejfelt MK, Chi SM and Antonarakis SE. Hypoxia-inducible nuclear factors bind to an enhancer element located 3' to the human erythropoietin gene. *Proceedings of the National Academy of Sciences of the United States of America*. 1991;88:5680-5684.

164. Bonnet S, Michelakis ED, Porter CJ, Andrade-Navarro MA, Thebaud B, Bonnet S, Haromy A, Harry G, Moudgil R, McMurtry MS, Weir EK and Archer SL. An abnormal mitochondrial-hypoxia inducible factor-1alpha-Kv channel pathway disrupts oxygen sensing and triggers pulmonary arterial hypertension in fawn hooded rats: similarities to human pulmonary arterial hypertension. *Circulation*. 2006;113:2630-2641.

165. Mizuno S, Bogaard HJ, Kraskauskas D, Alhussaini A, Gomez-Arroyo J, Voelkel NF and Ishizaki T. p53 Gene deficiency promotes hypoxia-induced pulmonary hypertension and vascular remodeling in mice. *American Journal of Physiology-Lung Cellular and Molecular Physiology*. 2011;300:753-761.

166. Huang DY, Lin YT, Jan PS, Hwang YC, Liang ST, Peng Y, Huang CY, Wu HC and Lin CT. Transcription factor SOX-5 enhances nasopharyngeal carcinoma progression by down-regulating SPARC gene expression. *The Journal of Pathology*. 2008;214:445-455.

167. Socha MJ, Manhiani M, Said N, Imig JD and Motamed K. Secreted protein acidic and rich in cysteine deficiency ameliorates renal inflammation and fibrosis in angiotensin hypertension. *The American Journal of Pathology*. 2007;171:1104-1112.

168. Fujita T, Shiba H, Van Dyke TE and Kurihara H. Differential effects of growth factors and cytokines on the synthesis of SPARC, DNA, fibronectin and alkaline phosphatase activity in human periodontal ligament cells. *Cell Biology International*. 2004;28:281-286.

169. Liang JF, Wang HK, Xiao H, Li N, Cheng CX, Zhao YZ, Ma YB, Gao JZ, Bai RB and Zheng HX. Relationship and prognostic significance of SPARC and VEGF protein expression in colon cancer. *Journal of Experimental and Clinical Cancer Research*. 2010;29:71.

170. Stroescu C, Dragnea A, Ivanov B, Pechianu C, Herlea V, Sgarbura O, Popescu A and Popescu I. Expression of p53, Bcl-2, VEGF, Ki67 and PCNA and prognostic significance in hepatocellular carcinoma. *Journal of Gastrointestinal and Liver Diseases*. 2008;17:411-417.

171. Dong Y, Sui L, Sugimoto K, Tai Y and Tokuda M. Cyclin D1-CDK4 complex, a possible critical factor for cell proliferation and prognosis in laryngeal squamous cell carcinomas. *International Journal of Cancer*. 2001;95:209-215.

172. Yang W, Wu Z, Yang K, Han Y, Chen Y, Zhao W, Huang F, Jin Y and Jin W. BMI1 Promotes Cardiac Fibrosis in Ischemia-Induced Heart Failure via the PTEN-PI3K/AKT-mTOR Signaling Pathway. *American Journal of Physiology Heart and Circulatory Physiology*. 2018.

173. Cheng J, Li Y, Liu S, Jiang Y, Ma J, Wan L, Li Q and Pang T. CXCL8 derived from mesenchymal stromal cells supports survival and proliferation of acute myeloid leukemia cells through the PI3K/AKT pathway. *FASEB Journal : official publication of the Federation of American Societies for Experimental Biology*. 2018:fj201801931R.

174. Li H, Wang Y, Chen L, Han L, Li L, He H, Li Y, Huang N, Ren H, Pei F, Li G, Cheng J and Wang W. The role of MIF, cyclinD1 and ERK in the development of pulmonary hypertension in broilers. *Avian Pathology*. 2017;46:202-208.

175. Fenouille N, Puissant A, Tichet M, Zimniak G, Abbe P, Mallavialle A, Rocchi S, Ortonne JP, Deckert M, Ballotti R and Tartare-Deckert S. SPARC functions as an anti-stress factor by inactivating p53 through Akt-mediated MDM2 phosphorylation to promote melanoma cell survival. *Oncogene*. 2011;30:4887-4900.

176. Goncharova EA. mTOR and vascular remodeling in lung diseases: current challenges and therapeutic prospects. *FASEB Journal : official publication of the Federation of American Societies for Experimental Biology*. 2013;27:1796-1807.

177. Krymskaya VP, Snow J, Cesarone G, Khavin I, Goncharov DA, Lim PN, Veasey SC, Ihida-Stansbury K, Jones PL and Goncharova EA. mTOR is required for pulmonary arterial vascular smooth muscle cell proliferation under chronic hypoxia. *FASEB journal : official publication of the Federation of American Societies for Experimental Biology*. 2011;25:1922-1933.

178. Hannigan G, Troussard AA and Dedhar S. Integrin-linked kinase: a cancer therapeutic target unique among its ILK. *Nature Reviews Cancer*. 2005;5:51-63.

179. de la Puente P, Weisberg E, Muz B, Nonami A, Luderer M, Stone RM, Melo JV, Griffin JD and Azab AK. Identification of ILK as a novel therapeutic target for acute and chronic myeloid leukemia. *Leukemia Research*. 2015.

180. Zhang Y, Chen K, Tu Y and Wu C. Distinct roles of two structurally closely related focal adhesion proteins, alpha-parvins and beta-parvins, in regulation of cell morphology and survival. *Journal of Biological Chemistry*. 2004;279:41695-41705.

181. Yamaji S, Suzuki A, Sugiyama Y, Koide Y, Yoshida M, Kanamori H, Mohri H, Ohno S and Ishigatsubo Y. A novel integrin-linked kinase-binding protein, affixin, is involved in the early stage of cell-substrate interaction. *The Journal of Cell Biology*. 2001;153:1251-1264.

182. Nikolopoulos SN and Turner CE. Integrin-linked kinase (ILK) binding to paxillin LD1 motif regulates ILK localization to focal adhesions. *The Journal of Biological Chemistry*. 2001;276:23499-23505.

183. Lee SL, Hsu EC, Chou CC, Chuang HC, Bai LY, Kulp SK and Chen CS. Identification and characterization of a novel integrin-linked kinase inhibitor. *Journal of Medicinal Chemistry*. 2011;54:6364-6374.

184. Desai N, Trieu V, Damascelli B and Soon-Shiong P. SPARC Expression Correlates with Tumor Response to Albumin-Bound Paclitaxel in Head and Neck Cancer Patients. *Translational Oncology*. 2009;2:59-64.

185. Gradishar WJ. Albumin-bound nanoparticle paclitaxel. *Clinical Advances in Hematology and Oncology*. 2005;3:348-349.

186. Gradishar WJ, Tjulandin S, Davidson N, Shaw H, Desai N, Bhar P, Hawkins M and O'Shaughnessy J. Phase III trial of nanoparticle albumin-bound paclitaxel compared with polyethylated castor oil-based paclitaxel in women with breast cancer. *Journal of Clinical Oncology* 2005;23:7794-7803.

187. Lai YC, Potoka KC, Champion HC, Mora AL and Gladwin MT. Pulmonary arterial hypertension: the clinical syndrome. *Circulation*. 2014;115:115-130.

188. Weissmann N, Gerigk B, Kocer O, Nollen M, Hackemack S, Ghofrani HA, Schermuly RT, Butrous G, Schulz A, Roth M, Seeger W and Grimminger F. Hypoxia-induced pulmonary hypertension: different impact of iloprost, sildenafil, and nitric oxide. *Respiratory Medicine* 2007;101:2125-2132.

189. McLoughlin P and Ward JP. Hypoxic pulmonary hypertension; the load on the right ventricle. Introduction. *Experimental Physiology*. 2013;98:1244-1246.

190. Malczyk M, Veith C, Fuchs B, Hofmann K, Storch U, Schermuly RT, Witzenrath M, Ahlbrecht K, Fecher-Trost C, Flockerzi V, Ghofrani HA, Grimminger F, Seeger W, Gudermann T, Dietrich A and Weissmann N. Classical transient receptor potential channel 1 in hypoxia-induced pulmonary hypertension. *American Journal of Respiratory and Critical Care Medicine*. 2013;188:1451-1459.

191. Norose K, Clark JI, Syed NA, Basu A, Heber-Katz E, Sage EH and Howe CC. SPARC deficiency leads to early-onset cataractogenesis. *Investigative Ophthalmology and Visual Science*. 1998;39:2674-2680.

192. Savani RC, Zhou Z, Arguiri E, Wang S, Vu D, Howe CC and DeLisser HM. Bleomycin-induced pulmonary injury in mice deficient in SPARC. *American Journal of Physiology-Lung Cellular and Molecular Physiology*. 2000;279:743-750.

193. Tada Y, Laudi S, Harral J, Carr M, Ivester C, Tanabe N, Takiguchi Y, Tatsumi K, Kuriyama T, Nichols WC and West J. Murine pulmonary response to chronic hypoxia is strain specific. *Experimental Lung Research*. 2008;34:313-323.

194. Dempsie Y, Nilsen M, White K, Mair KM, Loughlin L, Ambartsumian N, Rabinovitch M and Maclean MR. Development of pulmonary arterial hypertension in mice over-expressing S100A4/Mts1 is specific to females. *Respiratory Research*. 2011;12:159.

195. Brekken RA and Sage EH. SPARC, a matricellular protein: at the crossroads of cell-matrix. *Journal of the International Society for Matrix Biology*. 2000;19:569-580.

196. Bradshaw AD. Diverse biological functions of the SPARC family of proteins. *The International Journal of Biochemistry and Cell Biology*. 2012;44:480-488.

197. Novinec M, Kovacic L, Skrlj N, Turk V and Lenarcic B. Recombinant human SMOCs produced by in vitro refolding: calcium-binding properties and interactions with serum proteins. *Protein Expression and Purification*. 2008;62:75-82.

198. Vannahme C, Gosling S, Paulsson M, Maurer P and Hartmann U. Characterization of SMOC-2, a modular extracellular calcium-binding protein. *Biochemical Journal*. 2003;373:805-814.

199. Su JR, Kuai JH and Li YQ. Smoc2 potentiates proliferation of hepatocellular carcinoma cells via promotion of cell cycle progression. *World Journal of Gastroenterology*. 2016;22:10053-10063.

200. Sylva M, Li VS, Buffing AA, van Es JH, van den Born M, van der Velden S, Gunst Q, Koolstra JH, Moorman AF, Clevers H and van den Hoff MJ. The BMP antagonist follistatin-like 1 is required for skeletal and lung organogenesis. *PloS One*. 2011;6:e22616.

201. Zhao P, Guan HT, Dai ZJ, Ma YG, Liu XX and Wang XJ. Knockdown of SPOCK1 Inhibits the Proliferation and Invasion in Colorectal Cancer Cells by Suppressing the PI3K/Akt Pathway. *Oncology Research and Treatment*. 2016;24:437-445.

202. https://www.genetargeting.com/conditional-knockout/conditional-knockout-mouse-and-global-knockout-mouse/.

203. https://www.genoway.com/services/customized-mouse/knockout-models/constitutive-ko.htm.

204. https://www.taconic.com/genetically-engineered-animal-models/knockdown-mice/.

205. Harms DW, Quadros RM, Seruggia D, Ohtsuka M, Takahashi G, Montoliu L and Gurumurthy CB. Mouse Genome Editing Using the CRISPR/Cas System. *Current Protocols in Human Genetics*. 2014;83:1-27.

206. Sliva K and Schnierle BS. Selective gene silencing by viral delivery of short hairpin RNA. *Virology Journal*. 2010;7:248.

207. https://www.vectorbiolabs.com/shrna-aav-adenovirus/.